Università degli Studi di Roma "La Sapienza"

Facoltà di Ingegneria

Dipartimento di Ingegneria Strutturale e Geotecnica

Dottorato di Ricerca – XXV Ciclo

Evaluation of stability and integrity of a steel truss bridge in a forensic investigation

Candidate: Francesca Brando

Advisor: Prof. Franco Bontempi

Sapienza University of Rome

Co-Advisor: Prof. Rene B. Testa

Columbia University in the City of New York

Dissertazione presentata per il conseguimento del titolo di

Dottore di Ricerca in Ingegneria delle Strutture

A.A. 2012/2013

Alla mia Famiglia

Acknowledgements

I would like to express my gratitude to every person who has supported me during the course of my studies.

In particular, I would like to thank Professor Franco Bontempi for the trust he placed in me. His advice has enabled me to achieve important goals and encouraged me to face new challenges, both personally and professionally.

I would also like to thank Professor Rene Testa, whose guidance has allowed me to carry on my experience abroad and endorsed the collaboration with Columbia University in New York.

Furthermore, I would like to acknowledge Professor Giuseppe Rega, coordinator of the Doctoral School at Sapienza University of Rome.

Special thanks to Elisabeth Malsch, Senior Associate, and Gary Panariello, Managing Principal at Thornton Tomasetti, who made it feasible to develop research in New York.

Thanks to Simone, my parents and my brother who have always supported and encouraged me, every day, and stood by me in both stressful and joyful moments.

I cannot forget to thank my colleagues, peers and friends, and in particular the ones with whom I have shared countless hours of studying and memorable experiences. I believe that they are the ones who understand the satisfaction I feel from my achievements more than others.

I especially would like to thank my colleagues in New York, among them, Liling, Alexandra, Marguerite and Luis, as well as my colleagues in Rome, Filippo Gentili, Konstantinos Gkoumas, Francesco Petrini, Chiara Crosti, Stefania Arangio and Luisa Giuliani.

SYNTHESIS OF THE WORK

THESIS OUTLINE

ABSTRACT

AIM OF THE THESIS

THESIS OUTLINE

ABSTRACT

The studies presented in this Thesis have been developed in the frame of the forensic investigation into the causes of the collapse of the I-35West Bridge (I-35W) in Minneapolis, Minnesota, USA that occurred on August 1st, 2007. The failure of the I-35W represents a major case-study for the evaluation of stability and integrity of a steel truss bridge.

The Thesis has been developed at Columbia University and at the engineering firm Thornton Tomasetti (TT) which was hired by a national law firm, Robins, Kaplan, Miller & Ciresi, to perform a forensic investigation into the cause of the catastrophic collapse. According to the findings of the forensic investigation, the collapse was triggered by the buckling of an element of the main truss bottom chord in the main span close to the pier.

The Thesis focused on technical aspects and did not attempt to assign responsibility among the involved parties. In the first part of the thesis, the background and motivation for the forensic investigation are presented together with a description of the I-35W Bridge. The definition of bridge safety and related classifications are given. The concept of structural stability and integrity of steel structures are discussed. The nature of structures and their complexity are considered as well as the methodologies used to study them. An extensive description of the structural decomposition method is presented and detailed for the case study.

In this work, using the framework of a multilevel approach, the structural system has been broken down in order to perform a detailed analysis and evaluate the system performances at macro (global) and micro (local) levels. The effect of boundary conditions, thermal loads on the global system and post buckling capacity of the main truss bottom chord built up member on a local level have been studied.

First, a 3D finite element model has been developed in SAP2000 using frame elements. This global-level model reproduces the entire bridge based on original drawings, design and construction specifications. The model has been verified by comparing results with the available original design calculations. Member forces and reactions based on the as-designed conditions with the specified design loads have been confirmed. The model served to investigate the elastic behavior of the bridge and its overall response to various loading and boundary conditions. In particular, from the global model it has been possible to evaluate the static stress condition on the bridge showing how some of the temperature changes and the possible deterioration of the designed supports could affect the demand on the load carrying members. A specific lower chord member was identified as a critical member for temperature loading in particular.

Second, a 3D solid element model of the recognized critical load bearing member comprised of a welded built up section with perforated cover plates was built in Abaqus. This local-level model provided information on the post buckling behavior and capacity of the load bearing member. The effects of the perforations and boundary conditions have been outlined. Furthermore, the results have been compared against hand calculations following the provisions of the Code of Standard Practice for Structural Steel Buildings and Bridges (AISC, 2005) for built up members and the Timoshenko plate theory for columns with perforated cover plates.

Keywords: forensic investigation, steel truss bridge, stability, integrity, post-buckling capacity, welded built up sections.

AIM OF THE THESIS

The aim of the work has been to investigate the untested fragility of the bridge: its capacity to carry temperature loads and the post buckling behavior of the bottom chord member.

The I-35W was a state of the art structure when it was built in the early 1960s. The bridge was opened in 1967 and it consisted of a continuous truss bridge spanning 1000 ft. (305 m.) over four piers. Figure 1 shows a schematic overview of the I-35W Bridge. On August 1st, 2007 at 6:04 pm the bridge collapsed killing 13 people and injuring many more.

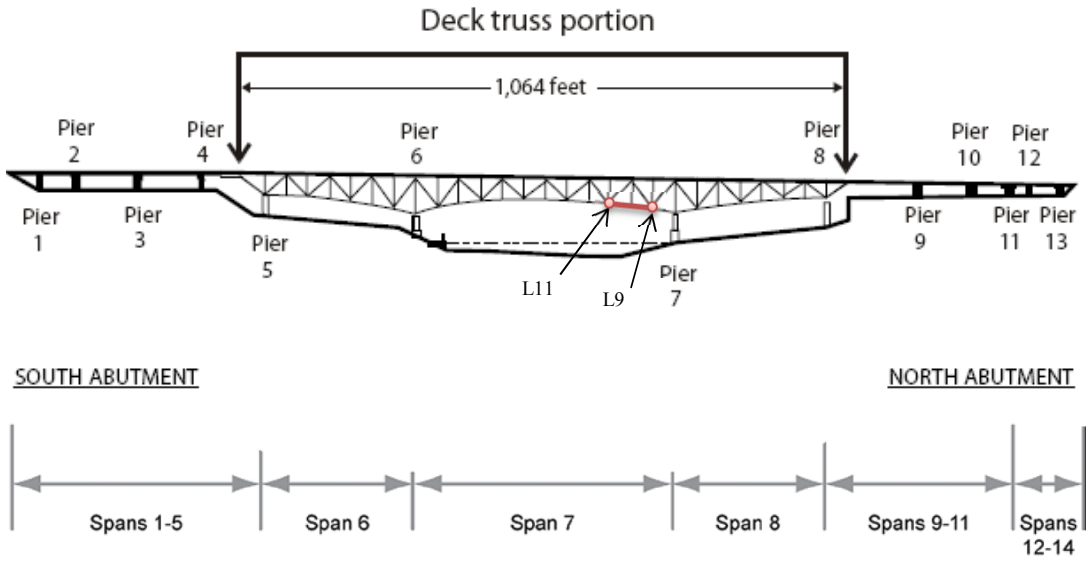

Figure 1 - Bridge schematic overview (NTSB, 2008b)

In the first part of the Thesis the forensic engineering practice and steps for a forensic investigation are defined.

In the second part, the systematic nature of a structure and its complexity are considered as well as the methodologies used to study it. The definition of structural safety requirements and bridge safety classifications are given. The concept of structural stability and integrity of steel structures are discussed.

In the third part, the structural decomposition method is presented and an extensive description of the I-35W Bridge is given. New technologies were employed in the construction of the I-35W Bridge such as: high strength steel provided designers with the possibility of creating more slender and weight efficient structure; a different type of manufacture (welds instead of rivets) for the steel sections construction was employed as

well as an intricate system of roller bearings and thin gusset plate connections; welded built up box section with perforated cover plates.

Following a multilevel perspective, the bridge structural system has been decomposed in order to evaluate the system performances at macro and micro levels in particular. See Figure 2.

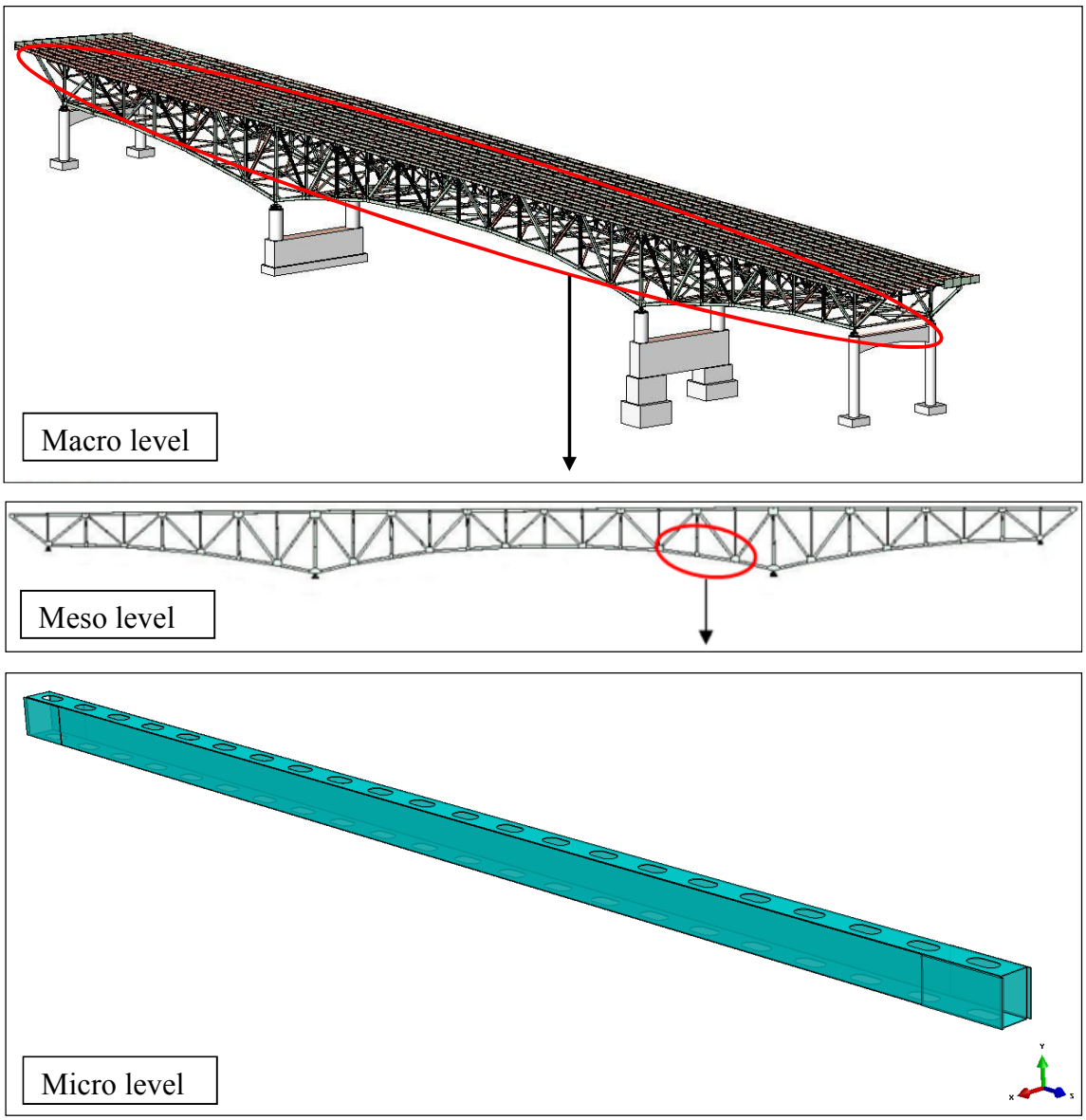

Figure 2 - Structural part identification used in the present study

The analyses here presented are divided into the following tasks:

- Development of a three dimensional (3D) global finite element model (FEM) of the entire bridge based on original drawings, design and construction specifications;
- Conduct analysis of the global structure;

- Development of a 3D FEM of a subsystem's component. In particular this study focus on the rectangular built up member with and without perforated cover plates located on the bottom chord of the main lateral trusses.
- Conduct subsystem component analysis.

First, a three dimensional finite element model has been developed in SAP2000 using frame elements. This global-level model reproduces the entire bridge based on original drawings, design and construction specifications. The model was verified by comparing results with the available original design calculations. Member forces and reactions based on the as-designed conditions with the specified design loads were confirmed. The model served to investigate the elastic behavior of the bridge and its overall response to various loading conditions. In particular, from the global model it has been possible to evaluate the static stress condition on the bridge showing how some of the temperature changes and the possible deterioration of the designed supports could affect the demands on the load carrying members. A specific lower chord member was identified as a critical member for temperature loading in particular.

Second, a three dimensional solid element model of the recognized critical load bearing member comprised of a welded built up section with perforated cover plates was built in Abaqus. This local-level model provided information on the post buckling behavior and capacity of the load bearing member using nonlinear Riks analysis (ABAQUS, 2010). Springs were applied to the member ends to simulate the effective boundary conditions between the individual element and adjacent members. The study focuses on the effect of perforations and boundary conditions on the behavior of the built up member. Furthermore, the numerical results of a buckling analysis obtained by detailed FEM analysis were compared with results obtained from the hand calculation. The hand calculation follows provisions of the 2005 AISC 360 Specification for Structural Steel Buildings (AISC, 2005) with the modified slenderness ratio (KL/r)m, and the Timoshenko theory for built up columns and plates, considering columns with perforated cover plates (Timoshenko, 1961). The separate local analysis helped to determine the effect of local design choices on the integrity of the I-35W steel truss bridge and therefore the role of buckling failure of one main truss's element with respect to the structural stability and sequential failures of other components and subsystem.

INTRODUCTION

1. INTRODUCTION

1 INTRODUCTION

The aim of building regulations and provisions is to build safe and sustainable structures. Nevertheless the design progress and developments are also the results of the lesson learned from failures occurred in the past. Many effects on structural behaviors were unknown before tragic events occurred. Each failure initiates an intense investigation process in order to understand the causes of the collapse and prevent any similar catastrophes in the future.

When catastrophic collapses occur, discovering the cause or causes is the first step to assuring the public and preventing future harm. Traditionally, the victims, the owners of the structure, and the professionals involved with design and maintenance of similar structures engage structural engineers as technical experts to collect evidence, filter the important data, analyze, and then communicate the results to society-at-large.

Forensic engineers have always been tasked with dual goals: primarily and most importantly to use their technical expertise and skills to mathematically determine the collapse mechanisms, but also to subsequently synthesize their results in order to suggest appropriate reactionary measures. In most of the cases the collapse results as combination of various reasons. In order to recognize and investigate the causes of a collapse, it is fundamental to know structural failures types and understand the different levels where they can occur. Failures can occur at material point, element section, structural element and structural system. It is essential to understand the system and to be able to decompose it in a structured and focused way (Bontempi, 2006). Therefore the knowledge of the system complexity, system relations and decomposition techniques are necessary to approach a forensic investigation.

Structural codes and provisions define principles, rules and methods to design structures and bridges complying with safety standards, with proper level of reliability and durability being aware of the different levels of complexity. To pursue the design aims fulfilling the safety requirements, different approaches can be used. The Limit State Design (LSD) is the most used nowadays as well as the Load and Resistance Factor Design (LRFD) used by the American Association of State Highway and Transportation Officials (AASHTO) for the design of bridges. The LSD method considers three principal limit states for which the capacity or strength is estimated under different conditions according to the required level of performance. The limit states considered are ultimate limit state, serviceability limit state and integrity limit state (ISO2394, 1998). The baseline of the LSD method is setting a limit beyond which the structure is considered unsafe. In general for steel members the most important types of structural failure are: large local plasticity, instability, fatigue cracking

related to cycling loading, ductile or brittle fracture, given fatigue cracking or preexisting defects, excessive deformation. The basic failure types do not occur simultaneously but more than one phenomenon may in principle be involved until the structure reaches the ultimate limit state (Paik, 2003).

One class of structures that often incorporates elements whose localized failure would trigger a progressive collapse is functionally non redundant bridges. Their intrinsic non-redundancy can make them susceptible to progressive collapse due to the loss of a series of adjacent members in a single loading event. Truss bridges without primary redundancy are particularly sensitive to progressive collapse. They rely exclusively on the redundancy in the secondary structural resistance to provide some measure of robustness. The term structural robustness in this work is intended as property of the structural system and it refers to the insensitivity to local failure (Starossek, 2006).

Redundancy plays a dominant role in providing robustness and preventing progressive collapse. While it is a strongly desirable feature in structural systems, there is no accepted measure of the degree or distribution of redundancy in a structure and it may be defined in various ways. One definition states that redundancy is "the absence of critical components whose failure would cause collapse of the structure" (Frangopol, 1987). Bridge redundancy is also defined in the (Gosh, 1998) as "the capability of a bridge to continue to carry loads after incurring damage or the failure of one or more of its members". This capability is mainly due to redistribution of the applied loads in transverse and/or longitudinal directions.

In general, redundancy can be seen as a property of the undamaged structure and it has a major impact on the risk of collapse. The absence of redundancy in a structure (i.e. statically determinate structure) may more likely lead to progressive collapse in the event of local damage and clearly represents a non-robust structure. On the other hand the presence of redundant (i.e. statically indeterminate structure) may or may not prevent progressive collapse depending on the robustness of the design and possibly on the existence of preexisting or hidden damage. Furthermore, even if in the primary action of the structure there is no redundancy, secondary action may introduce redundancy that can hinder progressive collapse and thus provide some measure of robustness.

In general, the main failure modes for a steel truss are listed below:

- Failure of truss members: compression members of a truss bridge can fail in overall buckling or in a local buckling mode and members in tension can fail in yielding of the gross area or fracture of the net area, leading to the truss global instability failure.
- Failure of truss connections such as the gusset plates, member splices and supports.

Each bridge has a unique design and intrinsic complexity related to the geometry and design choices and it is subjected to continuous (environmental or anthropic actions) and discrete (human error, accidental or deliberate actions) events which may affect its integrity and lead to collapse.

There are examples of truss bridges that have experienced connection failure without collapsing. One notable example is the Grand River Bridge in Ohio, USA (Figure 1-1). On May 24, 1996 the truss connection at joint L8' at the east end of the eastbound structure failed in the north and south trusses. The gusset plate supporting the verticals and the compression diagonals buckled and allowed the member ends to drop about 3 in (7,5 cm) and moved laterally about 3 in (7,5 cm). The damaged members were in the truss cantilever supporting the center suspended span (NTSB, 2008a). The cause originally was attributed to an overloaded semi-trailer truck. The bridge was closed nearly six months for repairs and lastly demolished and replaced in 2007.

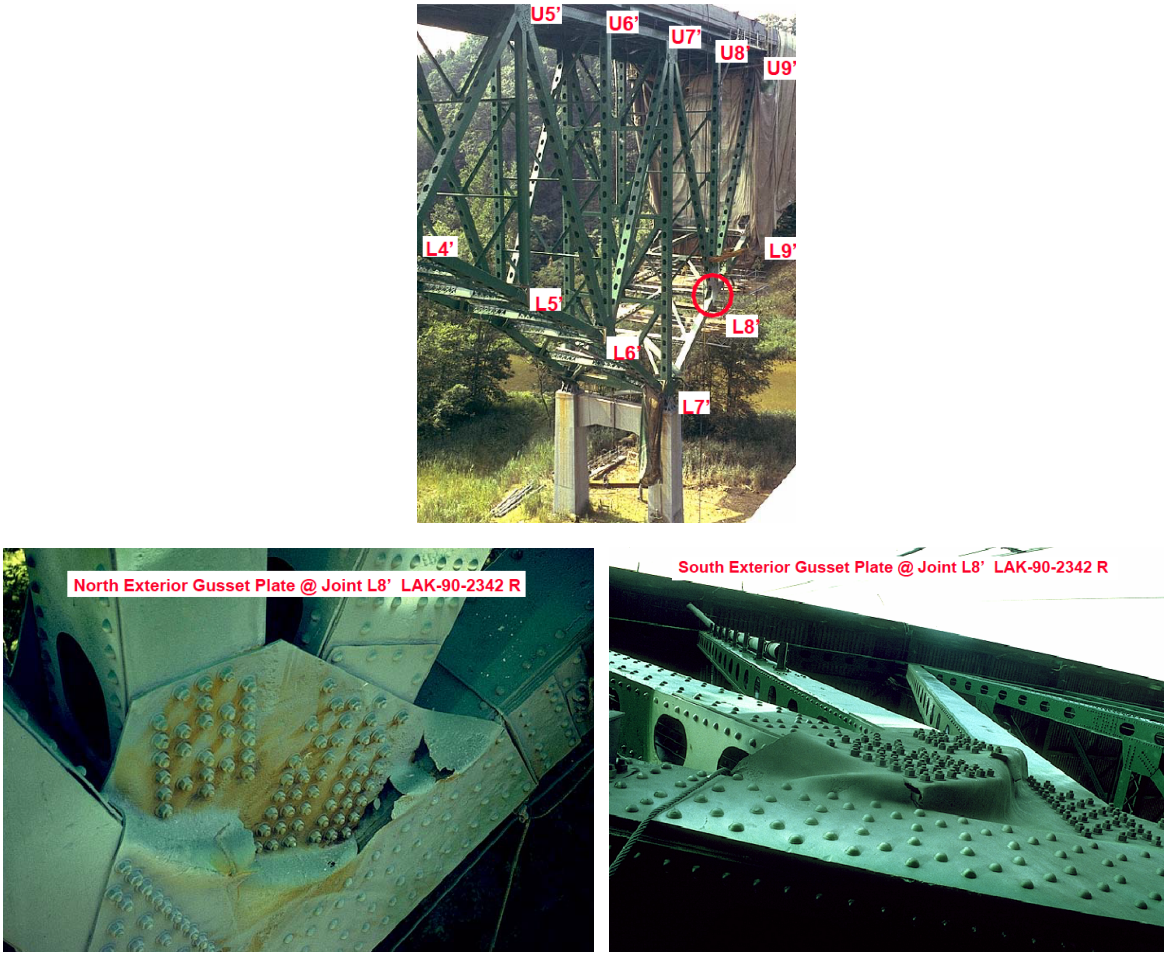

Figure 1-1- Damaged gusset plates, Grand River Bridge, Ohio, USA (NTSB, 2008a)

On the other hand, there are cases of truss bridges that, with the same design and geometry, collapsed tragically. On August 1st, 2007 at 6:04 pm the I-35W Bridge in Minneapolis, Minnesota collapsed killing 13 people and injuring many more (Figure 1-2). According to the findings of the forensic investigation performed at Thornton Tomasetti the combination of the seized bearings, thermal loads and minimal post buckling capacity triggered the local inelastic buckling of the west bottom chord member that spanned from panel point L9 to panel point L11 (L9-L11), hence initiating the collapse of the I-35W.

In this Thesis, a set of analysis results using finite element models and hand calculations are presented. In the framework of a multilevel approach, global and local models have been used to understand the effect of boundary conditions and thermal loads on the global system and the post buckling capacity of the main truss bottom chord built up member L9-L11 on a local level.

Figure 1-2 - I-35W Collapse - August 1, 2007

The I-35W was one of the first bridges to use welded built up box section with perforations, which are comprised of thin plates. Studies in literature show that for columns with welded box sections the reduction of buckling strength due to the presence of residual stresses is similar to that found for buckling of plates with residual stresses. Moreover the residual stresses present in a column cross section influence the local buckling strength even in the elastic range. The effect on the elastic-plastic buckling depends greatly on the width to thickness ratio of plates (Nishino, 1969). In the years before the Second World War a tendency developed, in the United States, to replace the lacing system or the batten-plates of built-up columns by perforated cover-plates. Lacing was ordinarily used on one flange only of a compression member. It was not counted as resisting compression and unbalanced the section. On the other hand, the perforated cover-plate metal could largely be counted in member area and tended to balance the section. It was soon realized that he perforated cover-plates increased the over-all stiffness of the members compared to laced built up columns and hence improved their behavior (White, 1956a,b).

PART I

FORENSIC INVESTIGATION

2. FORENSIC ENGINEERING
3. THE I-35W BRIDGE FORENSIC INVESTIGATION

2 FORENSIC ENGINEERING

Forensics engineering is essentially a branch of the engineering field focused on the study of failures, accidents, and other incidents involving engineered products. The purpose of forensic investigation is to locate the cause or causes of a failure performing a number of tests and analyses to reconstruct the chain of events which led to the failure.

Failures and accidents involving injury, loss of life, or property damage nearly always generate controversy. Hence, the investigation of such events is usually associated with litigation or the threat of litigation. Accident investigation and reconstruction, however, need not always be directly related to litigation. Sometimes the principal purpose of accident reconstruction is to determine causation so that the accident will not be repeated (Carper, 2001).

Forensic engineers can work for consulting firms, local governments, and legal firms, and they do a wide variety of work in the field and in the lab. The work can include analysis in the lab to determine which materials has been used, along with on-site inspection, interviews of people involved, and research into similar failures which may have happened in the past. When catastrophic collapses occur, discovering the cause is the first step to assuring the public and preventing future harm. Traditionally, the victims, the owners of the structure, and the professionals involved with design and maintenance of similar structures engage structural engineers as technical experts to collect evidence, filter the important data, analyze, and then communicate the results to society-at-large. See Figure 2-1.

Forensic engineers have always been tasked with dual goals: primarily and most importantly to use their technical expertise and skills to mathematically determine the collapse mechanisms, but also to subsequently synthesize their results in order to suggest appropriate reactionary measures and to communicate their findings. The inherent challenges to forensic investigation are multiple and quite varied and do not always play to the strengths of engineering skill and judgment. Over the course of any investigation, the engineer is challenged to continually translate between contradictory or incompatible languages in order to communicate to their multiple and quite varied audiences. Oftentimes the data that is collected from a variety of sources so vast and complex that it requires a great deal of filtration by the engineer in order to properly bound their analysis.

This requires engineering skill, but also a time-consuming document review process in order to achieve due diligence. This can be further complicated in modern investigations by outside factors such as legal or governmental processes that impose their own timeline and constraints on the analysis process.

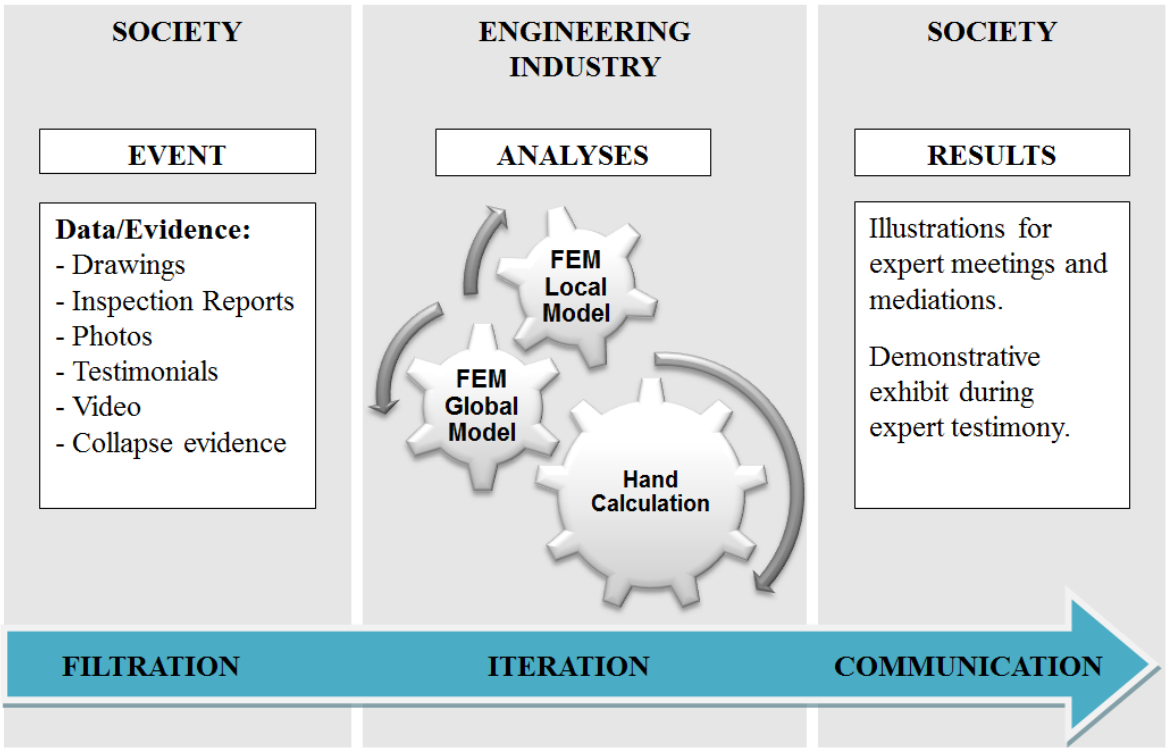

Figure 2-1- Forensic investigation flow chart (Brando, 2012)

Structural failures vary in size and complexity and similarly the subsequent investigations; however the basic steps are often the same and can be modulated to the specific condition a hand. The investigative plan is continuously revised to account or new information and evolving theories (Ratay, 2010).

2.1 DATA COLLECTION AND FILTRATION

Forensic engineers typically rely on site observations, document reviews and structural analyses to develop their expert opinions in the course of their investigations into catastrophic events. For some projects, the amount of documentation and the complex analytical behavior of the structure can make pinpointing the key factors in the forensic investigation quite difficult. The data collected to perform a structural forensic investigation include usually design and shop drawings of the structure, specifications from repair products, a lengthy inspection and maintenance history of the structure, photos and videos before and after collapse, written reports and analyses by consulting engineers tasked with studying and maintaining the structure prior to its collapse, witness testimonials of the collapse event itself and material evidence from the collapse site, among other items. The spectrum of these items presented what may seem to be a daunting task to the investigative team of filtering through the vast amount of documents in order to begin and effectively

analyze the structure. As is common in forensic investigations, the engineers work closely and in parallel to the consortium lawyers in order to facilitate the data collection process, as well as to advice on technical engineering matters. From a very early point, the first understandable difficulty is expressing both 3-D spatial geometry and mechanical concepts to the clients. In order to surmount these early obstacles, it is useful to create a 3-D model of the structure which instantly allowed the client to better understand the structure spatially as it was designed and built. Moreover, the use of forensic database for all collected data pertaining to the project is a handy filtration tool for the engineer throughout their analytical modeling process (Brando et al. 2012).

2.2 ITERATIVE ANALYSIS AND RESULTS

Most failure analysis requires accurate modeling of structural behavior than design analysis. Nonlinear effects and post-damage capacities need to be accurately evaluated. However caution is needed since the analysis carried out using computer can lead to wrong answers if they are not monitored and defined properly. It is critical to understand the default assumptions and underlying analysis techniques used in each finite element program to gauge their effect on the results. It is critically important that all models, hand or computer, accurately reflect the observed behavior of the structure (Ratay, 2010).

For these reasons, forensic database can be an instrumental tool in guiding the numerical modeling process and enabling the investigation team to focus the analyses on specific components of the structure with the aim of discovering patterns in the inspection information revealing possible trends which could lead and help to narrow down the possible causes of a collapse. A combination of priori and posteriori knowledge is the key to trace the collapse progression.

The analysis results and the complexity of the mechanical sequence of the catastrophic collapse still ultimately need to be translated into a universal language that conveys to a non-technical audience, the community-at-large.

Frequently in the course of a forensic investigation, product or procedural deficiencies are uncovered that extend beyond the specific case. One of the more rewarding aspects of forensic engineering practice is the opportunity to make recommendations on the basis of such an investigation. Forensic engineers have a role in disseminating information to design professionals to improve procedures and products so that failures or accidents are not repeated (Carper, 2001).

3 THE I-35W BRIDGE FORENSIC INVESTIGATION

The catastrophic collapse of the I-35W Bridge was one such event that deeply affected the entire nation by its gravity and required immediate action by federal, state and local governmental agencies in order to determine the causes, evaluate the extent of damage of remaining elements, and, if necessary, prescribe prompt preventative measures to other bridges across the country.

Immediately after the collapse of the I-35W rescue operations started and the US National Transportation Safety Board's (NTSB) took ownership of the site. They coordinated the recovery efforts and headed the official investigations. The salvaged members and sections of the Bridge were stored and organized by the US NTSB and the State of Minnesota.

Calculations performed subsequent to the collapse showed that the gusset plates at U10 and the corroded gusset plate at L11 in particular were under-designed by half. Investigations into the cause of the collapse performed by the US NTSB and others have focused primarily on the under-design of the U10 gusset plate and the effect of the dead and live loading on that connection on August 1st. The compressive load at the connection to U10 gusset plate of the L9-U10 member in particular was the focus of the NTSB investigation which concluded in their final report:

"The initiating event in the collapse of the I-35W Bridge was a lateral shifting instability of the upper end of the L9/U10W diagonal member and the subsequent failure of the U10 node gusset plates on the center portion of the deck truss".

At the same time, Thornton Tomasetti (TT) was engaged to independently investigate the cause of the I-35W collapse by Robins, Kaplan, Miller & Ciresi, L.L.P., a national law firm with offices in Minneapolis, MN, recruited and oversaw a consortium of 17 law firms that agreed to provide pro bono legal services to the survivors of the collapse. Since the limited physical access to the bridge's failed structural components, TT had to rely heavily on disclosed materials in order to begin the structural analysis process The data collected and reviewed in this investigation ultimately exceeded 50,000 documents, which included design and shop drawings of the structure, specifications from repair products, a lengthy inspection and maintenance history of the bridge, photos and videos before and after collapse, written reports and analyses by consulting engineers tasked with studying and maintaining the bridge prior to its collapse, witness testimonials of the collapse event itself and material evidence from the collapse site, among other items. Using a comprehensive new method of organizing and presenting findings, the Forensic Information Modeling (FIM), TT discovered patterns in the inspection information revealing a relationship between

expansion joints and notes on corrosion. FIM was an instrumental tool in guiding the numerical modeling process and enabling the team to focus the analyses on a specific component of the bridge, ultimately allowing TT to identify the origin of the bridge failure. In particular the attention focused on the roller bearings and the effect of their behavior on the structural system. More data from the FIM model, including design drawings, inspection reports and pre- and post-collapse photos, were used to calculate the in-situ capacity of the bearings by hand and verify that they were seized at the time of collapse. The frozen bearings informed the subsequent buckling capacity analysis of a bottom chord member in the bridge.

The focus of this latter investigation became the untested fragility of the bridge: its capacity to carry temperature loads. Over the years, bridge inspectors had catalogued the deterioration of the roller bearings. However, no analysis had been performed during past retrofits design to ascertain if the bridge could withstand the large temperature swings common in Minneapolis. The combination of the increased weight of the bridge due to the retrofits, the construction vehicles and material stationed on the bridge and the temperature load effect proved to be catastrophic for the lower chord member that spanned from L9-L11. Buckling of the bottom chord was the fuse that triggered the instability of the global system and initiated the collapse. A nonlinear bridge model was developed in LS-DYNA created by TT and enriched with the local element analyses presented in this Thesis. A combination of priori and posteriori knowledge was acting as a powerful tool to drive the analysis past the bifurcation points in the dynamic collapse simulation. The simulation confirms that the evidence does not support the NTSB conclusion that a lateral instability at the under-designed U10 gusset was the fuse that resulted in the collapse. Instead, the model confirms that collapse initiated by the buckling of the bottom chord best matches the bridge collapse video and local failure behaviors. The FIM was ultimately indispensable in order to achieve and communicate such a comprehensive understanding of the physical phenomena to the court and the society at large.

3.1 SAFETY RECOMMENDATIONS RESULTS OF I-35W ACCIDENT INVESTIGATION

On January 11, 2008, as results of this accident investigation, the FHWA provided an interim report on the adequacy of the gusset plates. Based on the findings in that interim report and the Safety Board's examination of the failed structure - and in the interest of possibly preventing similar catastrophic failures even while the investigation of this accident was underway—the Safety Board, on January 15, 2008, issued the following safety recommendation (H-08-01) to the FHWA:

"*For all non-load-path redundant steel truss bridges within the National Bridge Inventory, require that bridge owners conduct load capacity calculations to verify that the stress levels in all structural elements, including gusset plates, remain within applicable requirements whenever planned modifications or operational changes may significantly increase stresses".*

In coordination with the issuance of Safety Recommendation H-08-1, the FHWA issued:

- Technical Advisory T 5140.29, "*Load-carrying Capacity Considerations of Gusset Plates in Non-load-path-redundant Steel Truss Bridges*", on January 15, 2008.
- The FHWA Gusset Plate Evaluation Guidance – Part A and Part B with Illustrated Examples "*Load Rating Guidance and Example for Bolted and Riveted Gusset plates in truss bridges*" published on February, 2009 to provide guidelines to bridge owners in meeting the requirements of the FHWA Technical Advisory T 5140.29.

The technical advisory referenced Safety Recommendation H-08-1 and recommended that bridge owners take the following actions to supplement the guidance in the AASHTO Manual for Condition Evaluation of Bridges (NTSB, 2008b):

> • **New or replaced non-load-path-redundant steel truss bridges.** Bridge owners are strongly encouraged to check the capacity of gusset plates as part of the initial load ratings.
>
> • **Future recalculations of load capacity on existing non-load-path redundant steel truss bridges.** Bridge owners are strongly encouraged to check the capacity of gusset plates as part of the load rating calculations conducted to reflect changes in condition or dead load, to make permit or posting decisions, or to account for structural modifications or other alterations that result in significant changes in stress levels.
>
> • **Previous load ratings for non-load-path-redundant steel truss bridges**. Bridge owners are recommended to review past load rating calculations of bridges which have been subjected to significant changes in stress levels, either temporary or permanent, to ensure that the capacities of gusset plates were adequately considered.

PART II

STRUCTURAL COMPLEXITY, SAFETY AND INTEGRITY

4. STRUCTURAL SYSTEM COMPLEXITY
5. STRUCTURAL SAFETY
6. STRUCTURAL INTEGRITY
7. STRUCTURAL STABILITY

4 STRUCTURAL SYSTEM COMPLEXITY

4.1 DEFINITION OF STRUCTURAL SYSTEM

In Structural Engineering the idea of a system is represented by a structure. Adopting a broad definition, a structure can be defined as a physical entity treated as a unit, consisting of a comprehensive set of distinct elements positioned in space such that the character of the whole prevails on the interrelationships between the parties. The main purpose of a structure is to carry and transfer a certain set of load to the ground.

A simple example of structure is shown in Figure 4-1. Two separated elements, a circular plate and a tube, become a structure when they are connected in at least one point and their new state, as a unit, is able to channel weight to the ground and bear a defined set of loads.

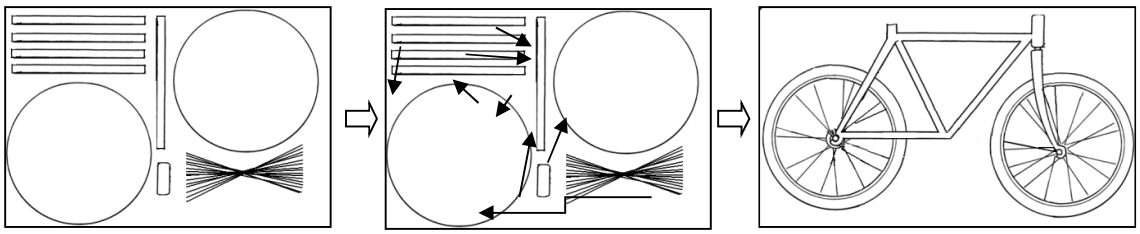

Figure 4-1 - Structure Composition

The structure has only one way of being interpreted due to the specific position and connection between its components. The global result of the structure is not possible if the comprising elements are not connected or positioned in a certain way so that the configuration functions as a whole unit and only secondarily as an array of discrete elements. All the elements in the configuration are necessary to "build up" that particular structure - concept of Synergy (Mella, 2007).

In general a structure has its own characteristic and state depending on its constitutive elements, characteristics and state notwithstanding that it does not identify with any of its elements. The state of each element is dependent on the state of at least another element and conditional on the state of the structure in its entirety. If the structure assumes or changes its state, then some elements must assume or change their state in response. The basic elements in the structure have a different role depending on their position in the structure and its own characteristics are stressed in a different way according to the overall structure aim. In general, there are different criteria to identify different functional levels and components of a structure. These criteria are:

- Functional, according to what the System Elements "do".

- Geographic/Architectural, according to where the System Elements "are".

It is possible to use either or both the criteria (i.e. Functional within the Geographic, or vice versa).

4.2 ASPECTS OF COMPLEXITY

A structure is essentially made up of only a small number of different types of elements. With basic structural elements it is possible to construct structural systems that can be very complex.

When studying a structure, it is important to consider and define the environment it built in. In general, the environment is the set of elements that, although not taking part in the system, they can lead to changes in the system's state. Moreover, it is important to understand what kind of relation exists among them and how they are defined. We can consider three types of relations (Bontempi et Al., 2010):

- *System interactions*: between the structure and the environment. These types of interactions refer to the behaviors and meaning that the system can have with and into the environment without losing its entirety.
- *Organizational relations*: between the structure and its components. These types of interactions define:
    - Function: the meaning of the reactions between the elements and the unity.
    - Functionality: the meaning of the interactions between the elements
    - Typology: the classification according to the time and space position of the elements in the structure.
- *Structural relations*: between the structure's components. These types of interactions define:
    - Specificity: shape, quantity and quality of the objects that compose the structure, its order and admissible deflection.
    - Connection: links, mechanisms and forces between the elements that are necessary to combine execute the structure.

In order to single out a system, one may proceed by:

- *Decomposition or analysis*: observing the whole object, identifying the elements that it is comprised of, the structural connections and the organization that gives the elements a function, functionality and topology in the structure (Top Down) (Figure 4-2).

- *Composition or synthesis*: observing the distinct elements, identify the interactions and the structural connections comprising the structure to study its entirety (Bottom Up) (Figure 4-2).

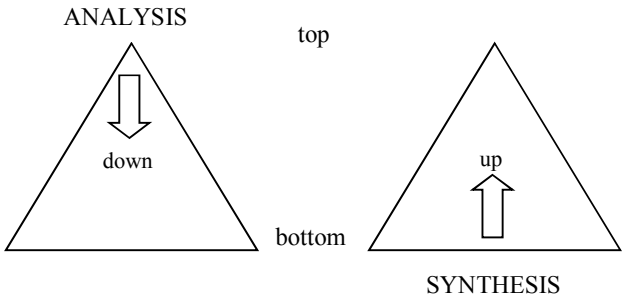

Figure 4-2 - Top-down and Bottom-up scheme

In particular:

- A **top-down** approach. Essentially breaking down a structure to gain insight into its compositional sub-systems. In a top-down approach an overview of the structure is first formulated, specifying, but not detailing any first-level subsystems. Each subsystem is then refined in yet greater detail, sometimes in many additional subsystem levels, until the entire specification is reduced to base elements. A top-down model is often specified with the assistance of "black boxes" that make it easier to manipulate. However, black boxes may fail to clarify elementary mechanisms or be detailed enough to realistically validate the model.

- A **bottom-up** approach. Piecing together structures to give rise to grander structures, thus making the original system's sub-systems of the emergent system. In a bottom-up approach the individual base elements of the structure are first specified in great detail. These elements are then linked together to form larger substructure, which then in turn are linked, sometimes in many levels, until a complete top-level system is formed. This strategy often resembles a "seed" model, whereby the beginnings are small but eventually grow in complexity and completeness. However, "organic strategies" may result in a tangle of elements and subsystems, developed in isolation and subject to local optimization as opposed to meeting a global purpose. The bottom-up approach is used when a system design has been decided already. Each component in the system on the lowest level is studied one-by one. Evaluates risks that the component incorrectly implements its functional specification.

From a general point of view the structural *complexity* increases with the number of elements, multiplicity of interactions and states that the structure can assume. It can be

described as an ideal space with the following dimensions as shown in Figure 4-3 (Bontempi, 2006):

- Behavior (Linear/Nonlinear);
- Ambiguity in the data or Uncertainty of the knowledge (Low/High);
- Coupling, Interactions and Connections among different parts of the problem (Tight/Loose).

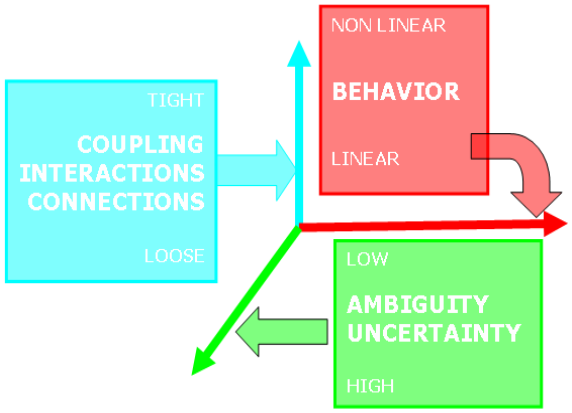

Figure 4-3 - Dimensions of complexity for a structural problem (Bontempi, 2006)

4.3 STRUCTURAL DECOMPOSITION METHOD

Most of the complex structures can be partitioned with a hierarchal configuration. This feature allows the choice of the particular level that is more relevant for analysis in any particular case.

In order to analyze a complex structure, it is useful to perform a *structural decomposition*. Using this technique a complex structure is deconstructed, in a targeted way, into independently basic substructures. This procedure, which is framed in the sub structuring methods, can be used for model updating and damage detection. In general, structural partitioning corresponds to the division of the complete structure into a number of substructures, identifying any variables and boundaries (Figure 4-4).

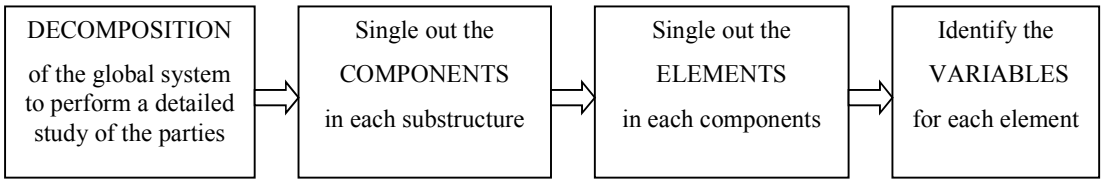

Figure 4-4 - Problem Decomposition Procedure

The structural parts can be categorized into three levels (Bontempi, 2006):

- *Macro-Level*: related to geometric dimensions comparable with the whole construction or with general role in the structural behavior. For instance, referring to a bridge there are essentially three systems:
    - principal, connected with the main resistant mechanism;
    - secondary, connected with the structural part loaded directly by highway and railway traffic;
    - auxiliary, related to specific operations that the bridge can normally or exceptionally face during its design life: serviceability, maintainability and emergency;
- *Meso-Level*: related to geometric dimensions still relevant if compared to the whole construction, but identifiable by their specialized roles in the structural system; the parts identified in this way are known as structures or substructures;
- *Micro-Level*: related to smaller geometric dimensions and specialized structural roles; these are components or elements.

The subdivision has the following manifold meaning:

- the organization of the structure is first of all connected with the load paths that must be developed by the structure itself;
- parts belonging to different levels of this organization require different reliability properties. With regards to structural failure conditions, this decomposition allows single critical mechanisms to be ranked in order of risk and consequences of the failure mechanism (so-called crisis canalization);
- there are strong relationships between life cycle and maintenance of the different parts. Referring to structural function, required safety levels and their reparability, structures and sub-structures are distinguished in primary components (critical, non-repairable or which require the bridge to be placed out of service for a consistent period in order to allow for repairs), and secondary components (repairable with minor restrictions on the operation of the bridge).

Figure 4-5 visualizes the system breaking down concept and Figure 4-6 shows an example. In general, the system is a composite of subsystems whose functions are integrated to achieve a mission / function (includes materials, tools, personnel, facilities, software, equipment); a subsystem is a composite of assemblies whose functions are integrated to achieve a specific activity necessary for achieving a mission; an assembly is a composite of subassemblies; a subassembly is a composite of components; a component is a composite of piece parts which is the least fabricated item, not further reducible. The system doesn't exist without interfaces: the interaction point(s) necessary to produce the desired /essential effects

between system elements (interfaces transfer energy / information, maintain mechanical integrity).

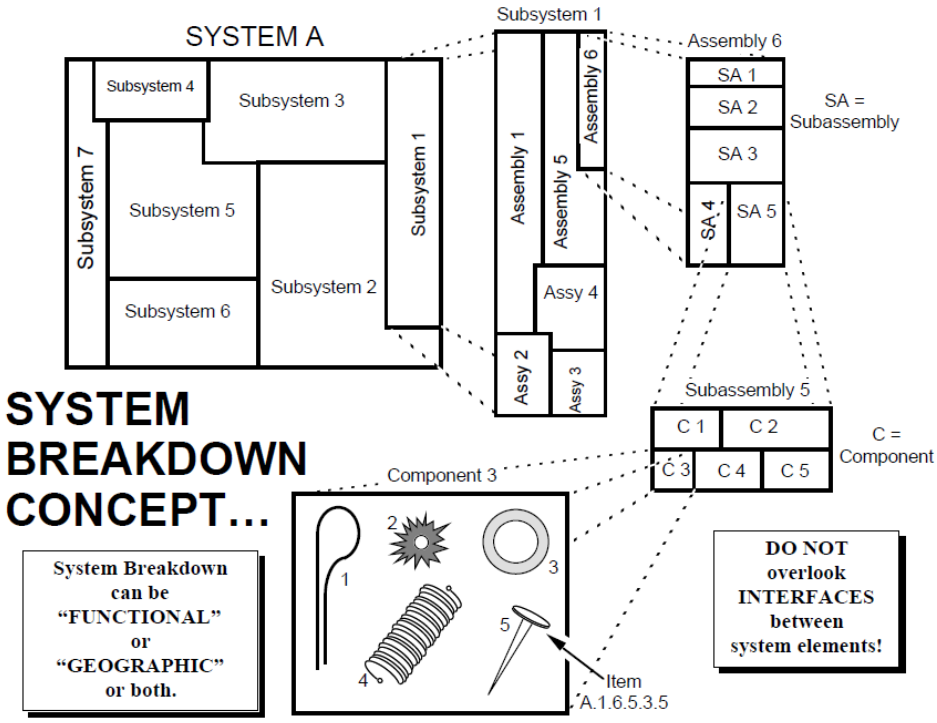

Figure 4-5 - System breakdown concept (Mohr, 1994)

SYSTEM BREAKDOWN EXAMPLE

System	Subsystem	Assembly	Subassembly
AUTOMOBILE	Cooling	radiator water pump coolant hoses/clamps engine block thermostat	
	Propulsion	fuel	storage delivery carburetor
		air	carburetor
		spark/ignition	battery generator plugs coil distributor
		engine	heads block pistons valves
		transmission	*(more…)*
	Braking	standard emergency	*(more…)* *(more…)*
	Chassis/Body	engine comp. passenger comp. storage comp. front bumper rear bumper fenders gages & indicators	
	Steering	*(more…)*	
	Electrical	*(more…)*	
	Suspension	*(more…)*	
	Operator	*(more…)*	

Some breakdowns combine Functional and Geographic approaches. This can help to ensure thoroughness.

Figure 4-6 - System breakdown example (Mohr, 1994)

4.4 PROBLEM DECOMPOSITION EXAMPLES

The multilevel approach has already been used to perform structural analysis in order to assess steel structure robustness and progressive collapse potential. It is suitable to mention the WTC tower investigation performed by the NIST.

After the terroristic attack on the World Trade Center on September 11, 2001, the Federal Emergency Management Agency (FEMA) and the American Society of Civil Engineers began planning a building performance study of the disaster. The goals of the investigation of the WTC disaster where to investigate the building construction, the material used, and the technical conditions that contributed to the outcome of the WTC disaster; to serve as basis for:

- Improvements in the way buildings are designed, constructed, maintained, and used;
- Improve tools and guidance for industry and safety officials;
- Recommends revision to current codes, standards, and practices;
- Improvements to public safety.

The unprecedented complexity and sophistication of these analyses required the use of various strategies for managing the computational demands while adequately capturing the essential physics. The overall approach combined mathematical modeling, statistical and probability-based analysis, laboratory testing, and analysis of photographic and video records.

The interdependence of the analysis of significant events is illustrated in Figure 4-7.

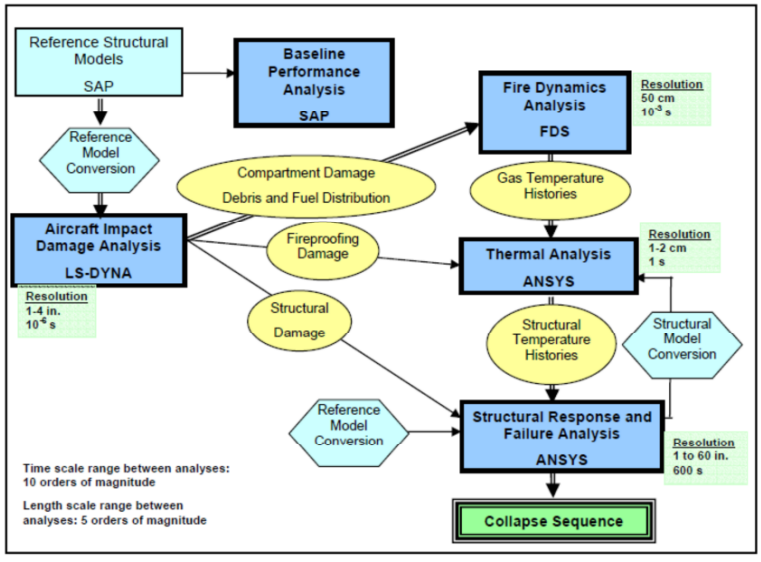

Figure 4-7 - Critical Analysis inter-dependencies (NIST NCSTAR 1-6 Draft, Executive summary)

The analysis approach used was a variant of the well-established sub structuring approach, adapted for the analysis of structure with highly non-linear behavior that progressed from individual components to major subsystems to global systems as shown in Figure 4-8.

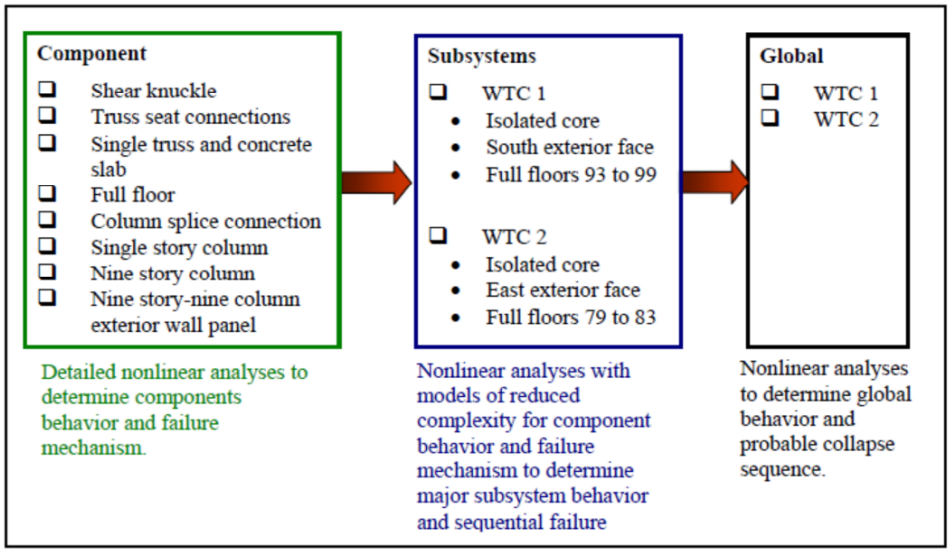

Figure 4-8- Structural Analysis Sequence (NIST NCSTAR 1-6 Draft, Executive summary)

The component analyses were conducted to identify critical behavior and failure mechanisms that contributed to the global structural response of each tower. The subsystem analyses incorporated the behavior and failure mechanisms identified in the component studies, with modifications to reduce the model size and complexity, thereby enhancing computational performance, without adversely affecting the quality of the results. Whenever modeling modifications were used, they were validated against the detailed component model results. The global analyses incorporated critical behavior and failure mechanisms, determined from subsystem analyses, while making necessary modifications in the level of modeling detail. (NIST NCSTAR 1-6 Draft, Executive summary)

Reference structural models were first developed and used to determine the baseline performance of each tower prior September 11, 2001. The results provided initial conditions for the related models. In Figure 4-9 a) the exterior wall subsystem and floor subsystem models (Figure 4-9) are shown.

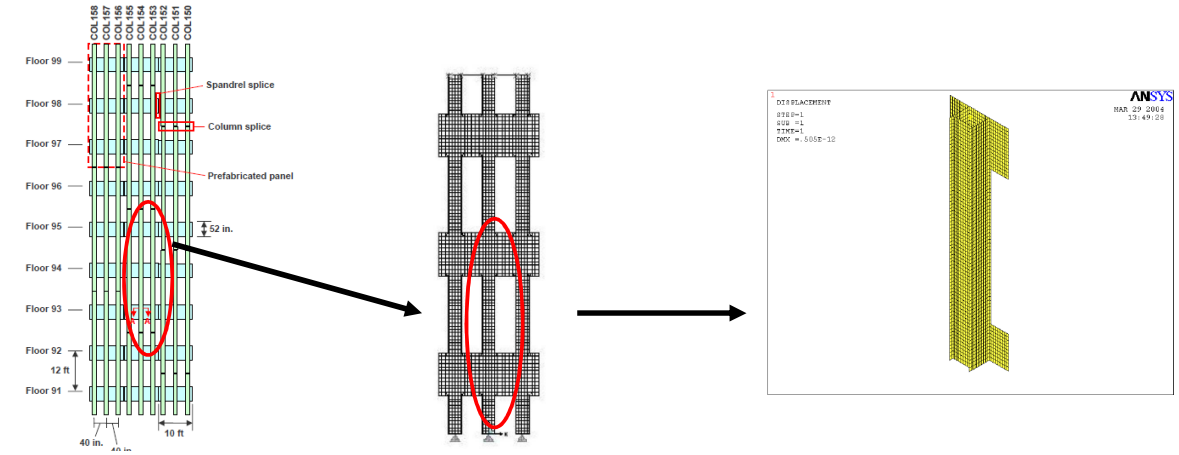

a)

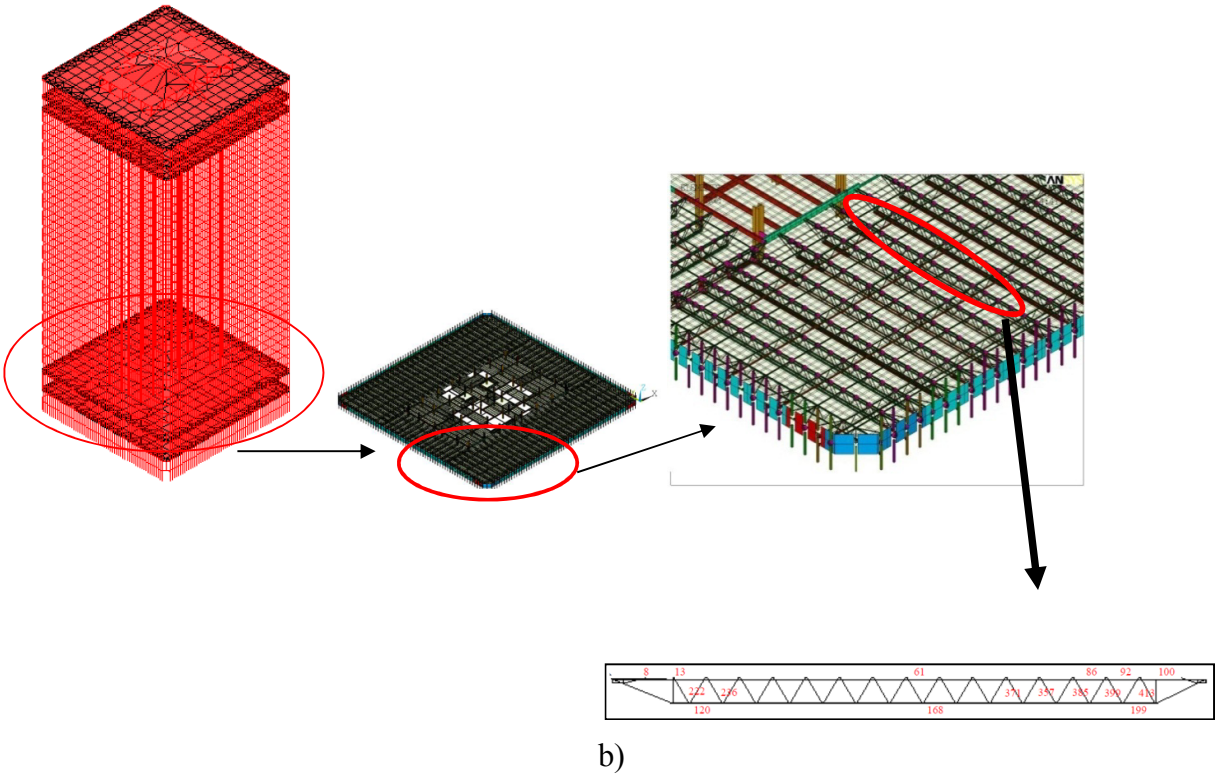

b)

Figure 4-9 - a) Exterior wall subsystem b) Floor Subsystem (NIST NCSTAR 1-6 Draft, Executive summary)

5 STRUCTURAL SAFETY

5.1 DEFINITION OF SAFETY

Every engineered system is the expression of the society needs and it should perform and have adequate margins of safety according to basic and essential requirements defined by Structural Codes and Standards in order to be used by the whole community.

Any typology of structure is designed for a specific and predefined set and magnitude of loads according to its destination. At the same time it deals with intrinsic levels of risk and uncertainties which could undermine its safety, the "critical event" mentioned in SIA260; according to the Swiss building code "*a structure can be declared safe if during a critical event, such as impact, fire, downfall, safety of people is assured"*.

Boundaries need to be drawn in order to ensure safety. The "limits states", are specific circumstances which trace the safe versus unsafe conditions for the structural system and they can be depicted from the definition of safety given by the International Standard (ISO 2394) which deems safety looking at the structural system itself:

> *"Structures and structural elements should be designed, built and maintained in such a way as to serve properly and economically their intended use during their design life. Particularly they should satisfy, with proper levels of reliability: Serviceability state requirements, Ultimate load state requirements, and Structural integrity requirements"*.

"Limit states" beyond which the structure is considered unsafe take into account as accurately as possible the indeterminate nature of the hazards, ensuring an appropriate level of reliability for each limit state, always considering attributes and variability in the quality of construction as well as the consistency of the construction materials which all together contribute and enforce the designed life of the structure hence its durability.

The aim of Structural Codes and Standards is to define principles, methods and rules to design structures complying with safety, reliability and durability being aware of the different level of complexity. The complexity of the design is at different levels: the load description and definition, the choice of the limit states applicable, the structural system complexity. The latter is discussed more extensively in Chapter 4.

5.1.1 Limit State Design

In order to pursue the design aims fulfilling the safety requirements, different approaches can be used. The Limit State Design (LSD) is the most used in nowadays Structural Codes and Standards. The LSD method uses the applicable capacity or strength of a structure

calculated under various conditions ("limit states" or "requirement" as defined in ISO2394) under which the structure may cease to fulfill its designed function and it uses the so calculated strength as limit for the design. The capacity or strength is estimated using simplified design formulations or using refined computations such as non liner elasto-plastic large deformation finite element analysis (Paik, 2003). Table 5.1-1 summarizes briefly the different Limit States which can be considered:

Limit State	**Object**	**Description**	
Ultimate (ULS) • Stability • Strength	Safety of people and the structure.	States beyond which there is loss of capacity and strength of the element or the structure expected to result from foreseeable actions, threatening safety of human life in and around the structure.	Loss of capacity and strength related to: • Loss of equilibrium of a part or the whole structure considered as a rigid body (e.g. overturning, uplift, sliding); • Loss of load bearing capacity of members due to exceeding the material strength (yielding, rupture, fracture, fatigue); • Very large deformation transformation into a mechanism overall instability (e.g. wind flutter ponding instability) [Ellingwood – A58].
Serviceability (SLS) • Stiffness • Maintainability • Availability	Structure under normal use, the comfort of people, and the appearance of the construction works.	States beyond which the function of the structure no longer fulfills their normal operation purposes under expected responses to foreseeable actions.	Loss of stiffness related to: • Excessive deflection or rotation affecting the appearance functional use or drainage of the building or causing damage to non-structural components and their attachment; • Excessive local damage (cracking or splitting, spalling, local yielding or slip) affecting appearance use or durability of the structure; • Excessive vibration affecting the scope of use of the structure.
Integrity (ILS) • Robustness	Structure under normal use and accidental event.	States beyond which the structure suffers of critical event.	• Collision, Impact; • Explosion, Fire; • Human error; • Structural damage or failure; • Spread of initial local failure into widespread collapse (progressive collapse or lack of structural robustness).

Table 5.1-1 - Limit states object and description

The aim of the limit state design methods is to determine the level of imposed loads which causes structural failure of individual members and overall structure.
The limit states can be checked at any level therefore is essential to understand the system and to be able to decompose it in a structured and focused way (Bontempi, 2006).

In Figure 5-1 the different level of failures are shown for a steel truss bridge:

1st level: Material point
2nd level: Element section
3rd level: Structural element
} Limit State Verification format
4th level: Structural system → Structural Robustness Assessment

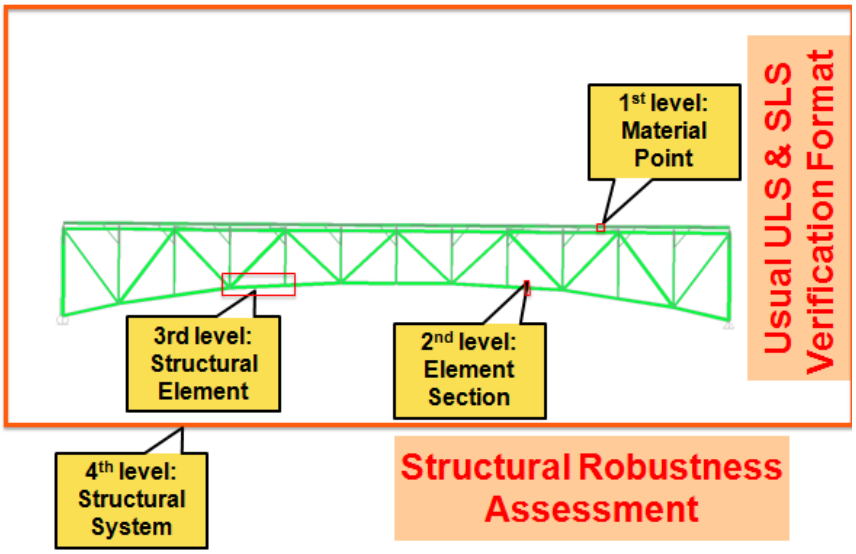

Figure 5-1 - Levels of verification (Bontempi, 2006)

It is extremely important to understand what types of structural failure could occur. For steel members the most important are:

- Large local plasticity;
- Instability;
- Fatigue crackling related to cycling loading;
- Ductile or brittle fracture, given fatigue cracking or preexisting defects;
- Excessive deformation.

The basic failure types do not occur simultaneously but more than one phenomenon may in principle be involved until the structure reached the ultimate limit state.

As the external loads increase, the most highly stressed region inside the structural member will yield resulting in local plastic deformation, and this decreases the member stiffness. With further increase in the loads, local plastic deformation will grow larger and/or occur at several different regions. The stiffness of the member with large local plastic region becomes quite small and the displacements increase rapidly, eventually becoming so large that the member is considered to have failed. Instability can occur in any structural member

which is predominantly subjected to loads that results in compressive effects in the structure (Paik, 2003).

5.1.2 U.S. Design codes methods

In the U.S. design codes and standards are issued by diverse organizations, some of which have adopted Limit States Design. The American Concrete Institute (ACI) Building Code Requirements for Structural Concrete (ACI 318) uses Limit State Design. The ANSI/AISC 360 Specification for Structural Steel Buildings, the ANSI/AISI S-100 North American Specification for the Design of Cold Formed Steel Structural Members, and The Aluminum Association's Aluminum Design Manual contain two methods of design side by side:

- Load and Resistance Factor Design (LRFD), a Limit States Design implementation;
- Allowable Strength Design (ASD), a method where the nominal strength is divided by a safety factor to determine the allowable strength. The design allowable strength is required to equal or exceed the effects of the factored loads for a set of ASD load combinations. ASD is calibrated to give the same structural reliability and component size as the LRFD method with a live to dead load ratio of 3 . Consequently, when structures have a live to dead load ratio that differs from 3, ASD produces designs that are either less reliable or less efficient as compared to designs resulting from the more rational LSD method.

5.2 U.S. BRIDGE SAFETY CLASSIFICATIONS

Safety and maintenance regulations applicable to all bridges over 20-feet (6 m) in length, located on publicly-owned highways and roads everywhere in the United States are formulated and enforced by the Federal Highway Administration (FHWA), through its Office of Bridge Technology. The bridge sufficiency rating is calculated per a formula defined in FHWA's Recording and Coding Guide for the Structure Inventory and Appraisal of the Nation's Bridges. This rating is indicative of a bridge's sufficiency to remain in service. A bridge sufficiency rating includes a multitude of factors: inspection results of the structural condition of the bridge, traffic volumes, number of lanes, road widths, clearances, and importance for national security and public use, to name just a few.

The FHWA defines structurally deficient bridges as those that "have been restricted to light vehicles, require immediate rehabilitation to remain open, or are closed." This classification should not be confused with "functionally obsolete," which are bridges whose capacities no longer support the roads they serve due to factors like inadequate lane width or load height clearance. Structurally deficient bridges are those considered the most likely to suffer

structural failure. Most structurally deficient bridges are left open to traffic while they undergo maintenance and repair.

Bridges are considered structurally deficient if significant load carrying elements are found to be in poor condition due to deterioration or the adequacy of the waterway opening provided by the bridge is determined to be extremely insufficient to point of causing intolerable traffic interruptions.

According to the American Association of State Highway and Transportation Officials (AASHTO) definition, a fracture critical bridge is a steel structure that is designed with little or no load path redundancy. Load path redundancy is a characteristic of the design that allows the bridge to redistribute load to other structural members on the bridge if any one member loses capacity. This designation is a function of the design of the bridge and not the condition. In fact, a brand new bridge can be fracture critical. If any of the fracture critical members, (steel tension member per AASHTO definition) fail, the bridge could be in danger of partial or total collapse. This does not mean the bridge is inherently unsafe, only that there is a lack of redundancy in its design.

The National Bridge Inspection Standards (NBIS) require that a fracture critical inspection be performed at least once every 24 months on bridge members identified as fracture critical. The Silver Bridge collapse in 1967, which spawned the NBIS, was due to the failure if a fracture critical member. The Mianus River Bridge collapse in Connecticut in 1983, which influenced the 1988 revisions to the NBIS, was also due to the failure of a fracture critical member. The consequences of these major bridge failures have been severe. They have included: loss of life; financial loss due to litigation; loss of capital investment in the bridge itself; economic loss to nearby businesses or industries that rely on the bridge for public transportation; loss of public confidence in bridge inspection programs and their ability to foresee or forestall such catastrophes (WSDOT, 2006).
The criteria for performing a refined analysis to demonstrate that part of the structure is not fracture critical have not been yet fully codified. Therefore, the loading cases to be studied, location of potential damage, degree to which the dynamic effects associated with fracture are included in the analysis, and finesses of models and choice of element type should be all agreed on by the owner and the engineer. Relief from the full factored loads associated with the conventional design-load combinations should be considered, as should the number of loaded design lanes versus the number of striped traffic lanes. While difficult to quantify, the use of high-performance steel and the associated welding techniques can add further robustness to truss bridges.

Fracture critical members can be found in steel truss systems. In general, most truss bridges employ only two trusses and are thus considered fracture critical. For inspectors, all truss

members in tension should be regarded as fracture critical members. The exception is, when a detailed analysis by an experienced structural engineer, verifies loss of a member would not result in collapse of the bridge or major component. The following elements within any truss bridge should also warrant special attention (WSDOT, 2006):

(1) Pin-connections: Any pin connections on a truss bridge should be considered fracture critical.

(2) Category D and E Welds: On a truss bridge, any tension member containing a Category D or E weld.

5.3 STEEL BRIDGES

Steel bridges are classified according to (ISDGA, 2012):

- the type of traffic carried:
  - Highway or road bridges;
  - Railway or rail bridges;
  - Road and rail bridges.
- the type of main structural system:
  - *Girder bridges:* Flexure or bending between vertical supports is the main structural action in this type. Girder bridges may be either:
    - *plate girder* (less than 50 m);
    - *box girder* (continuous span up to 250 m);
    - *truss bridges* (span range of 30 m to 375 m);
  - *Rigid frame bridges* (span range of 25 m to 200 m);
  - *Arch bridges* (span range of 200 m to 500 m);
  - *Cable stayed bridges* (span range of 150 m to 700 m);
  - *Suspension bridges* (long span bridges).
- the position of the carriage way relative to the main structural system:
  - *Deck Type*: The carriageway rests on the top of the main load carrying members. In the deck type plate girder bridge, the roadway or railway is placed on the top flanges. In the deck type truss girder bridge, the roadway or railway is placed at the top chord level.

- *Through Type Bridge* - The carriageway rests at the bottom level of the main load carrying members. In the through type plate girder bridge, the roadway or railway is placed at the level of bottom flanges. In the through type truss girder bridge, the roadway or railway is placed at the bottom chord level.
- *Semi Through Type Bridge* - The deck lies in between the top and the bottom of the main load carrying members. The bracing of the top flange or top chord under compression is not done and part of the load carrying system project above the floor level. The lateral restraint in the system is obtained usually by the U-frame action of the verticals and cross beam acting together.

5.3.1 Steel Truss Bridges

Truss bridges are one of the oldest types of modern bridges. They are used for their simple design and for the several others advantageous features. These kinds of bridges are still common in the United States.

A truss is composed by triangles which are the strongest and most rigid geometric figure. The typology of trusses depends on the arrangement of the framework of triangles which creates different patterns. The arrangement of the members determines the specific truss type. By arranging the framework of triangles in patterns the structure acquired different appearances and served different purposes. The bearing members are able to resist forces primarily in tension and compression. Large gusset plates and numerous rivets are used to connect the truss members. Figure 5-2 shows the truss structural members

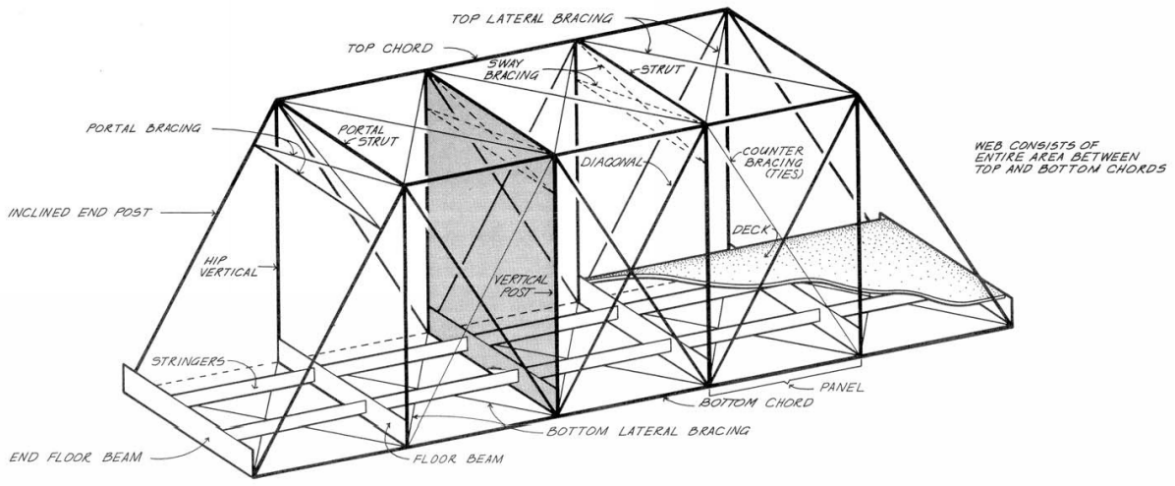

Figure 5-2 - Truss structural members (Jones, 1976)

There are also many “hybrid” trusses that do not fall into easily-defined categories. In such cases identification should be made as closely as possible in the terms of the standard

designs. Additionally, trusses often are inverted, creating outlines quite different from the original – tension members becoming compression members and vice versa.

Most bridges trusses are of three basic types. If the deck and/or rails are at the same level with the bottom chords, it is a through truss. A pony truss is a through truss with no lateral bracing between top chords. A deck truss carried the load level with the top chords. See Figure 5-3.

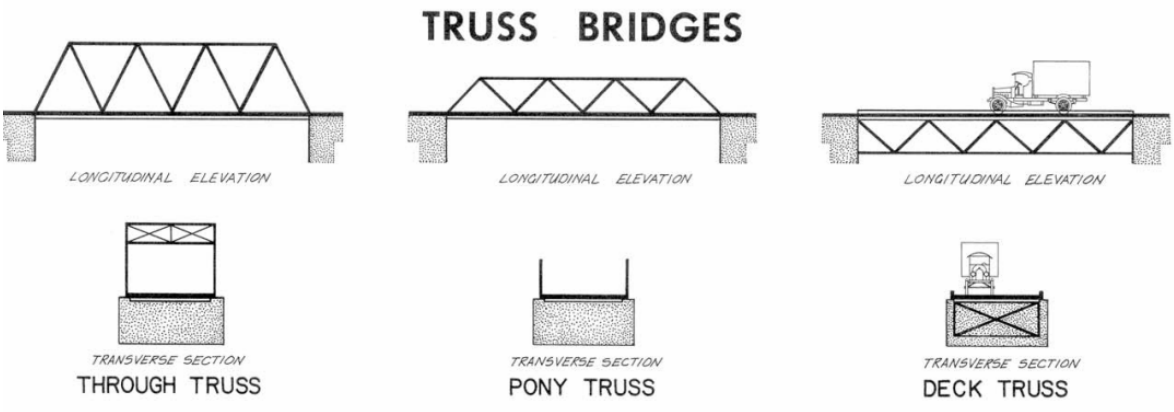

Figure 5-3 - Truss Bridges Identification: Nomenclature (Jones, 1976)

The pony truss, the smallest type and ordinarily confined to lengths under 140 feet (42.5 m), most of which under 100 feet (30 m), is distinguished by its low profile and absence of bracing above the roadway. The through truss by comparison is greater in length and height and consists of a tunnel, like structure that carries traffic through a system of overhead bracing which ties together the upper chords of the bridge. The choice of deck or through construction normally is dictated by the economics of approach construction. Designs created by English engineers Pratt and Warren, after demonstrating their strength and versatility on the railroads, became the preferred choice for building highway bridges. After 1890 almost exclusively fabricated of steel, connected at their joints with either pins or rivets, and became common sights on roads across the country and the epitome of America's dependence on the steel truss bridge. In the Pratt, vertical posts inserted between parallel chords carried compression while diagonal members sustained the stresses produced by loads moving across the bridge. The Warren, whose popularity peaked in the twentieth century, employed a series of triangles in the web to support both compressive and tensile forces, generally but not always constructed with verticals to reduce panel size. When rigid joints are used, such trusses are favored because they provide an efficient web system. Most modern bridges are of some type of warren configuration. The design of truss bridges usually follows the specifications of the America Association of State Highway and

Transportation Officials (AASHTO) or the Manual of the American Railway Engineering and Maintenance of Way Association (AREMA) (King, 1993).

Truss bridges are considered fractural critical structures. This means that there is a lack of redundancy in its design. The main failure modes for a steel truss are listed below (Crosti, 2011):

- Failure of truss connections such as the gusset plates and splices and supports;
- Failure of the truss members: compression members of a truss bridge can fail in overall buckling or in a local buckling mode and members in tension can fail in yielding of the gross area or fracture of the net area;
- Global instability failure of the truss: the compression chord can buckle and even the tension chord can move out of plane when the lateral braces are not stiff enough to provide the instability of the nodes.

6 STRUCTURAL INTEGRITY

6.1 DEFINITION OF STRUCTURAL INTEGRITY

Broadly, the term “integrity” recalls the concepts of wholeness and completeness which ideally are the requirements necessary to achieve the full functionality of any system. Indeed, in real life any structure may be subject to local abnormal loads in addition to conventional design loads, which are not considered to occur in its design life, causing adverse effect at a local level which could compromise the integrity of the whole system and therefore its designed/required functionality leading to a progressive collapse.

In engineering terms structural integrity can be defined as the ability of a structure not to be damaged to an extent disproportionate to the original cause, such as local failure producing a fatal effect on the entire structural system. In recent guidelines this requirement is also referred to as Structural Robustness: the property of the structure to be insensitive to local failure to endure an outstanding action without being damaged in a disproportionate way respect to the triggering cause. Structural integrity can be enhanced substantially improving redundancy and ductility of structures the overall integrity to withstand abnormal or unforeseen loads. This can be done introducing alternate load paths or redundancy within reasonable ranges of cost and time or by enhancing member capacities and ductility. The structural system integrity is sensitive to:

Continuous occurrence:

- *Environmental actions* (Corrosion, Material deterioration, Age)
- *Anthropic actions* (Fatigue, Additional retrofits loading, Increasing Traffic loading)

Discrete events:

- *Human error*
- *Accidental (unintentional) events*
- *Deliberate (intentional) attacks*

In Figure 6-1 the effect of the continuous and discrete events on the structural life path of a structure are represented.

6.1 ROBUSTNESS AND REDUNDANCY

Structural robustness and collapse resistance are research topics particularly relevant both in the design of new structures, and also for the safety assessment of existing structures. The

latter are prone not only to local failure due to accidental or malevolent attacks, but also due to long term material degradation (e.g. corrosion), bad design or construction.

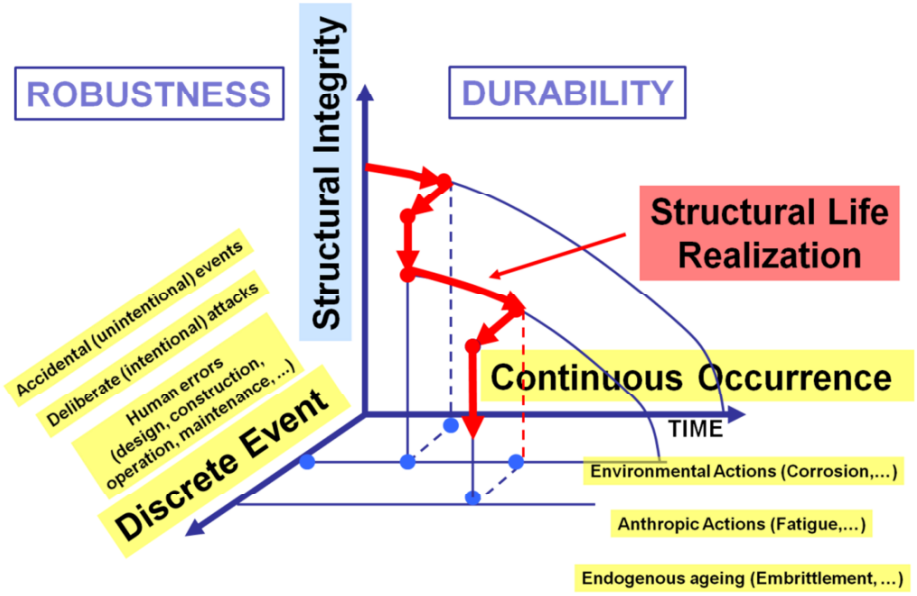

Figure 6-1 - Structural Integrity vs. Discrete event and Continuous occurrence (Crosti, 2011)

Behind this attention, there is the interest from a society that cannot tolerate death and losses as in the past. This is more evident after:

- recent terrorist attacks (a series of terror attacks in America and beyond, the deadliest being the September 11, 2001 attacks in New York at the World Trade Centre);
- recent bridge collapses due to deterioration or bad design or bad construction (for example, the De la Concorde overpass collapse in Montreal, 2006);
- difficult to foresee multiple hazard events from natural sources (wind, earthquake, flooding, wildfire, etc.) and from human sources (terrorism, fire, etc.) that lead to dramatic consequences, the most significant of which is the 2011 earthquake, off the Pacific coast of Tōhoku, that triggered powerful tsunami waves.

Among all other steel structures, many steel truss bridges in their various forms, very common worldwide, are now aged, not often optimally maintained, and need to be checked equally for safety and for serviceability. In this sense, also the optimal cost effective allocation of resources and the prioritization in the retrofitting phase is a very important issue.

Even though a variety of terms have been used in literature, robustness is commonly defined as the "*insensitivity of a structure to initial damage"* and collapse resistance *as the "insensitivity of a structure to abnormal events*" (Starossek and Haberland 2010).

Similarly, ASCE 7-05 (2005), defines "*progressive collapse as the spread of an initial local failure from element to element, eventually resulting in collapse of an entire structure or a disproportionately large part of it"*. Starossek and Haberland (2010) focus on the differences of progressive and disproportionate collapse, concluding that the terms of disproportionate collapse and progressive collapse are often used interchangeably because disproportionate collapse often occurs in a progressive manner and progressive collapse can be disproportionate.

From a historical perspective, progressive collapse came up as the first structural engineering concern, just after the collapse of the Ronan Point Tower, a residential apartment building in Canning Town, London, UK, in May 1968, two months following initial occupancy of the building. Ronan Point was a 22-story building, with precast concrete panel bearing wall construction. An explosion of natural gas from the kitchen of a flat on the 18th floor failed an exterior bearing wall panel, which led to loss of support of floors above and subsequent collapse of floors below due to impact of debris (Ellingwood 2002).

Concerning the above mentioned topics, there has been a lot of research in the recent years. Starossek and Haberland (2010), provide a terminology. A review of international research on structural robustness and disproportionate collapse is provided in Arup (2011). Regarding the quantification of robustness related issues, Canisius et al. (2007) provide an overview of methods. Starossek (2009) covers issues related to progressive collapse. Bontempi et al. (2007), Arangio et al. (2011) and Sgambi et al. (2012) provide a dependability framework, adapted from the electronic engineering field, where dependability attributes are either related to structural safety or serviceability. Focusing on structural safety, the attributes of structural integrity, collapse resistance, damage tolerance and structural robustness are investigated. Strategies and methods for the robustness achievement are discussed in Bontempi and Giuliani (2008), together with the robustness assessment of a very long span suspension bridge.

Even though many robustness research topics focus on explosions and terrorist attacks, as Table 1 suggests, there is a variety of reasons or events that could endanger a structure, eventually leading to a progressive collapse (Starossek and Haberland 2012). Potential failure scenarios specific for bridges are also provided in FHWA (2011), within a framework aiming at the resilience improvement.

The collapse likelihood of a structure is typically characterized in probabilistic terms. When an unexpected or critical event occurs, Ellingwood and Dusenberry (2005) describe, in probabilistic terms, the probability of a collapse in a structure as the product of the probabilities of three sub events:

- The extreme action associated with the event hits the structure;
- The structure is damaged in the area directly affected by the action;
- The local damage causes failures of other structural elements and leads to the collapse of a significant part of the structure.

Faults			Errors
External		Intrinsic	
Man-made (accidental or intentional)	Environmental (natural)		
Impact (car, train, ship, aircraft, and missile) Explosion (gas, explosives) Fire Excessive loading (live load)	Earthquake Extreme wind Heavy snowfall (excessive roof loads) Scour Impact (avalanche, landslide, rock fall, floating debris) Volcano eruption	Lack of strength Cracks Deterioration	Design errors Construction errors Usage errors Lack of maintenance

Table 6.1-1 Abnormal events that could threaten a structure (from Starossek and Haberland 2012)

The assessment of the risk associated with the event (commonly defined as the product of a probability of occurrence and of the corresponding consequence) can be performed using standard risk techniques. Several authors have focused on aspects of risk analysis and assessment in the civil engineering field - see for example Faber and Stewart (2003). Risk related special issues include the risk aversion for low-probability, high-consequence events (Cha and Ellingwood 2012) and the risk consistency in multihazard design for frame structures (Crosti et al. 2011).

Focusing on disproportionate collapse in probabilistic terms, Ellingwood et al. (2007) decompose the probability of disproportionate collapse P[C] as a result of an abnormal event, into three constituents: abnormal event, initial damage, disproportionate failure spreading. This is represented as the product of partial probabilities:

$$P[C] = P[C|D]\ P[D|E]\ P[E] \qquad 1$$

where, P[E] is the probability of occurrence of the abnormal event E that affects the structure; P[D|E] is the conditional probability of the initial damage D, as a consequence of the abnormal event, and P[C|D] is the conditional probability of the disproportionate spreading of structural failure, C, due to the initial damage D. The safety of structures with regards to the single elements contained in the equation, each characterizing the single sub-event mentioned above, is pursued in modern structural codes by the introduction of partial safety factors.

According to this approach, Giuliani (2012) identifies three design strategies for obtaining robustness:

- Prevention or mitigation of the effects of the event (increase collapse safety);
- Prevention or mitigation of the effects of the action (increase structural integrity);
- Prevention or mitigation of the effects of the damage (increase structural robustness).

These strategies are schematically depicted in Figure 6-2.

The assessment of structural robustness is also strongly related to the degradation state of the structures, caused by environmental agents: concrete carbonation, steel reinforcement corrosion, alkali aggregate reaction, freeze-thaw cycles can lead, over time, to an assessment of structural strength that is very different from that provided in the design phase (Biondini and Frangopol 2009). The effect of the above factors could compromise the structural response under a localized event.

Furthermore, different structural systems exhibit different degrees of robustness (Wolff and Starossek 2010), something neglected even in modern design procedures that use partial safety factors. Another issue very important in determining structural robustness for bridges is redundancy. Bridge redundancy, is defined by Ghosn and Moses (1998) as the capability of a bridge to continue to carry loads after incurring damage or the failure of one or more of its members. This capability is due to redistribution of the applied loads in transverse and/or longitudinal directions.

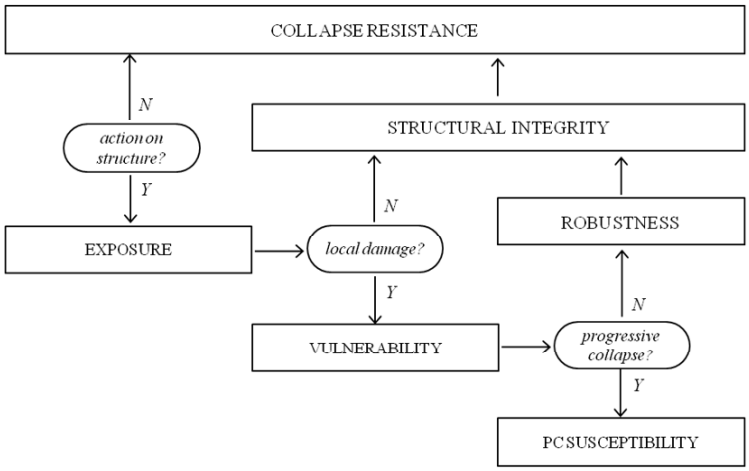

Figure 6-2 - Strategies for safety against extreme events and corresponding requirements (Giuliani, 2012)

Moreover, the inherent uncertainty associated with actions and mechanical, geometric and environmental parameters cannot be ignored since they affect the structural response (Biondini et al. 2004, Ciampoli et al. 2011, Garavaglia et al. 2012, Petrini and Ciampoli 2012).

Steel truss structures and bridges have been the subject of recent research on what concerns their ultimate strength and progressive collapse susceptibility. Choi and Chang (2009), focus on the vertical load bearing capacity of truss structures, using a sensitivity index that accounts for the influence of a lost element to the load bearing capacity. Miyachi et al. (2012) focus on how the live load intensity and distribution affect the ultimate strength and ductility of different steel truss bridges, similar to the one considered in this study. Malla et al. (2011) conduct nonlinear dynamic analysis for the progressive failure assessment of bridge truss members, considering their inelastic post-buckling cyclic behavior. Saydam and Frangopol (2011) use FE skills to investigate the vulnerability, redundancy and robustness of truss bridges, taking into account the stochastic time-dependent deterioration of the structure.

Progressive collapse literature indicates extensive research has been performed for the past few years on steel moment frames possibly owed to the fact that different design guidelines are issued in the US by the General Service Administration (GSA 2003) and the Department of Defense (DoD 2009). Kim and Kim (2009) conduct nonlinear dynamic analysis on benchmark buildings (3, 6 and 15-story) and compare the results with more straightforward linear static step-by-step analysis. Using nonlinear dynamic finite element simulations, Kwasniewski (2010) investigates the collapse resistance of an 8-story steel framed structure, and inquire on the uncertainties affecting the problem. Izzuddin et al. (2008a), provide a framework for progressive collapse assessment of multi-story buildings, considering as a design scenario the sudden loss of a column. Using this framework, the same authors (Izzuddin et al. 2008b) investigate possible scenarios, in the form of the removal of either a peripheral or a corner column, in a typical steel-framed composite building. Yuan and Tan (2011) investigate the progressive collapse of a 9-story building, at a global level, using a numerical spring-mass-damper model. Hoffman and Fahnestock (2011) investigate different column loss scenarios on 3 and 4-story steel buildings, focusing on different aspects of the problem, among else, the load redistribution and the column lost location. Galal and El-Sawy (2010) compare retrofitting strategies for 18-story buildings with different spans using 3D nonlinear dynamic analyses.

An important issue is the model complexity in the progressive collapse assessment. Alashker. et al (2011) deal with approximations in the numerical modeling, using a 10-story steel building as a case study, and compares four models of different levels of complexities (planar and 3D). Their conclusion is that, under restricted conditions, planar models can lead to reasonable results regarding the progressive collapse characterization, however, a full 3D analysis, in spite of its computational cost, may be the only sure way to rigorously investigate this aspect. Rezvani and Asgarian (2012), conduct different non-linear static and

dynamic analyses, among else, on an 8-story building, aiming at the progressive collapse assessment, and compare the results from the different analysis methods.

A relevant issue related to the structural robustness evaluation, is the choice of proper synthetic parameters describing the sensitivity of a damaged structure in suffering a disproportionate collapse. Recently Nafday (2011) discusses the usefulness of consequence event design (as opposed to using a probabilistic approach), for extremely rare, unforeseen, and difficult to characterize statistically events (black swans). In this view, the author, with reference to truss structures, proposes an additional design phase that focuses on the robustness, the damage tolerance and the redundancy of the structure. This proposed metric is based on the evaluation of the determinants of the normalized stiffness matrixes for the undamaged and damaged structure.

Concerning extreme loads on structures, a scientific debate takes place nowadays on the appropriate design methodology to adopt (see for example COST 2011). To this point, the member-based design is not efficient for contrasting extreme loads on structures that in general are unpredictable and not probabilistically characterized (Nafday 2011). Following the approach of HSE (2001) in the case of high uncertainties regarding the extreme loading likelihood, it is necessary to put emphasis on the consequences of the event.

One class of structures that often incorporates elements whose localized failure would precipitate progressive collapse is functionally non redundant bridges. Their intrinsic non-redundancy can make them susceptible to progressive collapse due to the loss of a series of adjacent members in a single loading event. Truss bridges without primary redundancy are particularly sensitive to progressive collapse. They rely exclusively on the redundancy in the secondary structural resistance to provide some measure of robustness. The term structural robustness in this work is intended as the property of the structural system and it refers to the insensitivity to local failure (Starossek, 2006).

Redundancy plays a dominant role in providing robustness and preventing progressive collapse. While it is a strongly desirable feature in structural systems, there is no accepted measure of the degree or distribution of redundancy in a structure. It may be defined in various ways besides the structural mechanics view of the number of resistances indeterminate by statics alone. One definition states that redundancy is “the absence of critical components whose failure would cause collapse of the structure” (Frangopol, 1987). Bridge redundancy is also defined in Gosh, 1998 as “the capability of a bridge to continue to carry loads after incurring damage or the failure of one or more of its members”. This capability is mainly due to redistribution of the applied loads in transverse and/or longitudinal directions.

In general, redundancy can be seen as a property of the undamaged structure and it has a major impact on the risk of collapse. The absence of redundancy in a structure (i.e. statically determinate structure) may more likely lead to progressive collapse in the event of local damage and clearly represents a non robust structure. On the other hand the presence of redundants (i.e. statically indeterminate structure) may or may not prevent progressive collapse depending on the robustness of the design and possibly on the existence of preexisting or hidden damage. Furthermore, even if in the primary action of the structure there is no redundancy, secondary action may introduce redundancy that can hinder progressive collapse and thus provide some measure of robustness.

7 STRUCTURAL STABILITY

7.1 DEFINITION OF STRUCTURAL STABILITY

Stable and unstable are words commonly used by everyone and in every field. Intuitively the term stable pictures something that is positive and rigid whereas unstable is connected to the possibility of a sudden loss of something. They are central concepts when studying the behavior of mechanical systems. In the civil and structural engineering field, these two words are the base of principles and theory for the structural design.

Stability is an important constituent of the ultimate strength limits. Therefore it is extremely important to know under which conditions a structural system can be considered stable or not. Establishing the limits for the stability of a structure allows the engineer to design a structural system that will have adequate margin of safety. A structural failure occurs when the stable limit state has been crossed and thus the system "falls" under an unstable condition.

A structure or a member of it, in an equilibrium state (stable), may become unstable under a given set of load when a small change in load causes a large change in displacement. The structure is not able to acquire a new stable equilibrium state after being disturbed showing therefore "instability". This instability can occur a different level: a local level (localized in a specific portion of a structure's member), at a member level, when the whole member become instable and it may precipitate to global system instability.

The load at which the structure ceases to be stable is usually referred to as "critical load". At the critical load there are infinite numbers of possible deformed position. Once the load is above the critical point the deformed shape of the structure will tend to the next configuration of stability for the system with the lowest energy state. See Figure 7-1.

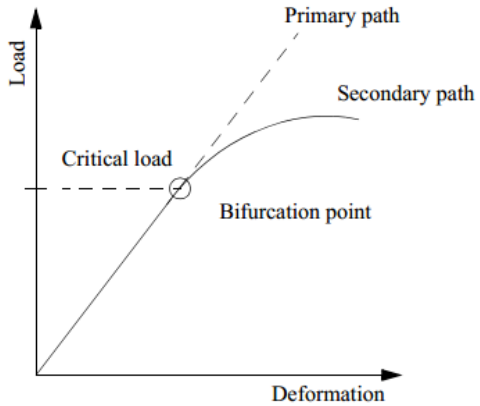

Figure 7-1 - Schematic description of the bifurcation of equilibrium

For initially straight columns the point where instability occurs is called “bifurcation point”. Meaning the point at which the column suddenly goes from unstable to stable position. It only exist for perfect straight column, the strength of such perfect straight column with perfect central loading ad well defined restraints and linear elastic material properties is the Euler load Pe or “buckling” load. The term “buckling” is nowadays used to define instability in the broad sense but it actually refers to a specific case of instability.

When the load applied reached the critical value (Pcr), or so called “buckling load”, the system enters the state of instability, or “buckling”. In general there are two types of buckling: bifurcation (initially straight columns) and limit load (any real structure which suffers of intrinsic imperfection by definition).

In order to predict the load at which the instability occurs, the load-deflection curve must be investigated. The curve can provide the critical load and also describe the equilibrium path. All structures deflect under loading and their behavior can be calculated using different methods as discussed by many authors (Galambos, 1968). The governing equilibrium equations of a structure can be written using different approaches which in turn reflect high order effect as shown in Figure 7-2.

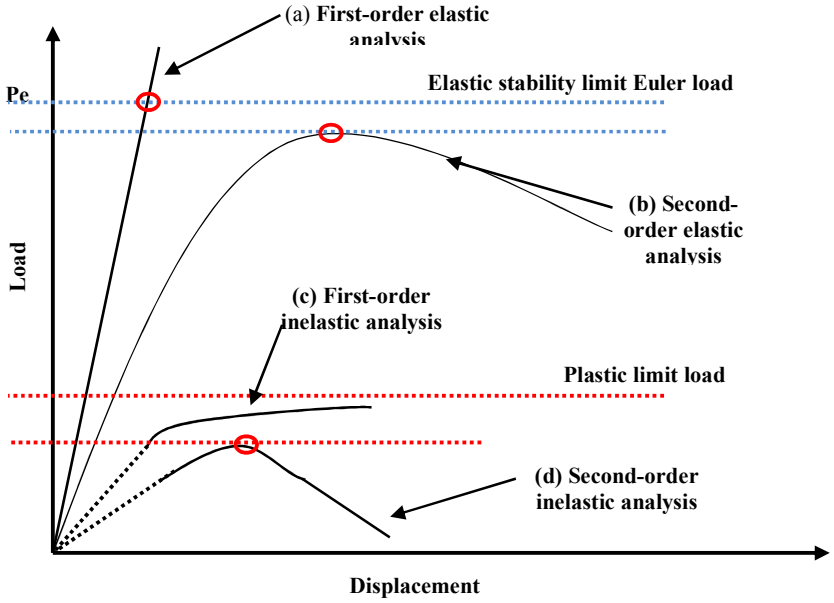

Figure 7-2 - Load-deflection curve

This method of analysis can capture geometrical and material non linearities of the structure. The calculation of forces and deformations in the structure after yielding requires iterative trial and error process because of the non linearity of the load deformation response, and the change in the effective stiffness of the cross section at inelastic region associated with the increase in the applied load and the change in structural geometry. The

post buckling behavior of such column shows how the lateral displacement occurs only if the load increases. The increase in load is due to the elastic unloading of some fiber in the cross section, which results in an increase in stiffness. But at the same time increasing the load results in further yielding, stiffness continues to be reduced and the load deflection curve achieves a peak beyond which it falls off.

Buckling loads for several simple configurations are readily available from tabulated solutions. Analysis software can also develop buckling loads. In real life, however, structural imperfections and nonlinearities prevent most structures from reaching their eigenvalue buckling strength predictions.

Instability depends on a variety of factors ranging from geometric properties to material properties and boundary conditions.

To discuss the effect of the initial imperfections on the column behavior under compressive axial load it is useful to look at the diagram in Figure 7-3 (Chen, 1987). Here there are a set of curves that describe the column behavior for different cases of imperfections. Curve (i) represent the Euler curve. Columns with initial crookedness or eccentric loads will laterally deflect at the instant a load is applied and show a load-deflection curve as (iia). The load deflection is smooth and it tends asymptotically to the Euler curve. Curve (iib) and (iic) show a large drop because of the inelastic assumption.

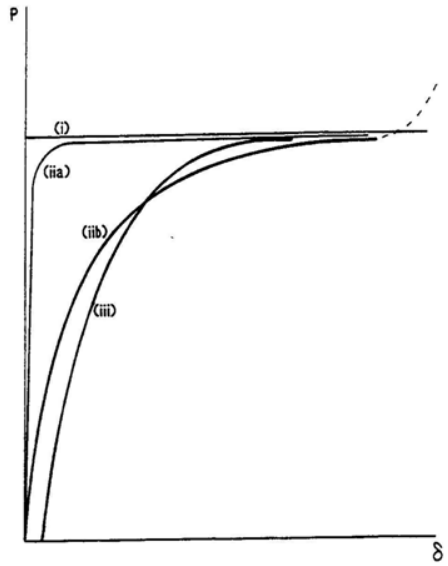

(i) perfectly straight column

(iia) column with small initial deflection

(iib) column with large initial deflection

(iii) column with eccentrically applied load

Figure 7-3 - Load-deflection curves (Chen,1987)

Beyond structural system stability and member stability there is a small but crucial further consideration: local stability. Member buckling strength cannot be developed if cross-section elements are so thin that local buckling occurs first. If the full section is needed for

strength, premature local buckling would mean member failure. Because I and H shaped cross section with thin flanges are susceptible to this phenomenon, width/thickness ratio limits for elements are used to distinguish between compact sections capable of developing full member strength and noncom pact sections for which capacity is reduced by the reduction factor Qs defined in the (AISC, 2005) Specification Section E. Limiting values of width-thickness ratios are also given in (AISC, 2005) Specification Section B4 - "Classification of sections for local buckling".

7.2 BUCKLING OF A BUILT UP SECTION

Three common types of built-up columns are illustrated in Figure 7-4. They are used when the loads to be carried are large or when a least-weight member or a member with similar radii of gyration in orthogonal directions is desired. Laced or latticed columns (Figure 7-4a) are frequently used in guyed antenna towers, in derrick booms, and in space exploration vehicles. In modern bridge construction perforated cover-plated columns (Figure 7-4b) are likely to be used rather than laced columns. Of the three, battened columns (Figure 7-4c) are the least resistant to shear and they are not generally used for bridge or building construction. Box columns with perforated cover plates designed to specification rules require no special considerations for shear effects (Ziemian, 2010).

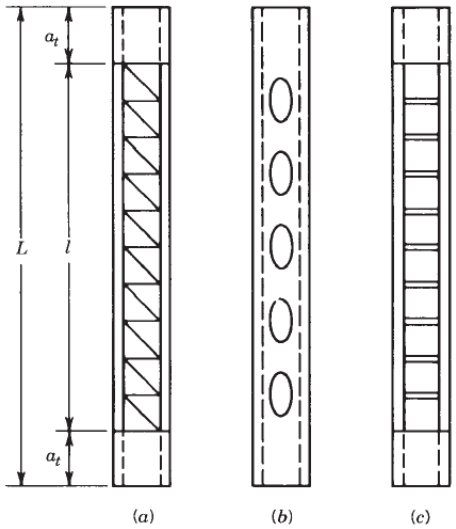

Figure 7-4 - Common types of built-up columns: (*a*) laced; (*b*) perforated cover plated; (c) battened (Ziemian, 2010)

Perforated cover plates effect

In the years before the Second World War a tendency developed, in the United States, to replace the lacing system or the batten-plates of built-up columns by perforated cover-

plates. Lacing was ordinarily used on one flange only of a compression member. It was not counted as resisting compression and unbalanced the section. On the other hand, the perforated cover-plate metal could largely be counted in member area and tended to balance the section. Additional advantages of an economical nature resulted in a reduction of fabrication and maintenance costs of such members. Furthermore, it was soon realized that he perforated cover-plates increased the over-all stiffness of the members compared to laced built up columns and hence improved their behavior (White, 1956a,b).

Tests were made to determine the mechanical properties of perforated plates. The results of the maximum compressive load test show that the net area of perforated plate columns may safely be used for estimating the strength of columns with perforated cover plates (Stang, 1948).

The studies performed by (White, 1956a,b) and (Stang,1948) refer to riveted built up columns with perforated cover plates. When perforated cover plates are used, the following provisions govern their design (Ziemian, 2010):

- The ratio of length, in the direction of stress, to width of perforation should not exceed 2.
- The clear distance between perforations in the direction of stress should not be less than the distance between points of support [i.e., $(c - a) \geq d$ in Figure 7-5a].
- The clear distance between the end perforation and the end of the cover plate should not be less than 1.25 times the distance between points of support.
- The point of support should be taken as the inner line of fasteners or fillet welds connecting the perforated plate to the flanges. For plates butt welded to the flange edge of rolled segments, the point of support may be taken as the weld whenever the ratio of the outstanding flange width to the flange thickness of the rolled segment is less than 7. Otherwise, the point of support should be taken as the root of the flange of the rolled segment.
- The periphery of the perforation at all points should have a minimum radius of 1½ in (38 mm).
- The transverse distance from the edge of a perforation to the nearest line of longitudinal fasteners, divided by the plate thickness, that is, the b/t ratio of the plate adjacent to a perforation (see Figure 7-5), should conform to minimum specification requirements for plates in main compression members.

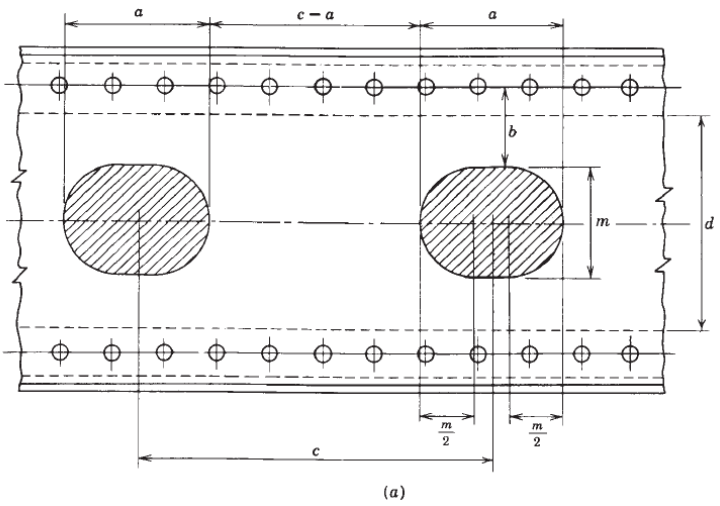

Figure 7.5a - Column with perforated web plates (Ziemian, 2010)

In order to derive the carrying capacity of steel built-up columns, the following must be studied:

- the elastic buckling load and the global behavior;
- the local behavior of the chords;
- the internal forces in the connecting members.

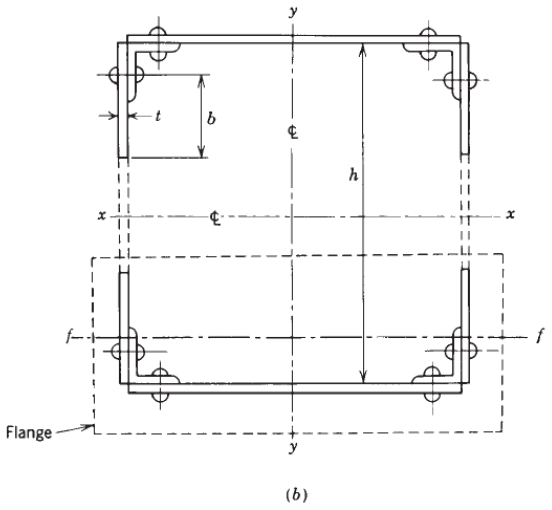

Figure 7-5b - Column with perforated web plates (Ziemian, 2010)

Timoshenko provides a methodology for calculating the critical load for a column with perforated cover plates. The properties of the net area can be used with sufficient accuracy. The element in Figure 7-6 (b) is considered to calculate the lateral displacement due to shearing force Q.

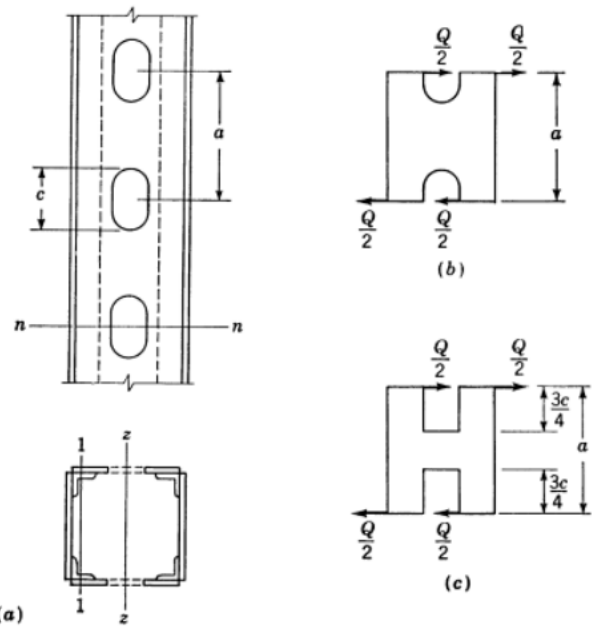

Figure 7-6 - Typical column with perforated cover plates (Timoshenko and Gere, 1961)

The horizontal cross member in the final idealized element shown in Figure 7-6(c) can be considered infinitely rigid. The length of the vertical projections, treated as cantilever beams, will be somewhere between c/2 and a/2, where c is the length of a perforation. The value 3c/4 is reasonable and gives results that agree with experiments (Timoshenko and Gere, 1961).

The equations used for columns with batten plates can be modified for this case. Since the cross member is infinitely rigid, the lateral displacement δ_1 produced by the bending can be considered equal to zero. The displacement produced δ_2 by the cantilever stubs can be obtained as follows:

$$\delta_2 = \frac{Q}{2}\left(\frac{3c}{4}\right)^3 \frac{1}{3EI_f} = \frac{9Qc^3}{128\,EI_f} \tag{2}$$

Where I_f represents the moment of inertia of the flange of the columns, that is, the entire effective area of the column on the side of the z axis taken about the centroid of the flange (axis 1-1 Figure 7-6 (a)). The angular displacement due to Q is

$$\gamma = \frac{\delta_1+\delta_2}{\frac{1}{2}a} = \frac{9Qc^3}{64aEI_f} \tag{3}$$

and therefore

$$\frac{1}{P_d} = \frac{9c^3}{64aEI_f} \tag{4}$$

from which it is obtained

$$P_{cr} = \frac{\pi^2 EI}{l^2} \frac{1}{1+\frac{\pi^2 EI}{l^2}\left(\frac{9c^3}{64aEI_f}\right)} \tag{5}$$

as the critical load for a column with perforated cover plates (Timoshenko and Gere, 1961).

Residual stresses effect

Residual stresses in welded structures are unavoidable. High tensile stress exists in the weld areas. It changes to compression in the areas away from the weld.

Fabrication by welding of built up sections introduces initial imperfections in the form of initial distortions and residual stresses and these may develop and affect the structural capacity.

There is a large number of investigations which have been carried out theoretically and experimentally in order to evaluate buckling and ultimate strengths of rectangular plates and welded box sections with perforated cover plates with welding stresses and/or deformation under compression. In general it was found that welding residual stresses and deformation reduce the buckling and ultimate strength and their affects become greater for thicker plates (Ueda, 1978).

Modeling and determining residual stresses induced by welding in the design phase of construction work may be a difficult issue.

Simplified distribution of the stress state after welding maybe estimated by using the suggested distribution according to the used design code or literature review. When local heating is input to structural steels, the heated part will expand, but because of adjacent cold parts it will be subjected to compressive stress and distortion. When the heated part is cooled down, it will be locally shrunk rather than revert to its initial shape and thus now be subjected to tensile stress. Idealized pattern of residual stress distribution is shown in Figure 7-7. The middle region of the plate is in compression before external loading is applied. The residual stresses are treated like any other load acting on the structure and super positioning these applied loads and stresses may give beneficial or detrimental effects for the structure.

Investigations and researches had been developed in the past to investigate the effects of residual stresses on steel plate buckling capacity. These initial imperfections affect the plate behavior before, as well as after, the bifurcation point as shown in Figure 7-8 and Figure 7-9.

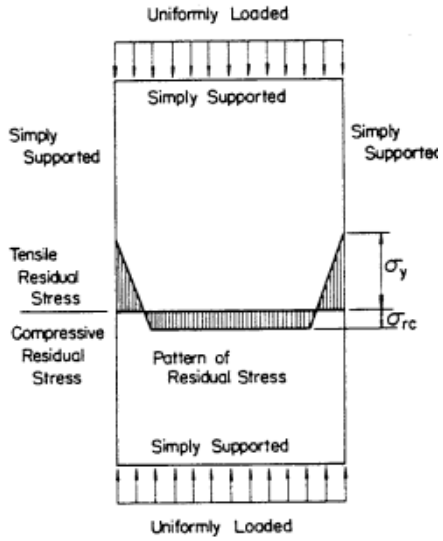

Figure 7-7 - Schematic distribution of residual stresses in an edge welded plate (Nishino, 1966)

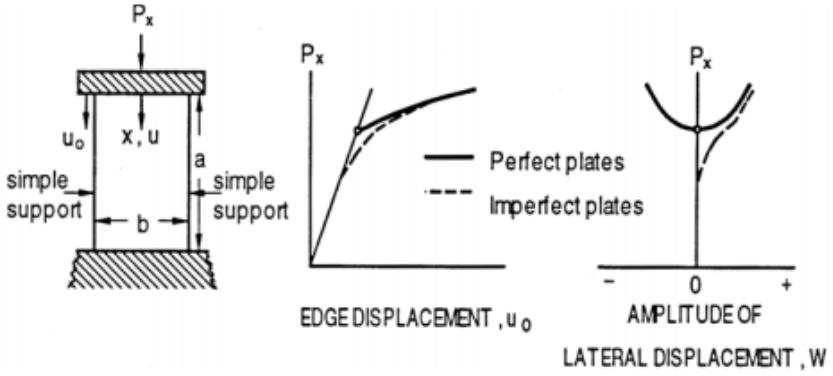

Figure 7-8 - The influence of initial imperfection in relation to a perfect plate (Farshad, 1994)

The elastic method used to calculate the critical stress level in a structural element subjected to compression can be straight forward but it leads to an upper bound solution. To capture the effects of initial geometric imperfections and residual stresses nonlinear models must be developed.

For plates, the reduction in the elastic buckling strength depends largely on the patterns of the distribution of residual stresses and its magnitude. For columns with welded box sections it should be mentioned that the reduction of buckling strength due to the presence of residual stresses is similar to that found for buckling of plates with residual stresses. Moreover the residual stresses present in a column cross section influence the local buckling strength even in the elastic range. The effect on the elastic-plastic buckling depends greatly on the width to thickness ratio of plates (Nishino, 1969).

The behavior under these large deformations or simply called “post buckling” behavior is a complicated area to describe. Nowadays, the finite element methods is the most powerful and common tool to study the post buckling behavior and capacity of a plate.

Under such initial conditions the post buckling equilibrium path becomes intricate. When the plate starts to buckle, the stresses are re-distributed in the plate showing how the ultimate load can significantly surpass the critical load level calculated according to elastic methods. Figure 7-9 shows schematically the influence on the behavior of a plate with or without residual stresses.

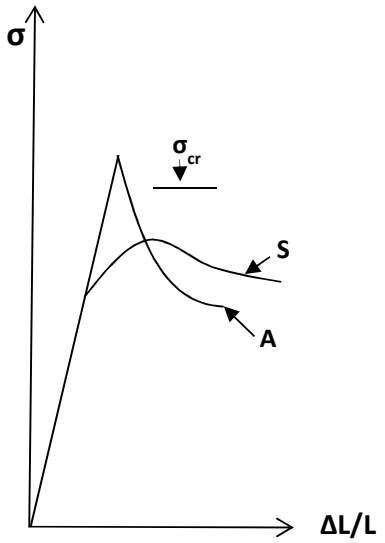

Figure 7-9 - Schematic influence on the behavior of a plate with (curve S) and without (curve A) residual stresses

PART III

CASE STUDY: I-35W BRIDGE NUMERICAL ANALYSES

8. I-35W BRIDGE COLLAPSE
9. I-35 W BRIDGE STRUCTURAL DECOMPOSITION
10. MODELS AND ANALYSES

8 I-35 W BRIDGE COLLAPSE

8.1 GENERAL DESCRIPTION

The I-35 West Highway Bridge (I-35W) spanned across the Mississippi River, Minneapolis. The bridge consisted of a three span continuous Warren deck truss with a cantilever overhang at each end, and 11 multi-girder and voided concrete slab approach span. A view of the deck truss from the north side of the I-35W Bridge is shown in Figure 8-1.

Figure 8-1 - View from the North side of the I-35W Bridge (NTSB, 2008b)

The bridge was oriented north to south and it carried three 12-ft (3,65 m) wide traffic lanes and one 12-ft (3,65 m) acceleration/deceleration lane in each direction. The total length of the bridge including the approach and deck truss was 1,907 feet (581 m). The piers and spans were numbered from south to north. Spans 1 through 4 and a portion of Span 5 were referred to as south approach spans and were steel multi-beam spans with a length of 416 feet (126,7 m) and a slight horizontal curvature. The deck truss made up a portion of Span 5, Spans 6 to 8, and a portion of Span 9 and the length of the truss portion was approximately 1064 feet (324,3 m) with a 456 feet (139 m) long river span and two 380 feet (115 m) long side spans that included two cantilever overhangs approximately 38 feet long (11,5 m). A portion of Span 9 and Spans 10 through 14 were referred to as north approach spans and consisted of a 3-span continuous welded steel multi-beam module and a 3-span continuous voided concrete slab module having a length of 427 feet (130 m). The north end of the south

approach spans and the south end of the north approach spans were cantilevered over their respective piers and were supported on the ends of the center deck truss portion of the bridge. (NTSB, 2008b)

The bridge was supported on reinforced concrete piers. The north and south abutments were stem wall-type abutments founded on piles. An elevation drawing of the entire bridge is shown in Figure 8-2 and a typical cross section through the deck truss at Pier 7 is shown on Figure 8-3.

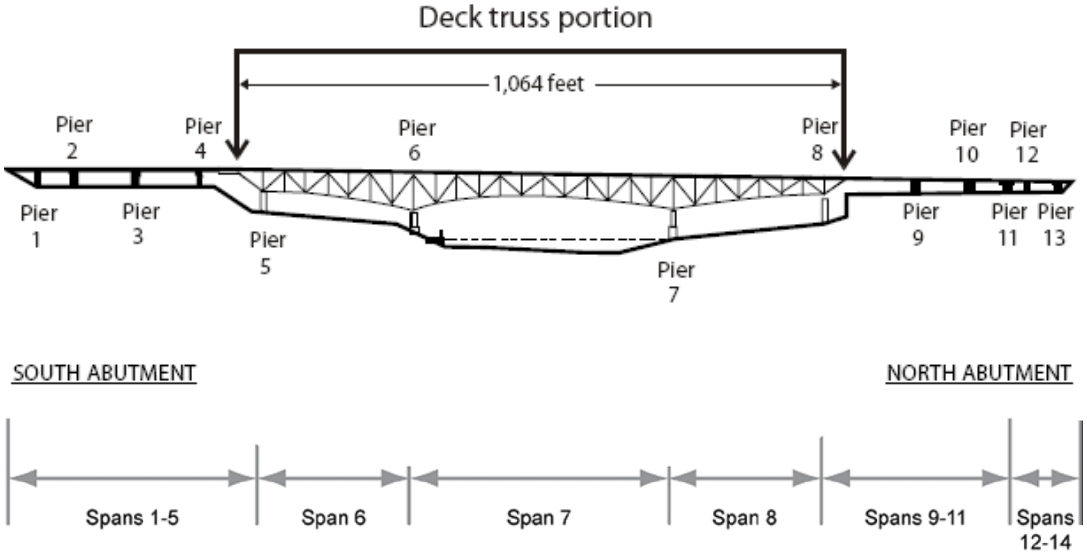

Figure 8-2 - Elevation of the I-35W Bridge (NTSB, 2008b)

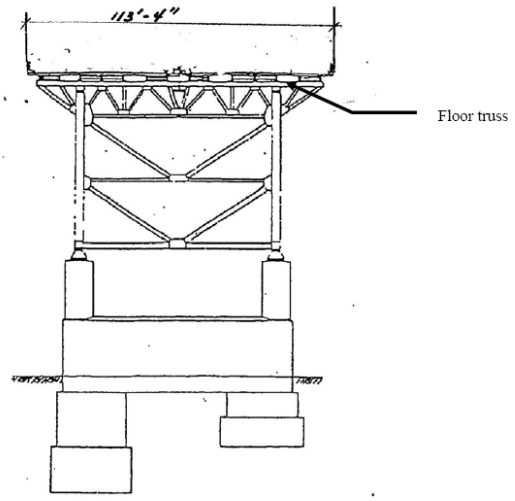

Figure 8-3 - Typical cross section trough the deck truss at pier 7 (NTSB, 2008b)

The bridge had been in continuous service since it was opened to traffic in 1967. The design was based on the 1961 AASHO *Standard Specifications for Highway Bridges* and 1961,

1962 *Interim Specifications*, and Minnesota Highway Department *Standard Specifications for Highway Construction, 1964.*

The "*As Designed*" condition refers to the geometry of the design plans for the bridge as described in the previous paragraph.

8.1.1 Materials

The steel deck truss member and approach framing were fabricated using M.H.D materials as specified in Table 7.2-1. The concrete deck strength was specified at 4,000 psi (27 MPa).

		MHD	ASTM	F_S (ASD) (psi) [MPa]	F_Y (ksi) [MPa]	F_U (ksi) [MPa]
Typical Steel	thickn. < 4" (10 cm)	3306	A 36	20,000 [138]	36 [250]	60 [410] to 80 [550]
HSLA Steel Plates	thickn.< 3/4"(2 cm)	3310	A 441	27,000 [186]	50 [345]	70 [480]
HSLA Steel Plates	thickn. >=3/4"(2 cm)	3309	A 242	27,000 [186]	46 [317]	67 [460]
High Str. Alloy Steel	Marked QT	3318	A 514	45,000 [310]	70 [483]	90 [620]
Rivets	7/8" diam. (2.2 cm)	3316, Type I	A 195	20,000 [138]	38 [262]	68 [468] to 82 [565]
Rivets	1" diam. (2.5 cm)	3316, Type IV	A 406	20,000 [138]	50 [345]	68 [468] to 82 [565]
High Strength Bolts	7/8" diam. (2.2 cm)	3391B, Style II	A 325	20,000 [138]	37.4 [258]	53.15 [366]
High Strength Bolts	1" diam. (2.5 cm)	3391B, Style II	A 325	20,000 [138]	49.1 [338]	69.7 [480]

Table 7.2-1 - Material Properties

8.1.2 Design Loads

The truss members were designed to resist a combination of Dead Load (DL), Live Load (LL), Impact (I), transverse Wind Load (W), Wind load on Live load (WL) and Centrifugal Forces (CF). The forces were combined as follows (Sverdrup, 1960):

Group I = DL + LL + I
Group II = DL + 75 pounds W
Group III = Group I + 30% W + WL + CF

An H20-S16-44 was used for the live load design. A 26,000 pound (12 Ton) concentrate load was also used in combination with lane live load. Code prescribed loading reductions was used.

The impact factors were applied to the live load as a function of the length of the loaded span and expressed as a percentage of the live load. The percentages varied from 13% for the back spans to 9 % for the mail span truss members. The cantilever overhangs at U0 and U0' had impact forces of 21% and 17%, respectively. Floor trusses, verticals (except U8-L8), and stringers received an impact of 30%.

The design was based on a maximum wind velocity of 100 miles per hour (161 Km/h) in accordance with the specifications. A temperature range from -30°F (-34°C) to 120°F (48°C) was considered with the design temperature equal to 45°F (7°C). In Table 7.2-2 are summarized the dead load description and values.

DESCRIPTION	LOAD		REFERENCE
Steel bridge structure	Self-weight		Sverdrup:1965, pp. 20-22
6 ½" (16.5cm) concrete deck	81.2 psf*	3,88 kPa	Sverdrup:1965, pg. 59
Safety curb	558 plf*	830 Kg/m	
Median curb	500 plf*	744 Kg/m	
Median rail and guardrail	20.4 plf**	30.4 Kg/m	
South approach span (72'-4") (22 m)			
Deck	2,940 plf	4,37 Ton/m	Sverdrup:1965, pp. 55 & 59
Edge curb and rail	20.9 kip	9,5 Ton	Sverdrup:1965, pp. 55 & 59
Median curb and rail	18.8 kip	8,5 Ton	Sverdrup:1965, pp. 55 & 59
Girder steel	4.61 kip	2,0 Ton	
North approach span (129'-4¼") (39.5 m)			
Deck	5,250 plf	8,6 Ton/m	Sverdrup:1965, pp. 58 & 59
Edge curb and rail	37.4 kip	17,0 Ton	Sverdrup:1965, pp. 58 & 59
Median curb and rail	33.6 kip	15,3 Ton	Sverdrup:1965, pp. 58 & 59
Girder steel	19.8 kip	8,9 Ton	

* 150 pcf (2403 Kg/m^3) Normal Weight Concrete

** 2'-3" Tall at 12'-6" o.c. spacing 5 WF 16 posts and two (2) 10 Ga. 12" deep Guardrails satisfying AASHTO M180 (ASHTOM:1961, pg. 393). The design weight of guard rails and fastenings is 200 plf (AASHTO:1961, § 1.2.2, pg. 8).

Table 7.2-2 - Dead Load Description and values

8.1.3 Composition of the Deck Truss

The deck truss structural framing is shown in Figure 8-4. The same identifying nomenclature provided in (MnDOT, 2009) design drawings and inspection reports had been used.

8.1.3.1 Main Trusses

The three span continuous deck truss was composed of two main trusses, designated East and West (E and W), that made up the primary load carrying members of this structure. The east and west trusses were spaced 72ft-4in. (22 m) apart and were connected by 27 transverse floor trusses spaced on 38-foot (11,5 m) centers along the truss and by two floor beams at the north and south ends. See also Figure 8-4. From south to north, the node locations of these trusses were designated 0 through 14 (mid-span) and 13′ through 0′. A U or L distinguished the upper and lower nodes at each of these locations respectively and these locations were referred to as Panel Points (e.g. Panel Point U8).

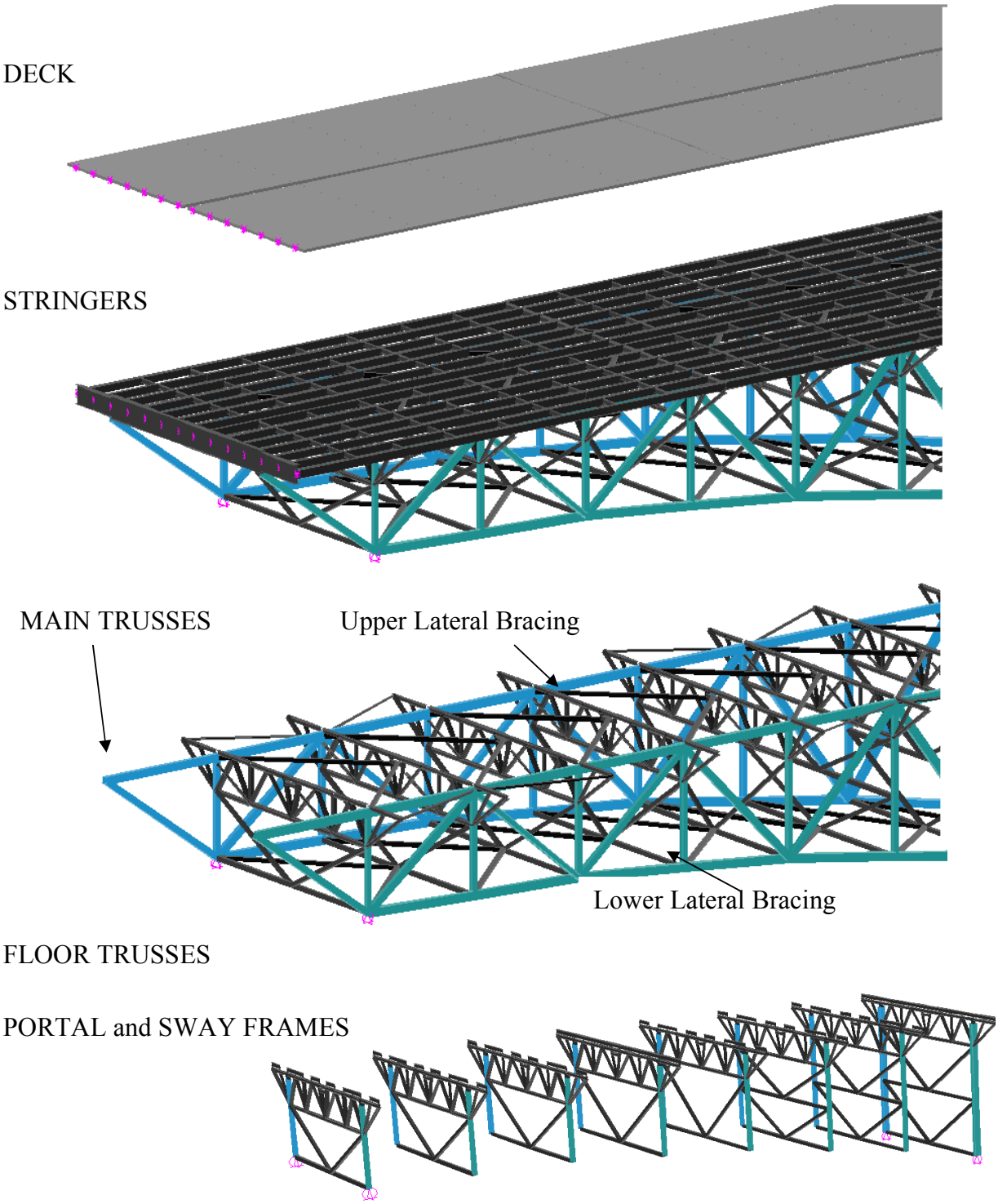

Figure 8-4 - Deck Truss Structural Framing

There were four types of members in the trusses: the upper chord members that extended the entire length of the truss, the lower chord members that extended between Nodes 1 and 1′, vertical members that vertically connected like-numbered nodes on the upper and lower

chords, and diagonals that connected adjacent nodes of the upper and lower chords. See in Figure 8-5 the East truss elevation and the different type of members.

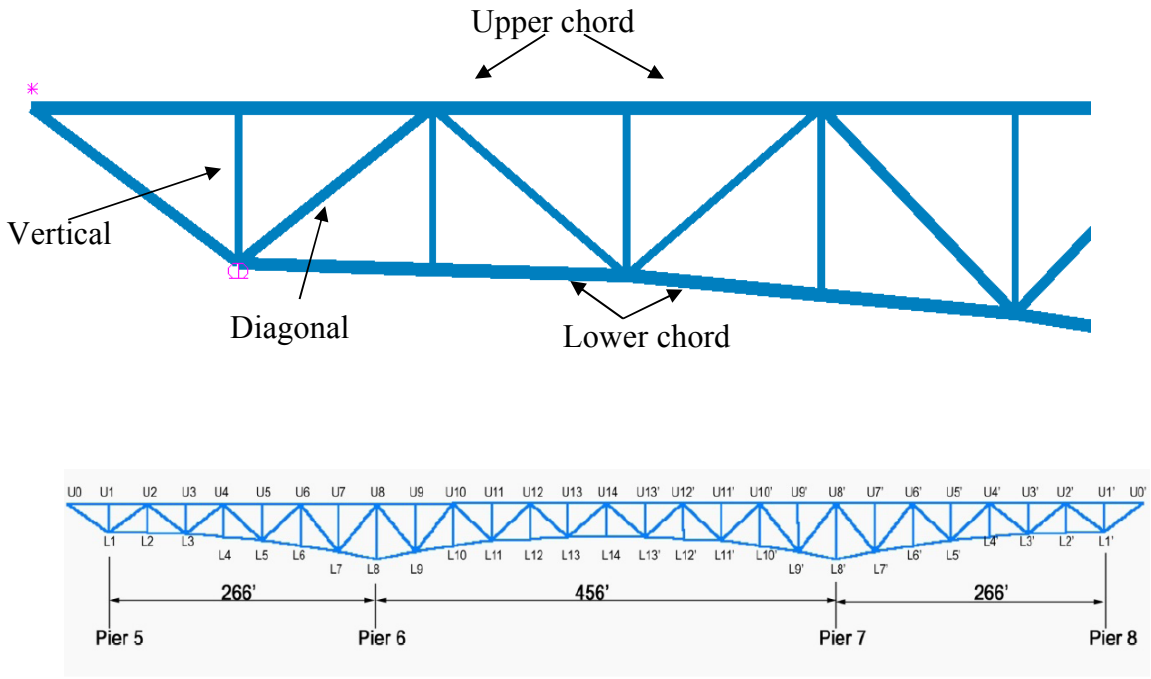

Figure 8-5 - East truss elevation and types of members

The members of the main trusses were composed of either box sections or H sections, connected using riveted joints at the nodes with gusset plates. The east and west sides of the box sections were referred to as side plates and the other two sides as cover plates. In many of the box members, one or both of the cover plates had access holes that are oval shaped and provided access for fabrication and inspection. The H sections have flanges that were welded to the web plate. The flanges and side plates were riveted into the gusset plates at the truss nodes.

8.1.3.2 Deck and Stringers

The deck of the bridge consisted of two reinforced concrete deck slabs separated by approximately 6 inches (15,24 cm). According to the design drawings, the cast-in-place* concrete deck slab had a minimum thickness of 6 ½ inches (16,51 cm) spanning one way east to west from stringer to stringer. Each deck slab carried four 12-ft-wide (3,65 m) traffic lanes and two 2-ft (60 cm) shoulders with interior and exterior barriers on both edges of the deck. The total width of the slabs was approximately 113 ft 4 in (34,5 m) as shown in Figure 8-6. The stringers supported the deck directly and were placed on top of the floor truss top chords. The elements were continuous longitudinally except at Panel Points U4, U8, U14, U8' and U4', due to the presence of expansion joints in the deck. In these particular points

there were also stringer expansions joints with one stringer end fixed to the floor truss top chord (the fixed side) and the other stringer end sitting on an expansion bearing support (the expansion side). The model had, in total, fourteen lines of stringers across the width of the deck truss all of which were W 27 x 94 sections.

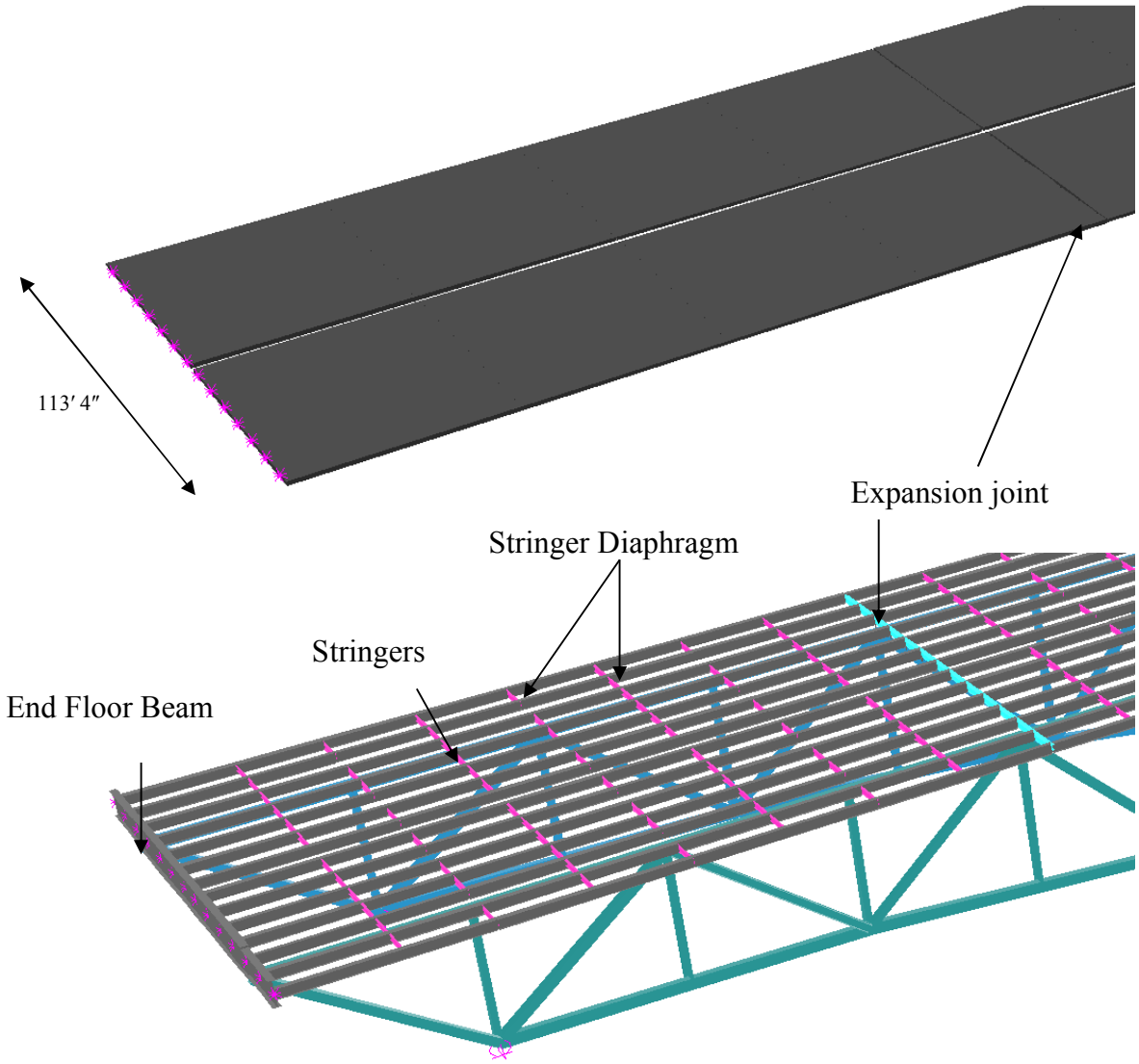

Figure 8-6 - Deck and Stringer Particular View

At each floor truss (panel location) and between two adjacent floor trusses (mid-panel point) there were stringer diaphragms to maintain the structural rigidity and position. The general section for stringers diaphragms were C 15x33.9 while at deck expansion joint locations there were W 16x36 wide flange sections.

8.1.3.3 Floor Trusses

The floor trusses were designated FT and framed into the upper nodes of the east and west main trusses. The floor trusses were primarily made from hot rolled wide flange (WF) sections and cantilevers approximately 16 feet (4,9 m) past the east and west main truss upper chords. The upper chord of each floor truss was supported on and connected to the upper chords of the main trusses at the like-numbered nodes. The lower chord of each floor truss connected to the main truss vertical member approximately 12-feet (3,65 m) below the floor truss upper chord. The lower chord of the floor trusses were longitudinally braced with diagonal members (kicker braces) at floor truss nodes L4 and L9. The braces extended upward from the floor truss lower chord to deck stringers on the south side of the floor trusses from Nodes 1 through 14 and on the north side of the floor trusses from Nodes 13′ to 1′. See Figure 8-7 for a floor truss general elevation.

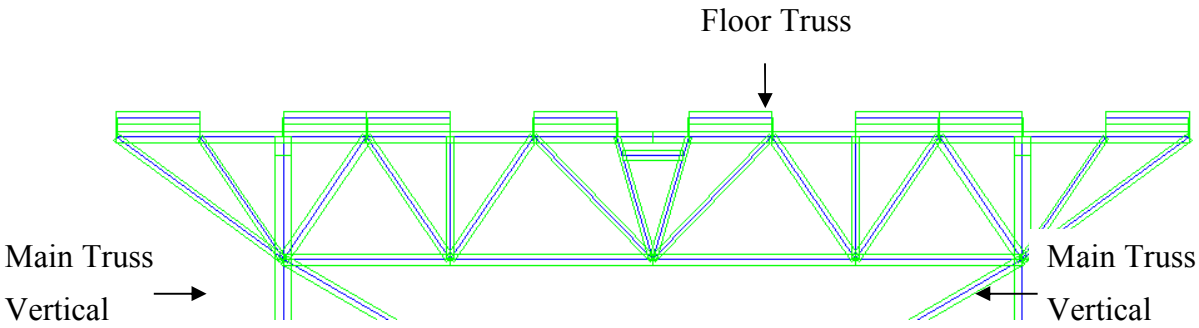

Figure 8-7 - General Floor Truss Elevation

8.1.3.4 Portal and Sway Frames

The trusses were braced by portal frames with K configurations at Panel Points L1, L1', L8, L8'. At intermediate panel points and not at bearings, the main trusses were braced by sway frames. The K-type sway frames consisted of box shaped members that were oriented transversely to the main truss in the plane of the same-numbered truss nodes. The deeper sections of the variable depth deck truss, Panel Point *6* through *10* and *10′* through *6′*, had a double layer of sway frames. The K configuration had a bottom strut connecting the lower nodes and in the presence of a double layer, an intermediate strut connecting vertical members of the main span at the point of mid-depth (between the lower node and the lower floor truss connection) providing lateral stability. Diagonals (the legs of the K shape) then spanned from the center of the struts to the vertical members on the main truss. The portal and sway bracing members were welded box sections without hand holes. In Figure 8-8 the Portal, Sway Frame and Floor Truss between Panel Point L0–L8 are shown.

8.1.3.5 Lower Lateral, Upper Lateral and Cantilever Bracing Members

There were three types of bracing in the structure: the upper lateral bracing for the upper chord of the main trusses, the lower lateral bracing for the lower chord of the main trusses, and the cantilever bracing for the cantilever portions of the floor beams outside the main trusses as shown in Figure 8-9. The lower lateral system was made up of diagonal members connecting lower chord nodes in the main truss and the center node of the bottom strut of the sway frame member at the next node immediately north of Nodes 1 through 13, and the lower chord nodes in the main truss and the center node of the bottom strut of the sway frame member at the next node immediately south of Nodes 13′ through 1′.

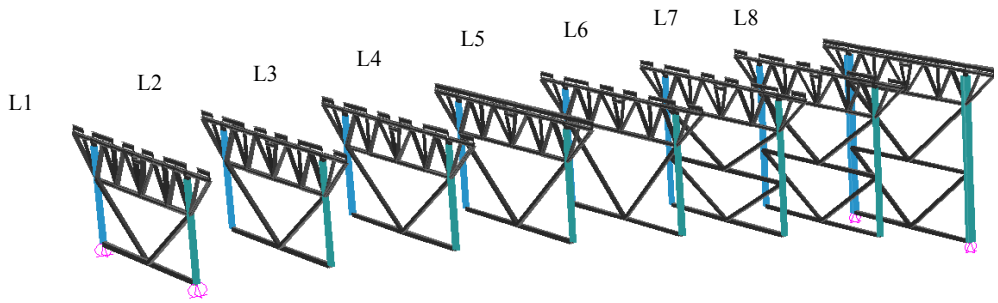

Figure 8-8 - Portal, Sway Frame and Floor Truss between Panel Point L0–L8

The upper lateral system was made up of diagonal members between upper chord nodes in the main truss and a connection at the center of the upper chord of the floor truss at the next node immediately north of Nodes 0 through 13, and between the upper chord nodes in the main truss and a connection at the center of the upper chord of the floor truss at the nodes immediately south of Nodes 13′ through 0′. An extension of the upper lateral bracing system existed for the cantilevered portion of the floor trusses, with diagonal members that connected east main truss Upper Nodes 2, 6, 11, 11′, 6′ and 2′ to the immediate north and south floor truss Upper-Chord Node 0, and diagonal members that connected west main truss Upper Nodes 2, 6, 11, 11′, 6′ and 2′ to the immediate north and south floor truss Upper -Chord Node 14.

8.1.4 Piers and Bearings

The main truss spans were supported on bearing assemblies at Piers 5, 6, 7, and 8 and are shown in Figure 8-10. A fixed bearing was provided for each of the main trusses at Pier 7, and expansion roller bearings were used at Piers 5, 6 and 8. The two expansion roller bearings at Pier 6 contain a lower bearing plate, four large diameter rollers, an upper bearing casting, a bronze domed casting, and a flange casting, which is bolted to the bottom of the node above. The bronze domed casting rests between the upper bearing casting and the flange casting, and these two members are held together with a hold-down stud. The

expansion roller bearings at Piers 5 and 8 are similar but contain three large diameter rollers. The spherical dome casting allows multi-directional rotation that provides concentric loading through the bearing. Overall height of the bearing assemblies (top of the concrete pier to the bottom of the truss) is 4 feet-11 ½ inches (1,5 m) for Pier 6 and 4 feet-1 inch (1,3 m) for Piers 5 and 8.

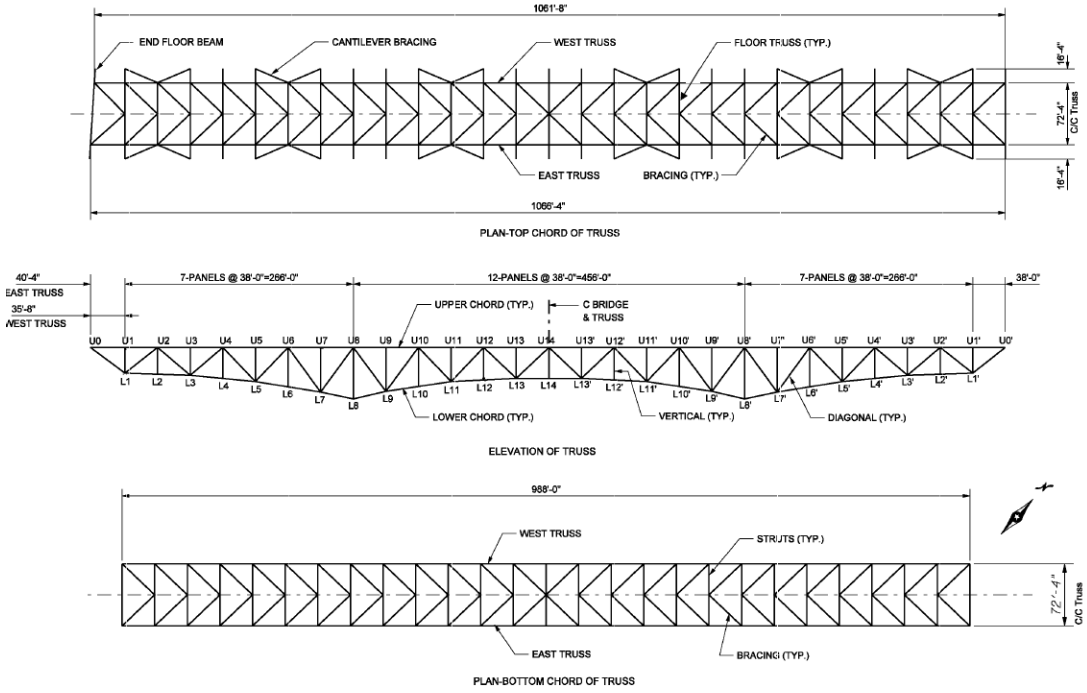

Figure 8-9 - Plan View of Lower Lateral and Upper Lateral System

The fixed bearing assemblies at pier 7 do not allow any displacement of the truss relative to the top of the pier and has an overall height of 3 feet-6 inches (1 m). The individual bearing locations are designated by the pier number and as either East or West. Expansion rocker bearings are used at nodes U0 and U0′. These bearings support the connecting approach spans on the deck truss cantilevered ends. The rocker bearings consist of 1 foot-6 inch (45cm) tall rocker castings.

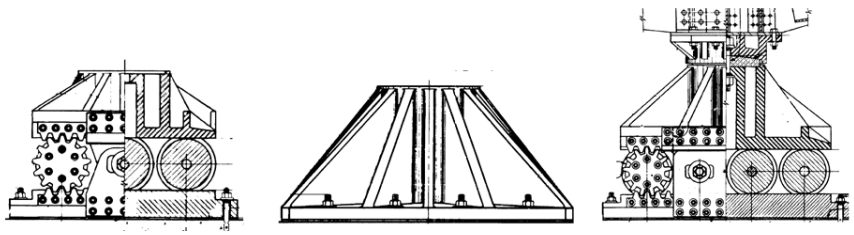

A) B) C)

Figure 8-10 - Bearings assemblies for each pier. A) Pier 5 and 8; B) Pier 7; C) Pier 6

8.1.5 Connections

Many of the member's connection were riveted. Welding was employed to build box members. The welded box, shaped members, except the top chord of the main trusses, had welded diaphragms near each end connections; the top chord members had bolted diaphragms. Additional intermediate diaphragms spaced at not more than 15 feet (4,6 m) were used for all box members. The wide-flange shapes in the floor truss were welded to gusset plate. High strength bolts were used primarily on the floor trusses. Shear connection between the deck and the stringers was accomplished with welded studs. The main truss was not design to be composite with the deck system.

8.2 COLLAPSE DESCRIPTION

8.2.1 Conditions at Collapse

The gravity loading on the bridge at the time of the collapse consisted of:

- Weight of structural steel and weight of concrete deck and concrete features including overlay material and other items that had been added to the bridge following the original construction.("As Built" Condition).
- Construction materials and equipment in the four lanes that were closed to traffic as part of an ongoing construction project.
- Vehicle traffic in the four open lanes.

"As Built" Condition

The "*As Built*" conditions reflect all changes made during the service life of the bridge and increased the dead load on the structure. The bridge had been modified from its original construction in 1977 by the addition of a 2-inch-thick concrete overlay that was added to the deck on the main trusses and approach spans. In 1998 a new concrete face was added to the inside of the original rails along the exterior edges of the deck and new median barriers replaced the rail on the inside edges of the deck on both the truss spans and approach spans. Figure 8-11 a) shows the original exterior and interior barrier at the time of the design and Figure 8-11 b) shows the exterior and interior barrier added in the 1998 retrofit. Table 7.2-3 summarizes the changes due to the Retrofit in 1977 and 1998 (NTSB, 2007).

Figure 8-11 a) exterior and interior barrier as Designed in 1965, b) barriers at the time of the collapse

Construction Loading and Traffic at time of the Collapse

At the time of the collapse roadway work was underway. The work involved removing and replace 2 inches thick (5 cm) concrete overlay. At the time of the collapse, four of eight lanes were closed to traffic. The preexisting wearing surface was still in place on the two inside lanes northbound, where the average deck thickness was 8.7 inches (22 cm). The new overlay was already in place on the two outside northbound lanes and the two outside southbound lanes. The surface of the two inside southbound lanes had been milled for the entire length of the bridge, removing about two inches of material. Based on interviews, photos, and weight tickets, the NTSB compiled the best estimate of construction loads and their respective position on the bridge at the time of the collapse.

DESCRIPTION	INITIAL DEAD LOAD		CHANGES DUE TO 1977 RETROFIT	CHANGES DUE TO 1998 RETROFIT
Steel bridge structure	Self-weight			
6 ½" concrete deck	81.2 psf	3,88 kPa	Add 21.1 psf (1 kPa)	
Safety curb	558 plf	830 Kg/m		Add 333 plf (495 Kg/m)
Median curb	500 plf	744 Kg/m		Add 1,060 plf (1,577 Kg/m)
Median rail and guardrail	20.4 plf	30.4 Kg/m		Remove 20.4 plf (30,35 Kg/m)
South approach span (72'-4")				
Deck	2,940 plf	4,82 Ton/m	Add 763 plf (1,25 Ton/m)	
Edge curb and rail	20.9 kip	9,5 Ton		Add 12.0 kip (6 Ton)
Median curb and rail	18.8 kip	8,5 Ton		Add 37.6 kip (18.8 Ton)
Girder steel	4.61 kip	2,0 Ton		
North approach span(129'-4¼")				
Deck	5,250 plf	8,6 Ton/m	Add 1,360 plf (2 Ton/m)	
Edge curb and rail	37.4 kip	17,0 Ton		Add 21.5 kip (10.75 Ton)
Median curb and rail	33.6 kip	15,3 Ton		Add 67.2 kip (33.6 Ton)
Girder steel	19.8 kip	8,9 Ton		

Table 7.2-3 - Load values due to the retrofit in 1977 and 1998

Figure 8-12 shows the position of equipment and materials stages between Node 8 and Node 14. An estimate 578.5 kips (289 Ton) of construction loads were present in this region, including a total weight of 383,200 pounds of aggregate. Thanks to post accident vehicle positions, photographs, and witness statement, it was possible to determine the types and general position of the 111 vehicles on the bridge at the time of the collapse (NTSB, 2007).

Weather Conditions

Weather at the time of the bridge collapse was clear and hot. Records from the University of Minnesota for the 24-hour period of August 1, 2008 show an air temperature at the 6:05 pm time of the collapse of 92.1 °F after a peak temperature reading of 92.9 °F at 4:30 pm.

Figure 8-13 is a temperature plot for August 1, 2007. Weather records at the nearby Lower St. Anthony Falls weather station indicated a peak of temperature of 93 °F. Weather records for this time of period also indicated light to moderate winds out of the southwest between 10 to 18 mph.

Figure 8-14 shows the wind and gust data for August 1, 2007. No precipitation was recorder within 24 hours of the collapse.

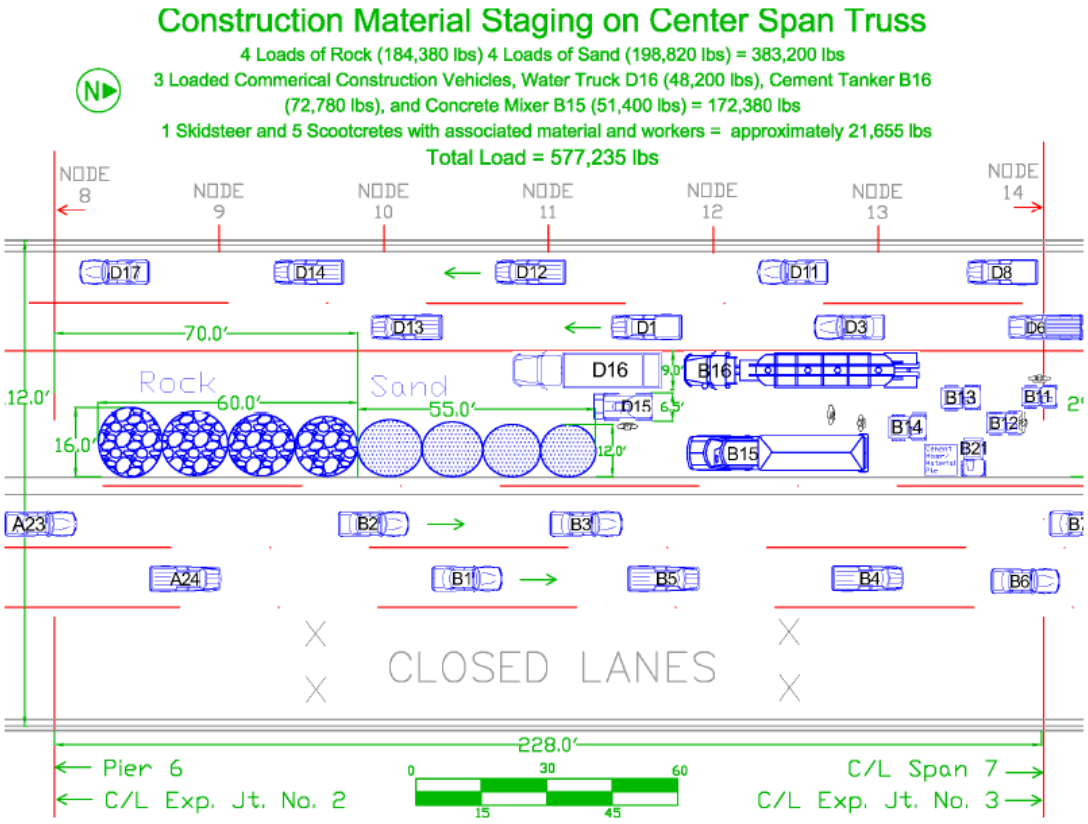

Figure 8-12 - NTSB best estimate of construction loads and their respective positions on the bridge at the time of the collapse (NTSB, 2007)

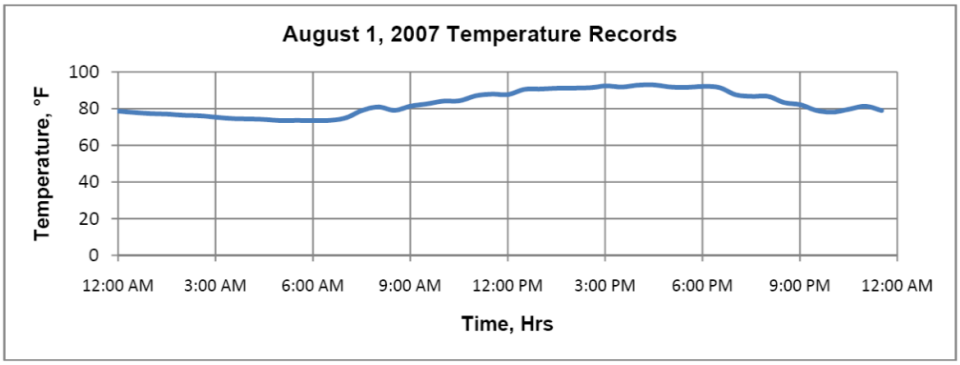

Figure 8-13 - Temperature plot for August 1, 2007 (NTSB, 2007)

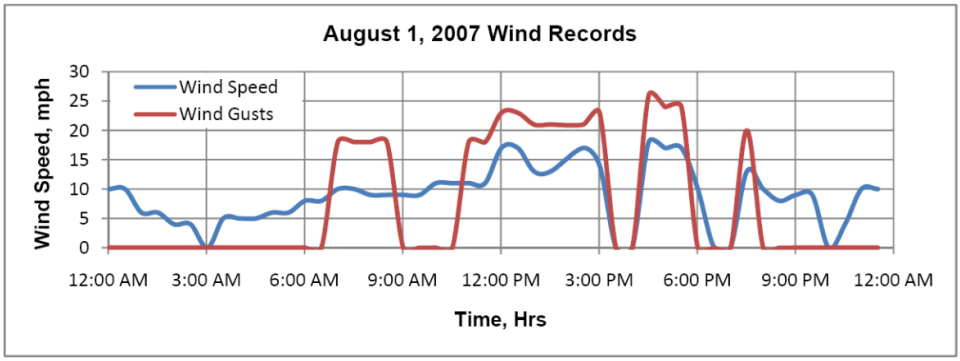

Figure 8-14 - Wind and gust data for August 1, 2007 (NTSB, 2007)

Bearings

The truss span was supported by a fixed bearing at Pier 7 and three roller bearings at Pier 5, 6 and 8 respectively. From the Mn/DOT's June 2004 inspection report the bridge bearing were noted to being poor condition. All the roller bearing did not appear to be functioning uniformly as designed with section loss, flacking and surface rust with moderate corrosion. Figure 8-15 shows the URS photo of Pier 6W bearing Ù8.

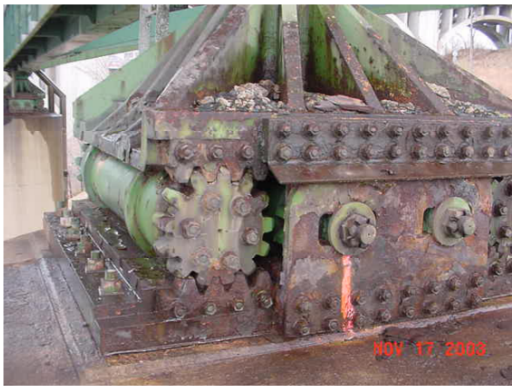

a)

b)

Figure 8-15 - a) 2003 URS photo of Pier 6W bearing U8 (WJE); b) Re-assembled Pier 6 bearing

9 I-35W BRIDGE STRUCTURAL DECOMPOSITION

Following the structural problem decomposition technique discussed in Chapter 3, the I-35W Bridge in this study has been partitioned as follows:

Macro level:

- Principal structural system with deck truss system and piers;

Meso level: Main substructures characterized by their specific roles:

- Stringers and Deck. Resist and transfer applied vertical loads;
- Main trusses. Resist and transfer to the piers the loads transferred by the stringer and deck system, the steel self-weight and the horizontal load transmitted by the portal system;
- Portal. Provide lateral stability and transfer/adsorb lateral loads;
- Piers. Transfer loads to the foundation system.

Micro level: Single elements characterized respect to their smallest geometric dimension and specialized roles:

- Vertical, diagonal, top and bottom chords members pertaining to the main truss substructure;
- Floor truss and sway frame members in the portal substructure;
- Concrete deck, stringers and diaphragm in the stringer and deck substructure.

The partitioning for Macro (global) to Meso (substructure) to Micro (local) levels as shown in Figure 9-1 may be employed. More specifically, if attention focuses in a segment of the bottom chord of one truss, the decomposition in Figure 9-2 may be considered.

In this multilevel approach the global response to any loading can be found from a coarse model at the Macro level after which, at the Meso level, a more refined model can give interaction of the Meso level structure with the selected focal elements.

Finally, a very detailed model can be used to study the behavior of the selected bottom chord element at the Micro level. By this process all sensitivity elements or substructures at the Micro level can be analyzed in detail in order to assess potential failure and role in the robustness of the system.

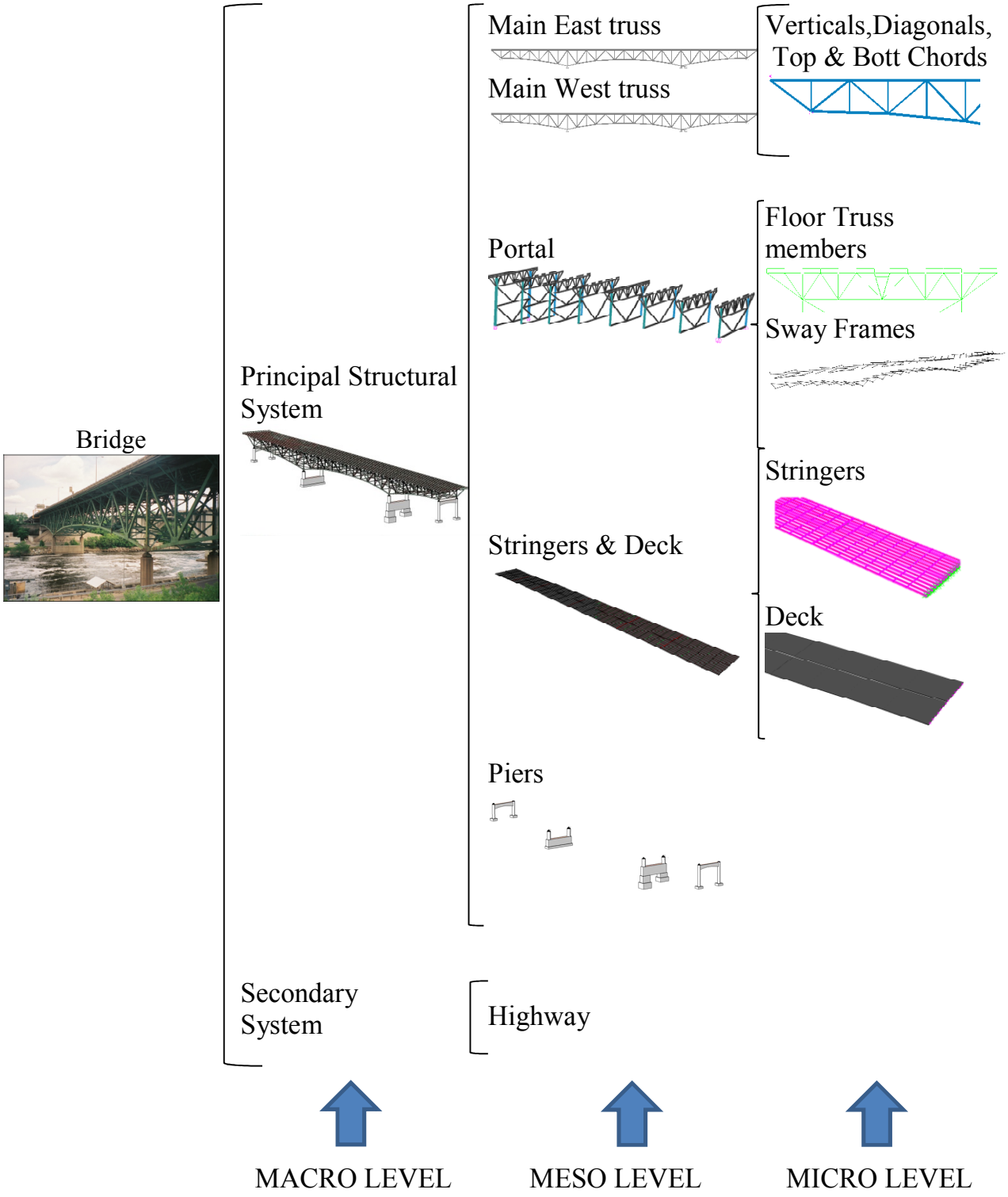

Figure 9-1 - Case Study Structural Partitioning

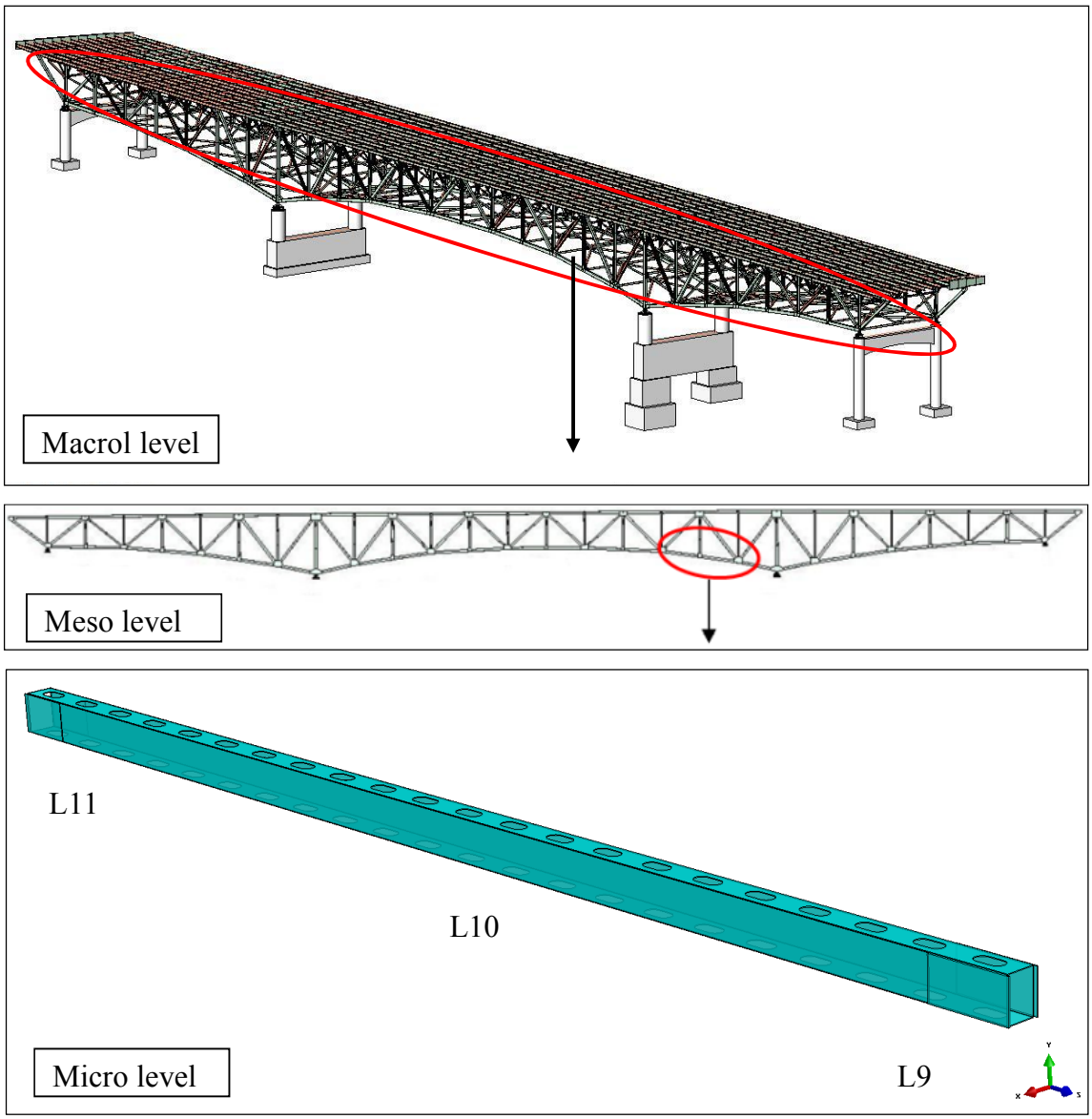

Figure 9-2 - Structural parts identification used in the present study

10 MODELS AND ANALYSES

The study is divided into the following tasks:

- Develop a three dimensional (3D) global finite element model (FEM) of the whole bridge based on original drawings, design and construction specifications;
- Conduct analysis of the global structure;
- Develop a 3D FEM of a subsystem's component. In particular this study focus on the rectangular built up member with and without perforated cover plates located on the bottom chord of the main lateral trusses;
- Conduct subsystem's component analysis.

10.1 GLOBAL FINITE ELEMENT MODEL

A global study of the whole bridge in the light of seasonal and daily temperature changes has been performed building a 3D FEM of the entire bridge.

The effect of the seasonal and daily temperature changes, applied at different portion of the bridge, has been investigated for different bridge bearings conditions in order to evaluate the demand changes in the main truss members and in particular at the bottom chord member on both trusses.

10.1.1 Model Description

The 3D FEM of the deck truss portion of the bridge was realized using SAP2000 software (CSI, 2004). The SAP model is made up using frame element and it includes the main trusses, deck and stringers, floor trusses, portal and sway frames upper and lower lateral elements. Longitudinal restraint at all main pier bearings have been applied. Figure 10-1 is an overview of the 3D FEM. Figure 10-2 and Figure 10-3 are closer views of the side span and center span of the model, respectively.

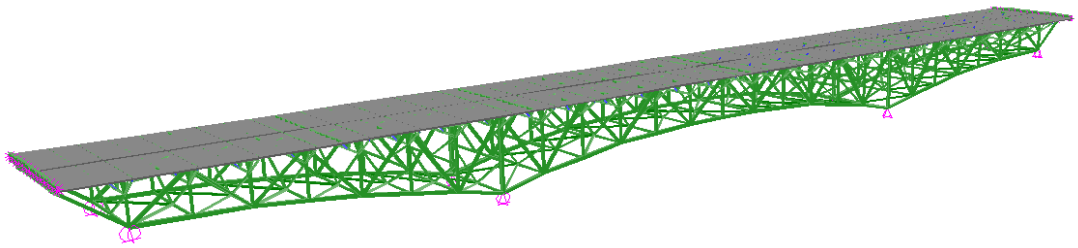

Figure 10-1 - Overview of the I-35W 3D Computer Model Solid view

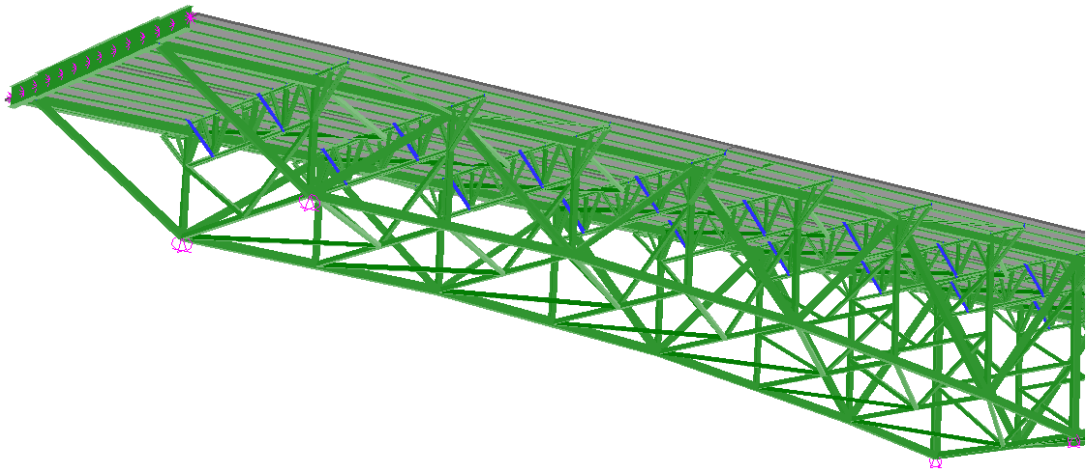

Figure 10-2 - Side Span of the I-35W 3D Computer Model Solid view

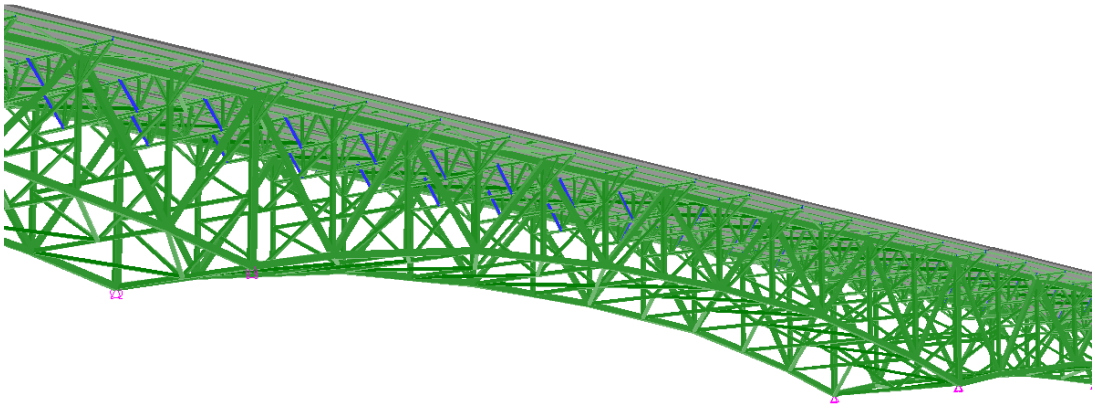

Figure 10-3 - Center Span of the I-35W 3D Computer Model solid view

The truss was modeled using the geometries and member sizes outlined in the design plan using the following assumptions:

- The vertical slope and the small horizontal curvature of the structure at both the north and south ends were neglected.
- The two trusses were assumed to be identical.
- The cross slope of the structure was neglected and thus both trusses have the same elevation.
- All steel members were modeled with “space frame” members that have six degrees of freedom at each joint.
- The beam members were placed along the centerlines of the actual members they represent between joints.

- The members are rigidly connected to the joints except where it is necessary to release certain forces per end support conditions.
- The reinforced concrete deck was modeled with quadrilateral linear shell elements and each joint has six degree of freedom. The transverse and longitudinal deck joints were properly included in the model.
- The Approach spans were integrated into the main truss model as point loads applied at each end of the main truss.
- The material properties used are the same specified in the original design documents.
- All main truss members were modeled with two elements along their length to ensure any effects that might occur during the buckling analysis.

The material used for steel members and deck is listed in Table 10.1-1.

Material	Unit Weight lb/in^3 [Kg/m^3]	Unit Mass Kip-s^2/in^4 [Kg/m^3]	E1 Kip/in^2 [GPa]	G12 Kip/in^2 [GPa]	U12	Fy Kip/in^2 [MPa]	Fu Kip/in^2 [MPa]	EffFy Kip/in^2 [MPa]	EffFu Kip/in^2 [MPa]
Steel A36	0.28 [7´800]	8.9933E-07 [0.79]	29000 [200]	11500 [79,3]	0.3	36 [250]	58 [400]	54 [372]	63.8 [440]
Concrete	0.0868 [2´400]	2.248E-07 [0.2]	3605 [24,855]	1502 [10,35]	0.2	-	-	-	-

Table 10.1-1 - Material Properties 3D SAP Model

10.1.1 Linear Static Analyses

The accuracy of the SAP model was checked in a number of ways. Using structural loads and bearing conditions consistent with those assumed in the original design, member forces of interest and support reactions were compared to values listed in the original design drawings as reported in Table 10.1-2 and

Table 10.1-3.

This exercise indicated that the model was performing well, as the member forces obtained from the model were typically very close to the original design values.

Member	Dead Load As Designed		Dead Load SAP Model		Error	Design Service Load Original Dwg.	
	kips	kN	kip	kN		kip	kN
L8-L9	2,543 c	11´311	2,566 c	11´414	1 %	3,420 c	15´212
L9-L11	559 c	2´486	628 c	2´794	12 %	919 c	4´087
L11-L13	1,311 t	5´831	1,116 t	4´964	14 %	2,011 t	8´495
L13-L13'	2,036 t	9´056	1,782 t	7´926	14 %	2,975 t	13´233

Table 10.1-2 - Truss Member Group I Design Forces

PIER	SAP MODEL		ORIGINAL PROJECT		Error
	Kip	kN	Kip	kN	%
PIER 5_E	1,000	4′448	1,098	4′884	8.8
PIER 5_W	1,001	4′ 452			
PIER 6_E	3,698	16′449	3,660	16′280	1.0
PIER 6_W	3,699	16′543			
PIER 7_E	3,691	16′418	3,589	15′964	2.8
PIER 7_W	3,691	16′418			
PIER 8_E	1,058	4′706	1,446	6′432	26.8
PIER 8_W	1,058	4′706			

Table 10.1-3 - Group I Reactions

In order to estimate the effects of thermally–induced restraint forces in key structural elements the model has been subjected to a variety of temperature scenarios, consistent with the weather conditions at the time of the collapse and the maximum and minimum temperature values for the month leading up to collapse, and various bearing restraint conditions. All the analyses were performed in a linear elastic hypothesis. The variables used in the analysis are:

- **Uniform applied temperature**
  Three different temperatures, listed in Table 10.1- 4, are chosen.

	T		*ΔT*	
Min temperature month leading up to collapse	59 °F	15 °C	12 °F	8°C
Max temperature month leading up to collapse	102 °F	38.8 °C	57 °F	31.8°C
Max temperature day of collapse	92.9 °F	33.8 °C	47.9 °F	26.8°C

Table 10.1- 4 – Temperature applied to SAP model ($\Delta T = T - 45$ °F)

- **Bridge portion subjected to temperature**
  The uniform temperature has been applied on the following bridge portions:
    - Main East Truss
    - Main West Truss
    - Bridge centerline to East truss
    - Centerline to West truss
    - All steel elements
    - All steel elements and deck

- **Bridge boundary conditions**

The initial bearing conditions in the "As Design" conditions of the bridge described in Chapter 9 are represented in Figure 10-4. Two different boundary condition modeling approaches (BC CASE1, BC CASE2) have been used and are discussed in the next section.

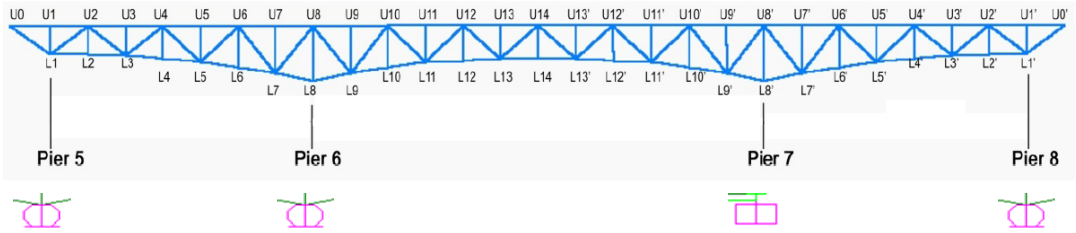

Roller	**(R)**	
Pin	**(P)**	
Fix	**(F)**	

Figure 10-4 - Bearing position and "As designed" restraints

BC CASE 1: The first set of analyses has been carried out using roller, pin and fix restraints to model the bridge bearing conditions. The boundary conditions of the SAP model were changed alternatively to simulate the different stages of deterioration for a total of 27 possible combinations. Table 10.1-5 shows all the combinations used in the analysis. All the symmetric configurations have been deleted. The results obtained considering the supports restrained in such ways give an upper and lower bound estimate of the demand on the bridge load bearing members.

Combo	PIER 5	PIER 6	PIER 7	PIER 8
1	R	R	F	R
2	P	R	F	R
3	R	R	F	P
4	P	P	F	R
5	R	P	F	P
6	P	R	F	P
7	P	P	F	P
8	F	P	F	P
9	P	F	F	P
10	P	P	F	F
11	P	F	F	F

Combo	PIER 5	PIER 6	PIER 7	PIER 8
12	F	P	F	F
13	F	F	F	F
14	F	R	F	R
15	R	R	F	F
16	R	F	F	F
17	F	R	F	F
18	P	F	F	R
19	R	F	F	P
20	F	P	F	R
21	F	R	F	P
22	P	R	F	F
23	R	P	F	F

Table 10.1-5 – Bearing Combinations

BC CASE 2: To better understand the actual stress condition of the bridge on the day of the collapse, springs can be used to model the presence of concrete piers. Therefore, the stiffness of the piers has been estimated using the approximation shown in Figure 10-5 and Table 10.1-6. In particular, from inspection reports performed during the life of the bridge, Pier 6 showed accumulation of debris and corrosion. It is plausible to consider that the roller was not able to move as designed. The calculated Pier 6 stiffness has been implemented in the sap model adding a lateral spring element at Pier 6 supports and this model has been used for a second set of analysis (BC CASE2).

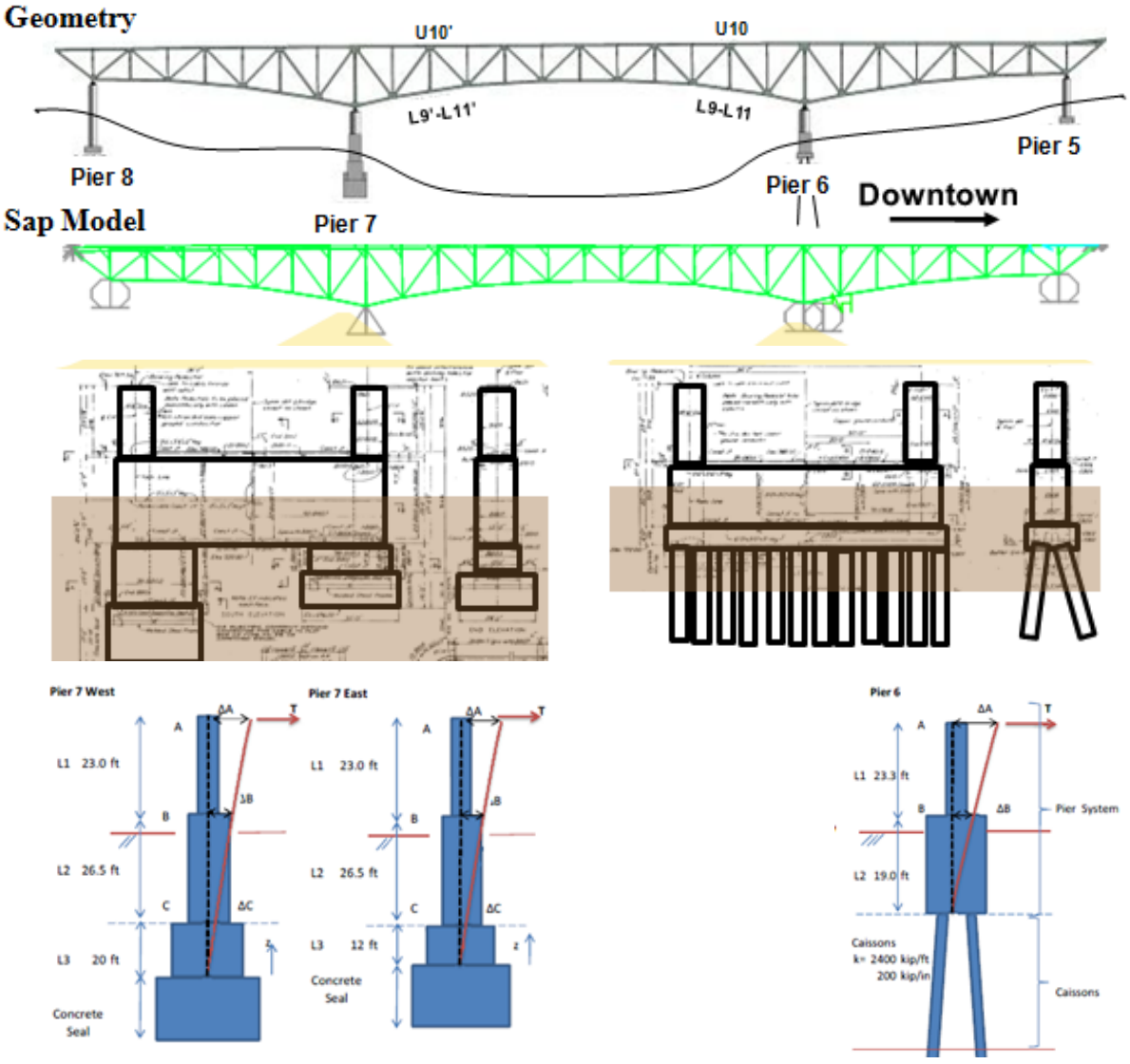

Figure 10-5 – Piers stiffness calculation

- **Load Combinations**

The load combinations used are summarized in Table 10.1-7 and they represent combination of dead and live load existing on the bridge at the time of the collapse as well as the different temperature change scenarios.

	ELASTIC		CRACKED	
	$K_{1\ column}$		$K_{1\ column}$	
	[kip/in]	[kN/m]	[kip/in]	[kN/m]
Pier 5	4,28	74´934	2,99	52´349
Pier 6	2,384	417´391	1,729	302´713
Pier7 E	1,875	328´275	1,313	229´880
Pier7 W	1,550	271´374	1,085	189´962
Pier 8	104	18´208	73	12´781

Table 10.1-6 – Piers stiffness

A = DL + RET + 12°F	DL= bridge dead load; RET=additional load applied as results of retrofits; AUG= traffic and construction loads the day of the collapse (NTSB,2008b)
B = DL+RET+AUG+47°F	
C = DL + RET + 57°F	
D = DL+RET+AUG+12°F	
E = DL+RET+AUG+57°F	

Table 10.1-7 - Load Combinations

10.1.2 Analyses Results

10.1.2.1 BC CASE 1

Among all the load combinations, the combination B (DL+RET+AUG+47°F) has been chosen for the purposes of this study since it is the one that considers the loads and temperature on the day of the collapse. Set the load combination, we can proceed discussing in detail the influence of the bearing conditions. Considering the restraints combinations listed in Table 10.1-5 has been found that the compression load increases when bearing combinations 5, 7 to 13, 19 and 23 are used, independently by the portion of bridge irradiated. The mentioned combinations are the most disadvantageous because they show an increase in demand in the bottom chord member L9-L11 West and East. Table 10.1-8 shows the maximum compression values of the member L9-L11 West and East.

BEARING COMBINATION (Table 10.1-5)	Axial force	
	kip	kN
5	2,121	9´434
7-13	2,165	9´633

19	2,268	10´090
23	2,268	10´088

Table 10.1-8 - Maximum compression force in L9-L11 member - Disadvantageous bearings combinations (BC CASE 1)

Besides, the combinations 3, 6, 15, 17 and 21 give a positive contribute, relieving the compression in the member L9-L11. Listed in Table 10.1-9 are the maxim compression values of the L9-L11member between the west and east truss.

BEARING COMBINATION (Table 10.1-5)	**Axial force**	
	kip	**kN**
5	1,190	5´294
7-13	1,587	7´063
19	1,190	5´293
23	1,588	7´063

Table 10.1-9 - Maximum compression force in L9-L11 member - Advantageous bearing conditions (BC CASE 1)

10.1.2.1 BC CASE 2

For the same load combination B (DL+RET+AUG+47°F), using the springs to model the stiffness of piers 6 the resulting maximum compression force in L9-L11 is shown in Table 10.1-10.

	Axial force	
	kip	**kN**
Dead Load	560	2´491
Retrofit	130	578
Aug1	80	355
Temp.	1,090	4´848
Total	1,860	8´273

Table 10.1-10 - Maximum Compression force in L9-L11 (BC CASE 2)

In the light of the forensic investigation the load combination which considers the actual loading condition on the bridge on the day of the collapse has been taken into account.

The two boundary condition modeling approaches used show the sensitivity of the main members demand to the bearings support conditions. As the roller bearings gathered corrosion and debris ever larger forces were required to cause the bearing to move. As a result, seized bearings turned a functionally non-redundant truss into an indeterminate structure. This led to a significant increase of forces in the bottom chord as the temperature increased which were not accounted for in the original design (Cao, 2012).

Form the analyses set (BC CASE1) the upper bound results show a compression force in the member of about 2,300 kips (10′230 kN), the lower bound a compression force of about 1,200 kips (5′337 kN). The model BC CASE2 where the spring at pier 6 has been used indicates a maximum compression force of 1,860 kips (8′274 kN) in the L9-L11 member.

It becomes fundamental, in order to assess the bridge integrity and for the purposes of the forensic investigation, to investigate the buckling and post buckling capacity of the main truss bottom chord member L9-L11.

10.2 LOCAL FINITE ELEMENT MODEL

The study focuses on the effect of perforations and boundary conditions on the behavior of the built up member. This local-level model provided information on the post buckling behavior and capacity of the load bearing member using nonlinear buckling analysis. Different models have been used in order to understand the effect of perforation and boundary conditions. A three dimensional solid element model of the recognized critical load bearing member L9-L11 comprised of a welded built up section with perforated cover plates was constructed in Abaqus based on the original drawings Figure 10-6 and springs were applied to the member ends to simulate the effective boundary conditions between the individual element and adjacent members.

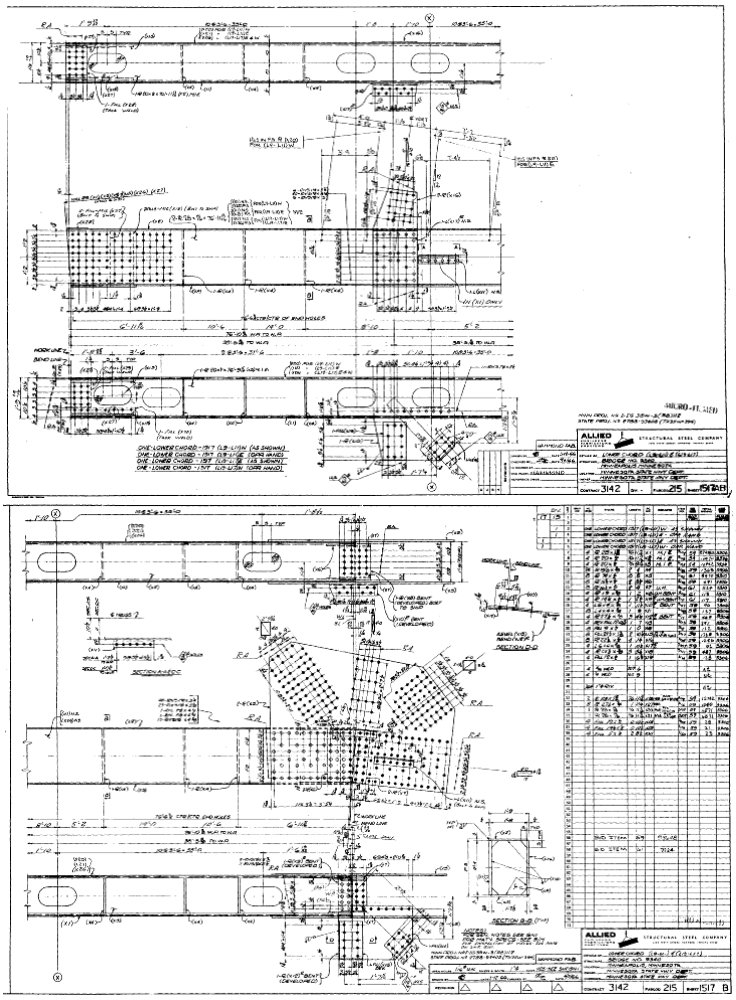

Figure 10-6 - Member L9-L11 shop drawings (MnDoT, 2012)

10.2.1 Model Description

All the models analyzed are built using continuum (solid) element C3D8R assembled to form a rectangular built up section. Some of the models included the opening on the top and bottom plates. A view of a typical 3D model is shown in Figure 10-7. The gusset plates are modeled only partially just to account of the extra steel thickness that they provide at the ends.

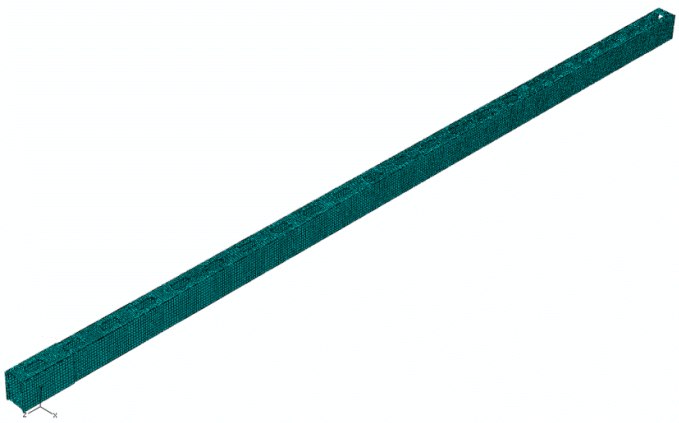

Figure 10-7 - Rectangular built up section with perforations – Overview

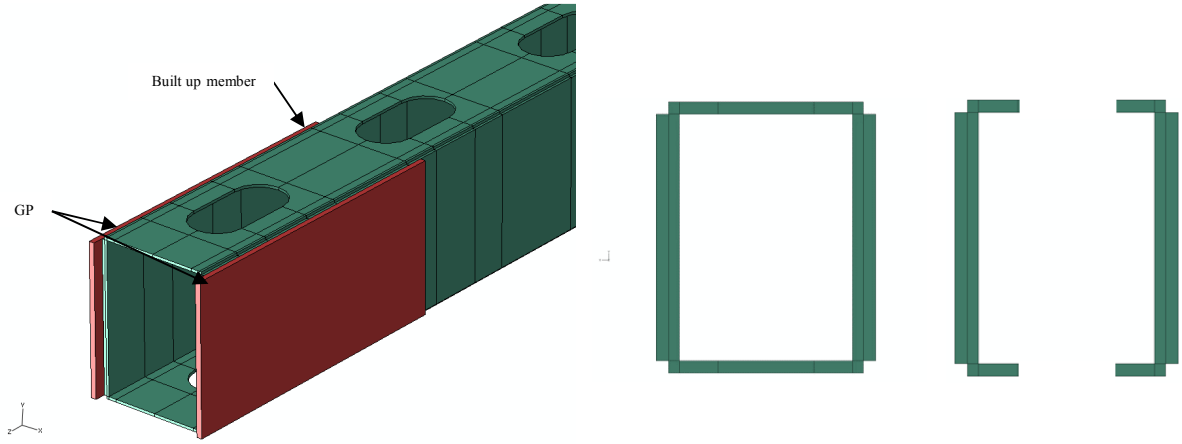

Figure 10-8 – Built up section geometry

Built up Section See (Figure 10-8)

Top /Bottom plate Thickness = 0.5 in (1,27cm) Lateral plate Thickness = 0.94 in (2,38 cm)
Length = 20 in (50,8 cm) Length = 28 in (71,12 cm)

Total Area =72.64 in^2 (468,6 cm^2)

Built up Member:

Total Length = 922 in (23,41 m) Total Volume = 63046.22 in^3 (1,03 m^3)

Gusset plate and Perforated cover plate (Figure 10-9)

Holes Spaced 3'-6'' (106 cm) center to center.

GP **L9:** plate thickness = 1in (2,54 cm) **L11:** plate thickness = 0.5in (1,27 cm)
Offset from box section cut plane = 2in Offset from box section cut plane = 2''

20 ''

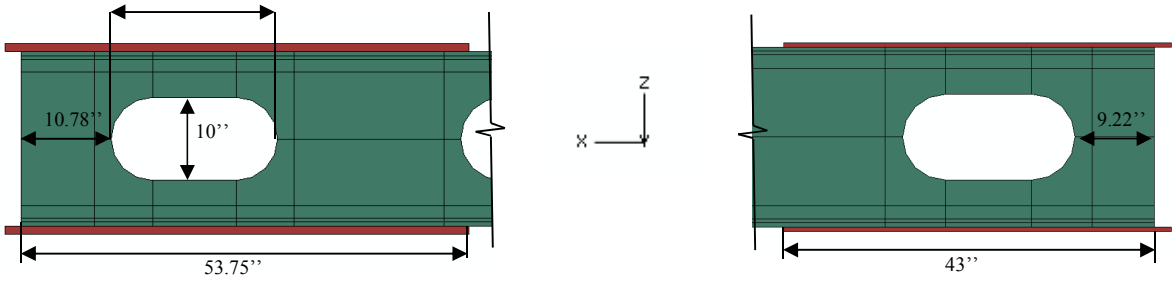

Figure 10-9 – Perforation spacing

Material

Two different types of steel materials, 50 ksi (345 MPa) and 36 ksi (250 MPa) steel, were used for the components in the 3D model. The steel was represented as an isotropic elasto-platic material with the material properties shown in Table1 and the true stress-plastic strain curve shown in Figure 10-10. The stiffness, Poisson's ratio, coefficient of thermal expansion and elasto-plastic properties of the steel were provided by NTSB and FHWA (NTSB, 2008c) and shown in Table 10.2-1. A higher stiffness value was used for the 50 ksi (345 MPa) steel to take into account the real geometrical configuration of the whole gusset plate system at the panel point L9 and L10. In the Abaqus model the 36 ksi (250 MPa) steel has been used for the L9-L11 main truss lower chord member and the 50ksi (345 MPa) steel has been used for the gusset plate. Beyond the maximum input plastic strain, the material behavior would be assumed to be perfectly plastic.

Material	**Elastic Modulus (ksi) [GPa]**	**Poisson's ratio**	**Density (lbm/in^3) [Kg/m^3] [Kg/m^3]**	**Yield strength (ksi) [MPa]**	**CTE (in/(in-°F)) [mm/m/°C]**	**Specific heat (Btu/lbm °F) [kcal/kg]**	**Conductivity (Btu/(hr-in-°F) [kcal/m °C]**
36 ksi	29,000 [200]	0.26	0.28 [7´850]	36.0 [250]	6.5 x 106 [0,0123]	0.11 [0,12]	2.4 [68]
50 ksi	31,900 [220]	0.3	0.28 [7´850]	50.0 [345]	6.5 x 10^6 [0,0123]	0.11 [0,12]	2.4 [68]

Table 10.2-1 - Steel properties

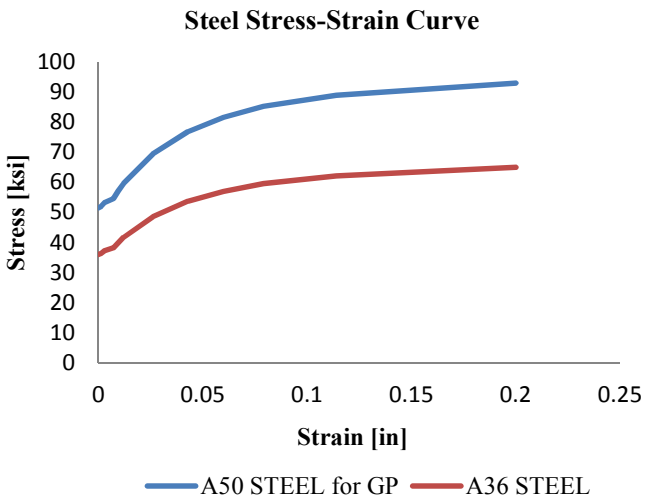

Figure 10-10 - Steel Stress-Strain Curves

Boundary Conditions

One important aspect to take care of, studying the structure following a decomposition approach, is the modeling of the exact boundaries conditions for the elements that has been extrapolated. The isolated subsystem model, in fact, lacks in the restraint offered by the subsystem. To consider the effective boundaries conditions for the local model springs elements SPRING1 were applied to model the connection with the global model. See Figure 10-11. SPRING1 is a linear connectors; a spring between node and ground, acting in a fixed direction.

The stiffness has been estimated using a formula for equivalent stiffness combination of springs as shown in Figure 10-12 and the values used in the model are shown in Table 10.2-2.

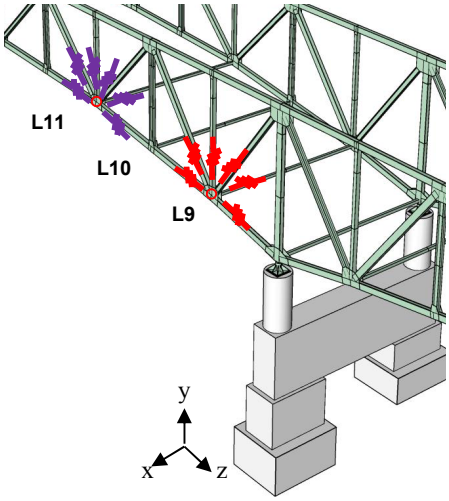

Figure 10-11 - Spring system - Revit Model Rendering (TT)

Spring Combination	Stiffness Formulas for System
6. 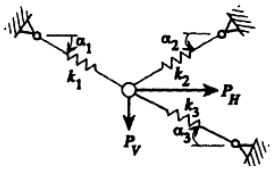	$k_H = \sum_i k_i \cos^2 \alpha_i$ $k_V = \sum_i k_i \sin^2 \alpha_i$ where k_H = horizontal stiffness k_V = vertical stiffness

Figure 10-12 - Stiffness formula for spring system at panel point

	PP L11	PP L10	PP L9
kx	Fix	Fix	Fix
ky	7770 kip/in 13607 kN/cm	Fix	7770 kip/in 13607 kN/cm
kz	1470 kip/in 2574 kN/cm	Free	1470 kip/in 2574 kN/cm
krx	Fix	Free	Fix
kry	3E+8 in-lb/rad 33900 kN m/rad	Free	4E+8 in-lb/rad 45200 kN m/rad
krz	Fix	Fix	Fix

Table 10.2-2 - Spring stiffness at panel point (PP) L9, L10, L11 (Pilkey,1994)

10.2.2 Linear Buckling and Post Buckling Analyses

A linear eigenvalue buckling analysis is generally used to estimate the critical buckling loads of stiff structures and may be sufficient for design evaluation. This type of analysis is a linear perturbation procedure, and buckling loads are calculated relative to the base state of the structure; but if there is concern about material nonlinearity, geometric nonlinearity prior to buckling, or unstable post-buckling response, a load-deflection analysis must be performed to investigate the problem further (Simulia, 2009).

Geometrically nonlinear static problems sometimes involve buckling or collapse behavior, where the load-displacement response shows a negative stiffness, and the structure must release strain energy to remain in equilibrium. In a typical geometrically nonlinear static analysis, it is common for the analysis to diverge at the stability limit of the structure. To investigate the post buckling capacity other analysis method can be employed, such as a dynamic analysis procedure or a modified Riks method.

The modified Riks method allows material non linearity, geometric non linearity and could predict complex unstable responses; often follows an eigenvalue buckling analysis to provide complete information about a structure's collapse and can be used to speed convergence of ill conditioned or snap through problems that do not exhibit instability. This method is used for cases where the loading is proportional; that are where the load

magnitude is governed by a single scalar parameter. The load magnitude and the displacement are unknown variables and are solved together. The load could increase or decrease, depending on the structure's stiffness. The Riks method uses the load magnitude as an additional unknown; it solves simultaneously for loads and displacements. Therefore, another quantity must be used to measure the progress of the solution; Abaqus/Standard uses the arc length along the static equilibrium path in load-displacement space. This approach provides solutions regardless of whether the response is stable or unstable.

In Abaqus/Standard the Riks method can be used to solve post buckling problems, both with stable and unstable post buckling behavior. However, the exact post buckling problem often cannot be analyzed directly due to the discontinuous response (bifurcation) at the point of buckling. To analyze a post buckling problem, you must turn it into a problem with continuous response instead of bifurcation, which can be accomplished by introducing a geometric imperfection pattern in the "perfect" geometry so that there is some response in the buckling mode before the critical load is reached. Imperfections are usually introduced by perturbations in the geometry. Abaqus offers three ways to define an imperfection: as a linear superposition of buckling eigenmodes, from the displacements of a static analysis, or by specifying the node number and imperfection values directly. Only the translational degrees of freedom are modified. Abaqus will then calculate the normals using the usual algorithm based on the perturbed coordinates. Unless the precise shape of an imperfection is known, an imperfection consisting of multiple superimposed buckling modes can be introduced. The usual approach involves two analysis runs with the same model definition, using Abaqus/Standard to establish the probable collapse modes and either Abaqus/Standard or Abaqus/Explicit to perform the post buckling analysis. The Riks procedure can also analyze post buckling and collapse due to thermal straining. The loads generated by the thermal strain contribute to the "reference" load specified for the Riks analysis and are ramped up with the load proportionality factor. In Abaqus, nodal temperatures can be specified as "Predefined fields". Any difference between the applied and initial temperatures will cause thermal strain if a thermal expansion coefficient is given for the material.

The models used and the results of the analyses performed are discussed in the next section.

10.2.3 Models and Analyses Results

Different models have been used in order to understand the effect of perforation and boundary conditions.

First, the eigenvalue analysis is used to obtain estimates of the buckling loads and modes. The numerical results of the buckling analyses obtained by detailed FEM models were

compared with results obtained from the hand calculation. For the L9-L11 member, the hand calculation follows provisions of the AISC 360-05 Specification for Structural Steel Buildings (AISC, 2005), with the modified slenderness ratio (KL/r)m, and the Timoshenko theory for built up columns and plates, considering columns with perforated cover plates (Timoshenko,1961) as shown in details in Appendix A.

The second phase of the study is the performance of load-displacement analyses using the Riks method, where imperfections consisting of the critical buckling modes obtained in the previous analyses are introduced as well as temperature loading and different boundary conditions.

The following list summarizes the models used:

- CASE 1 – Box – Without Perforated Cover Plates - Two supports;
- CASE 2 – Box – With Perforated Cover Plates - Two supports;
- CASE 3 – Box – Without Perforated Cover Plates – Three supports;
- CASE 4 – Box – With Perforated Cover Plates – Three supports;

At last, in order to investigate the behavior of the I-35W bridge bottom chord member, springs have been applied as well as temperature gradient in order to simulate as closely as possible the actual condition of the member the day of the collapse.

- CASE 5 – L9-L11 member.

CASE 1 – Box – Without Perforated Cover Plates - Two supports

In Case 1 a 3D solid element model comprised of a rectangular built up element without perforations has been analyzed. Three different support conditions have been considered. Figure 10-13 shows the deformed shape of the members into the elastic buckling and post buckling response and the related critical value.

Simply supported member:

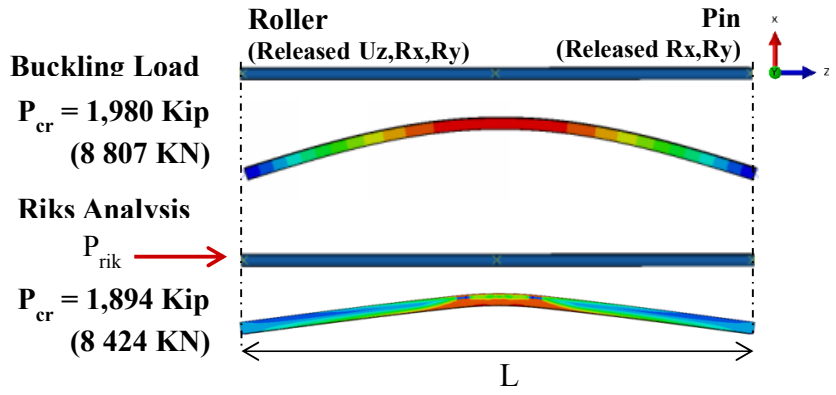

Roller-Fix member:

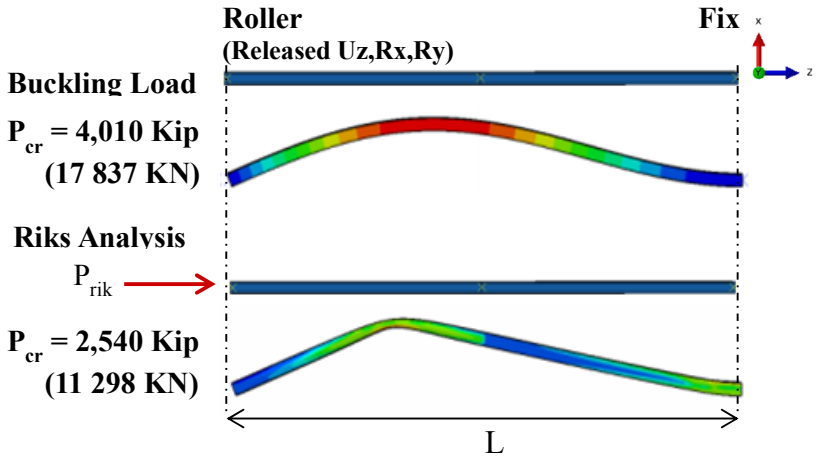

Fix -Fix member:

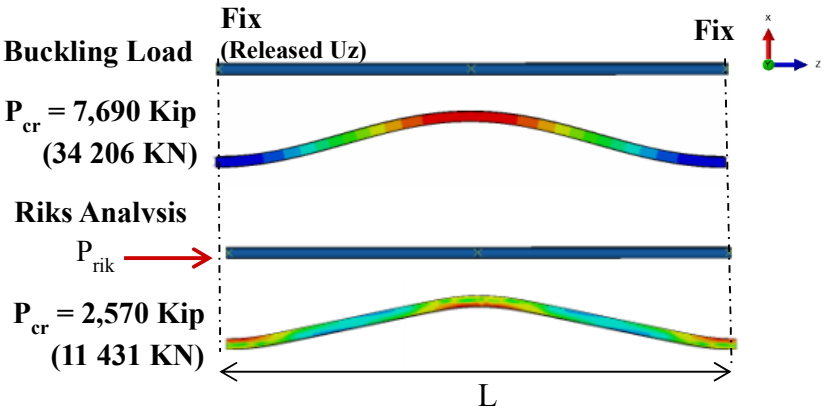

Figure 10-13 - Case 1 - Deformed shape into elastic and post buckling response

CASE 2 – Box – With Perforated Cover Plates - Two supports

Case 2 analyzes 3D solid element models comprised of a rectangular built up element with perforations. Three different support conditions have been considered. Figure 10-14 shows the deformed shape of the members into the elastic buckling and post buckling response and the related critical value.

Simply supported member:

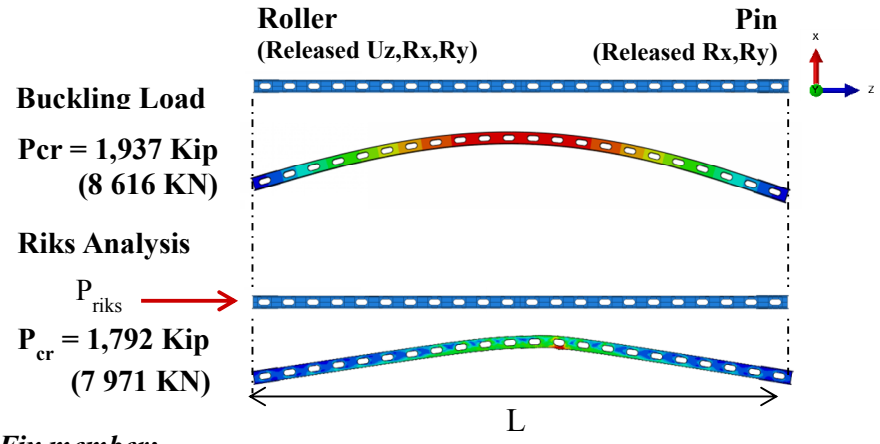

Roller-Fix member:

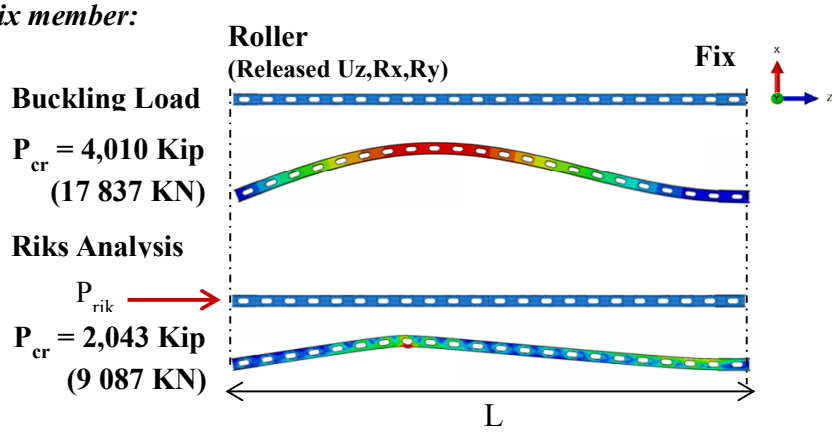

Fix -Fix member:

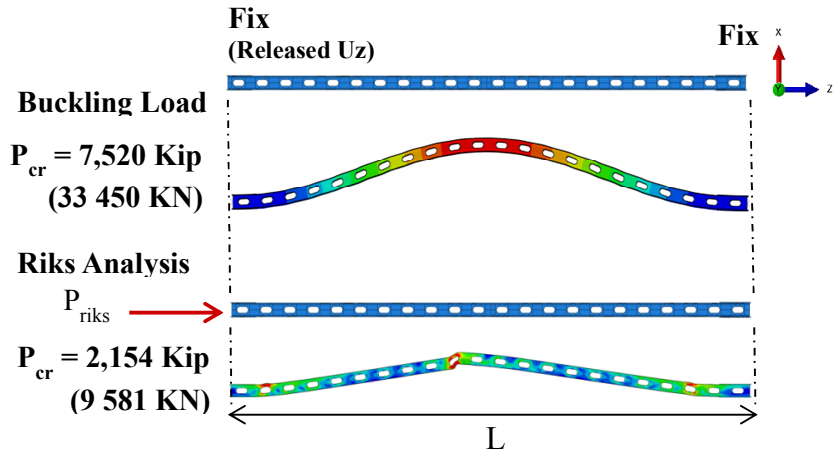

Figure 10-14 - Case 2 - Deformed shape into elastic and post buckling response

Figure 10-15 shows the applied load against the axial displacement of the reference node at the end of the member.

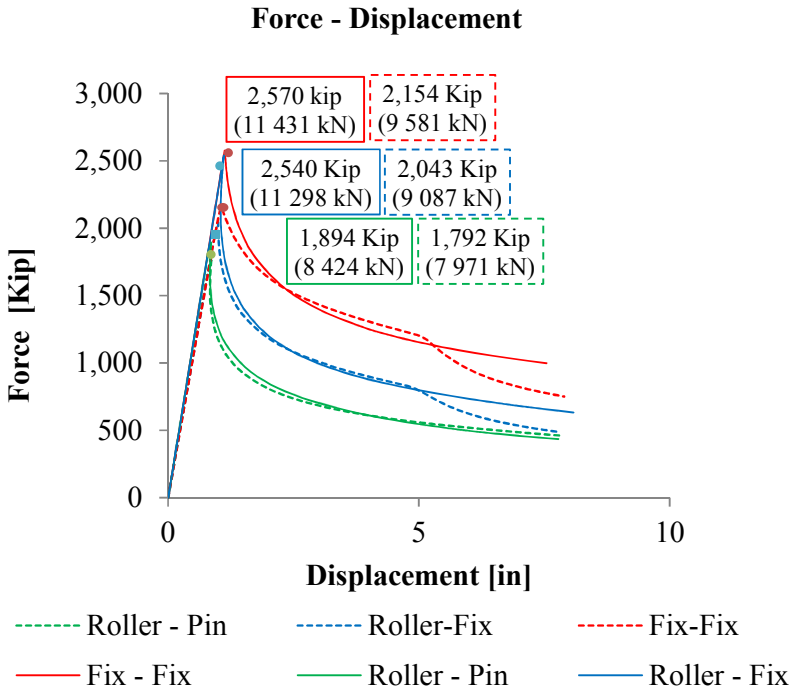

Figure 10-15 - Force-Displacement curves comparison for CASE 1 and CASE 2

Figure 10-15 shows that all the curves for the different models have a similar trend. It can be noted that the peak load is sensitive to the boundary conditions. In particular softening the supports reduce the critical load by 16% when the cover plates are perforated and by 26 % when the cover plates are not perforated.

It should also be noted that the critical load calculated using the AISC 360-05 K - values are reasonably close to the post buckling peak values whereas the eigenvalue obtained from the linear buckling analysis largely overestimate the capacity of the member. See Table 10.2-3.

		$P_{cr} = \frac{\pi^2 EI}{(KL)^2}$		**ABAQUS Linear Buckling**		**ABAQUS Riks Analysis**	
	K	Kip	KN	Kip	KN	Kip	KN
Pin - Roller	**1**	1,987	8´838	1,980	8´807	1,890	8´470
Roller - Fix	**0.7**	2,700	12´010	4,000	1´779	2,540	11´298
Fix - Fix	**0.5**	3,119	13´874	7,000	31´137	2,570	11´431

Table 10.2-3 – Critical Load Comparison

CASE 3 – Box – Without Perforated Cover Plates – Three supports

Case 3 analyzes a 3D solid element models comprised of a rectangular built up member without perforations. Two different support conditions have been analyzed. Figure 10-16 shows the deformed shape of the members into the elastic buckling and post buckling response and the related critical value.

Fix-Roller-Roller member:

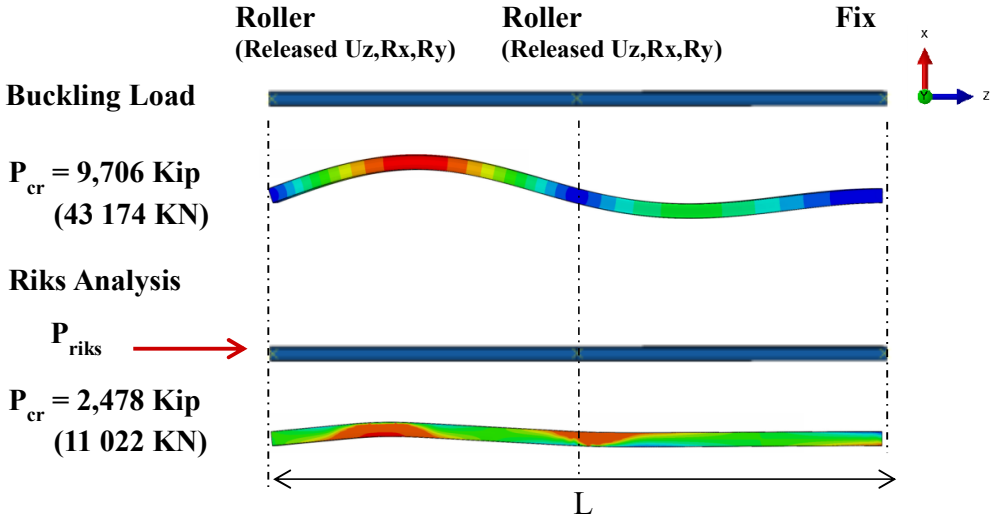

Pin-Roller-Roller member:

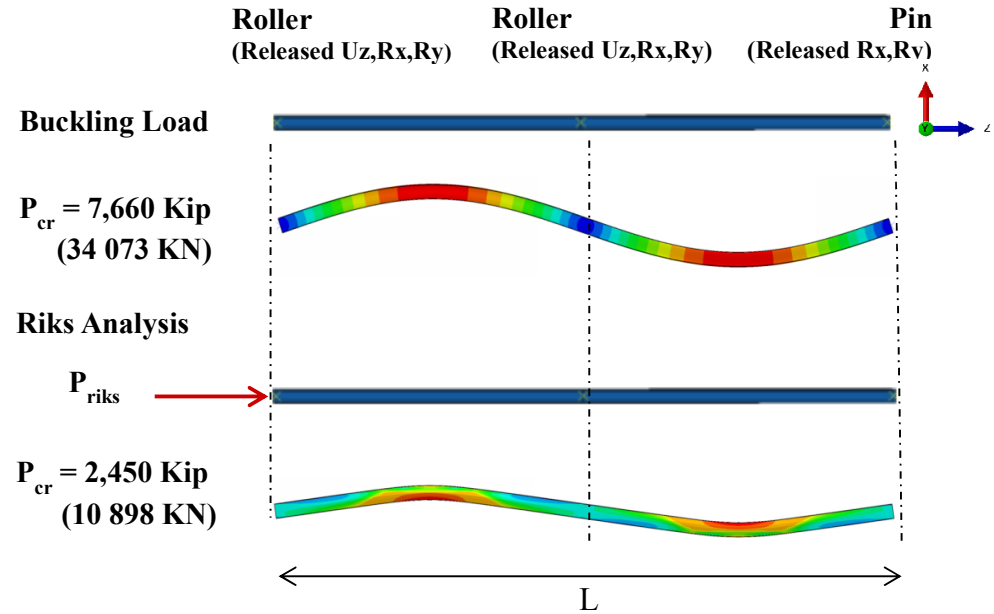

Figure 10-16 - Case 3 - Deformed shape into elastic and post buckling response

CASE 4 - Box – With Perforated Cover Plates – Three supports

Case 4 considers 3D solid element models comprised of a rectangular built up member with perforations. Two different support conditions have been analyzed. Figure 10-17 shows the deformed shape of the members into the elastic buckling and post buckling response and the related critical value.

Fix-Roller-Roller member:

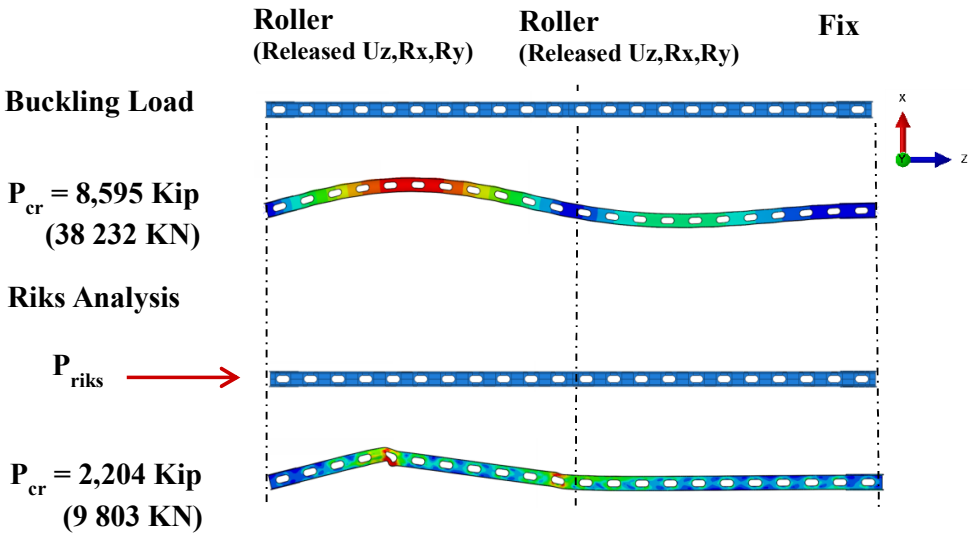

Pin-Roller-Roller member:

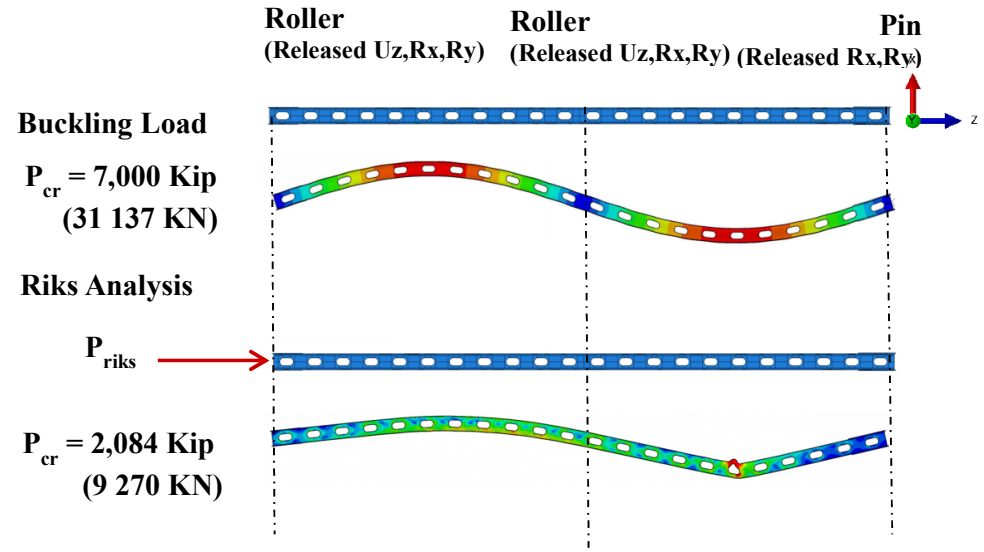

Figure 10-17 - Case 4 - Deformed shape into elastic and post buckling response

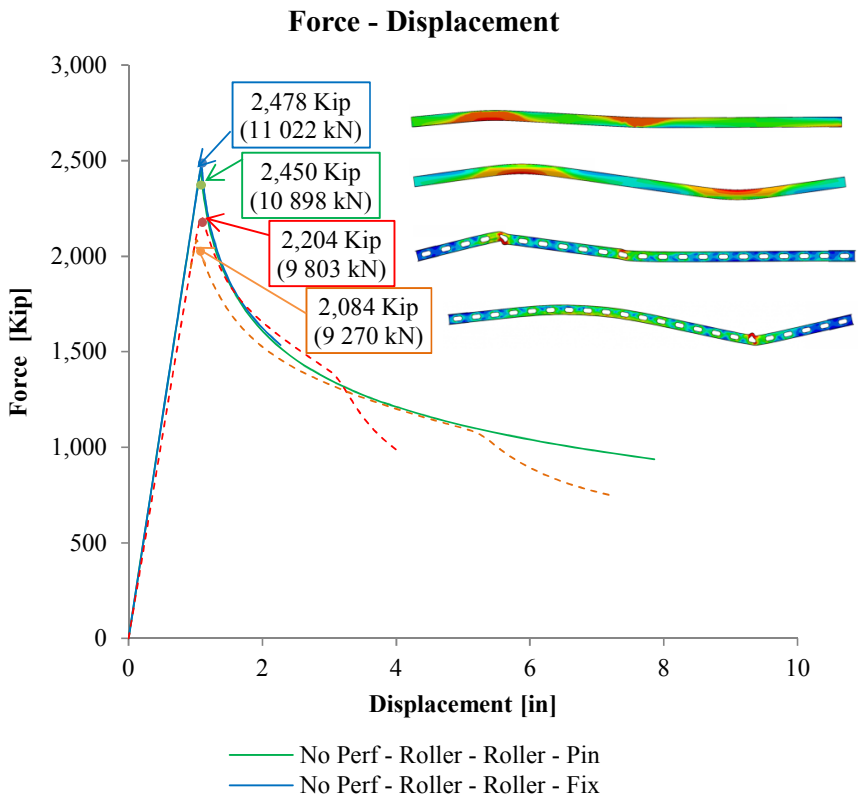

Figure 10-18 - Force-Displacement curves comparison for CASE 3 and CASE 4

Figure 10-18 shows that all the curves for the different models have a similar trend. It can be noted that the peak load is sensitive to the boundary conditions. In particular softening the support reduces the critical load by 5% when the cover plates are perforated and by 1% when the cover plates are not perforated.

The reason why the difference is smaller between CASE 3 and CASE 4 than it is between CASE 1 and 2 is due to the presence of the third support which shorten the un-braced length therefore mitigating the effect of the fixity or softer support on one side.

CASE 5 – L9-L11 member.

In order to investigate the behavior of the L9-L11 bottom chord member, the 3D FEM model has been constrained using springs which stiffness have been calculated in Section 10.2.1.

North West Side

Secondary moments obtained from the global SAP model have been applied at L9, L10, L11 panel points as well as temperature gradient to consider the thermal strain induced by temperature to the member. A scaled buckling mode shape has been used as initial

imperfection. It can be seen in Figure 10-19 that the member without any temperature or initial imperfection has a quite large post buckling capacity. The critical load decreases and the curve sudden drops showing a poor post buckling capacity when imperfections and temperature are introduced in the model.

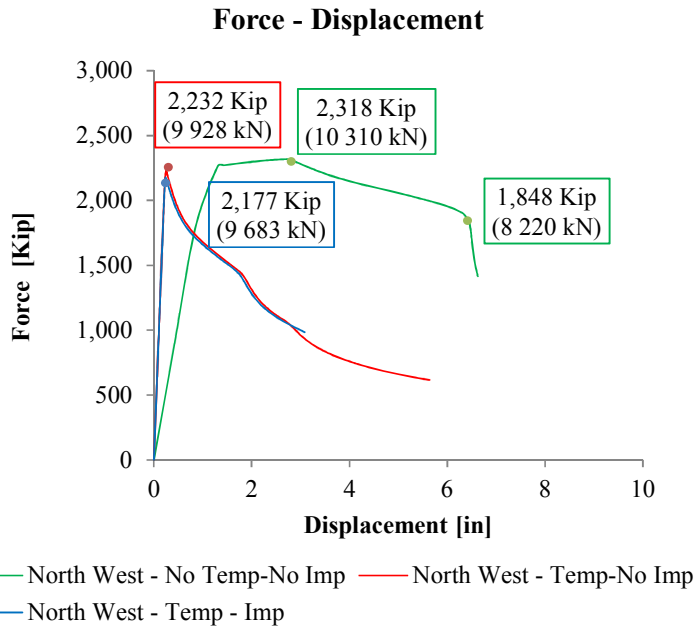

Figure 10-19 – North West member - Load-Displacement curves

The locations of the plastic hinges found in the Abaqus deformed shape shown in Figure 10-21 match the visible deformation on to the recovered member after the collapse. Figure 10-20 shows the location of the bottom chord member located on the bridge schematic overview as well as the deformed member recovered after the collapse.

Figure 10-20 - View of the North West Side member L9'W -L11'W

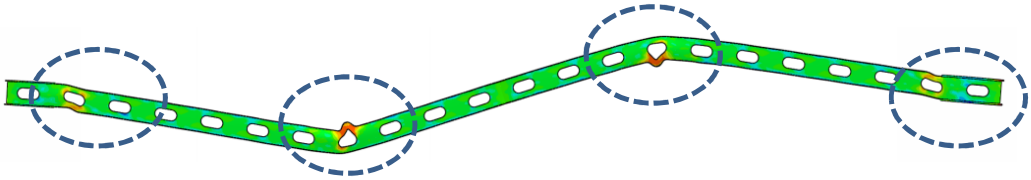

Figure 10-21 – Deformed shape into post buckling response

South West Side

Secondary moments obtained from the global SAP model have been applied at L9, L10, L11 panel points. The post buckling deformation and force – displacement plot in Figure 10-22 shows a large drop which results in a sudden loss of capacity for the member and the formation of a plastic hinge, similar to the behavior of the North side L9-L11 member. Once the capacity of the deformed member is overcome by the actual load the collapse is triggered.

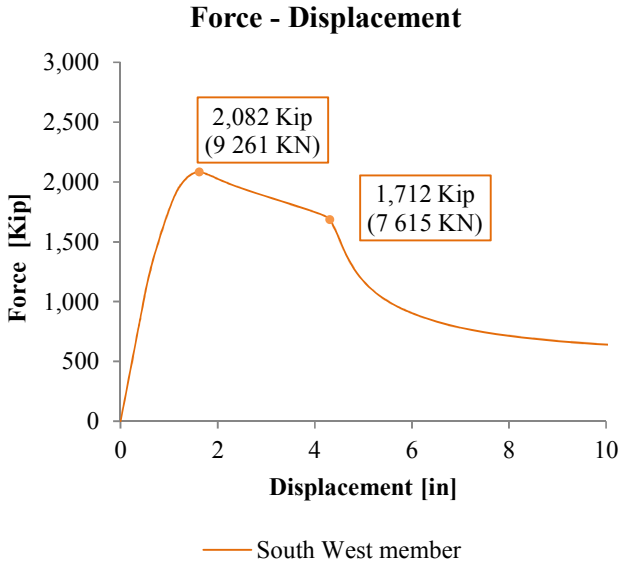

Figure 10-22 – South West member - Load-Displacement curves

The post buckled deformed shape obtained has also been compared to the recovered deformed member and it is shown in Figure 10-23 and Figure 10-24 the matching plastic hinge and deformations.

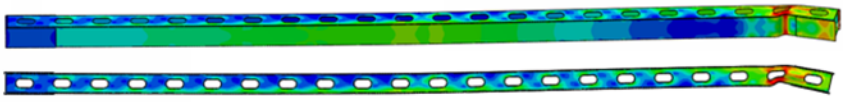

Figure 10-23 –Deformed shape into post buckling response

Figure 10-24 - View of the South West Side member L9W-L11W

CONCLUSIONS

11 CONCLUSIONS

The thesis has been developed in the frame of the forensic investigations into the causes of the collapse of the I-35W Bridge. The structural failure brought the bridge to catastrophically plunge into the Mississippi river on August 1st, 2007, in Minneapolis, MN, USA.

The I-35W Bridge was a state of the art structure when designed and built in 1960s. It was a continuous truss bridge spanning 1000 ft. (305 m.) over four piers. Over the years, bridge inspectors had catalogued the roller bearing's deterioration. However, no analysis had been performed during past retrofits design to ascertain if the bridge could withstand the large temperature swings common in Minneapolis. The combination of the increased weight of the bridge due to retrofits, construction vehicles, material stationed on the bridge and temperature load effect proved to be catastrophic for the lower chord member that spanned from L9-L11. Buckling of the bottom chord was the fuse that triggered the instability of the global system and initiated the collapse.

The failure of the I-35W represents a major case-study for the evaluation of stability and integrity of a steel truss bridge. The aim of the work has been to investigate the bridge's untested fragility using the multilevel analysis approach: globally its capacity to carry temperature loads and locally the post buckling behavior of the bottom chord member. In general, if a compression member has enough post buckled capacity, it can absorb some overstress and release it by deforming while still being able to carry the loads thus indicating a local source of robustness. For this functionally non-redundant bridge the initiating buckle and local plastic hinges resulted in a global instability and total collapse.

The global-level model reproduced the entire bridge based on original drawings, design and construction specifications. The model has been verified by comparing results with the available original design calculations. Member forces and reactions based on as-designed conditions with the specified design loads were confirmed. The model served to investigate the bridge's elastic behavior and its overall response to various loading conditions. In particular, from the global model it has been possible to evaluate the static stress condition on the bridge showing how some of temperature changes and possible deterioration of the designed supports could affect the load carrying members' demand. In the case of the I-35W Bridge the bearings were designed to accommodate both the static loads imposed by the superstructure's self-weight and the dynamic forces generated by vehicle traffic, wind, temperature variations. The analyses performed highlighted how the non-functioning roller bearings would likely result in an increase in compression forces in the lower chords from

thermal expansion. This is particularly true in places like Minnesota where there are significant temperature extremes during the course of a year.

As results of the global model analysis, two boundary condition approaches used showed the sensitivity of the main members demand to the bearings support conditions. Seized bearings turned a functionally non-redundant truss into an indeterminate structure. This led to a significant increase of forces in the bottom chord as the temperature increased which were not accounted for in the original design. In particular for the L9-L11 member, the upper bound results show a compression force in the member of about 2,300 kips (10´230 kN), the lower bound a compression force of about 1,200 kips (5´337 kN). The model where springs at pier 6 have been used indicates a maximum compression force of 1,860 kips (8´272 kN) in the bottom chord member, L9-L11.

In the light of the results obtained from the global analyses and in order to investigate their effect on the structural integrity and stability of this non-redundant bridge, it became fundamental to investigate the buckling and post buckling capacity of the member L9-L11.

At a local level, different models have been used in order to understand the effect of perforations and boundary conditions on the L9-L11 member. The rectangular built up member has been modeled in Abaqus with and without perforated cover plates and nonlinear buckling analyses have been carried out.

First, linear eigenvalue analyses have been used to obtain estimates of the buckling loads and modes. In the last part of the study load-displacement analyses using the Riks method have been performed, where imperfections consisting of the critical buckling modes obtained in the previous analyses were introduced as well as different boundary conditions. In order to represent as closely as possible the I-35W bridge bottom chord member, springs have been applied as well as temperature gradient in order to simulate as closely as possible the actual condition of the member the day of the collapse. Secondary moments from the global have also been applied to the element.

The numerical results of the buckling analyses obtained by detailed FEM models were compared with results of hand calculated elastic buckling loads. In general, it has been found that the post buckling analyses using Riks method depict a critical compression load closer to the hand calculated critical value then the elastic buckling analysis. The hand calculation follows provisions of the 2005 AISC 360 Steel Design Guide-Specification for Structural Steel Buildings with the modified slenderness ratio (KL/r)m, and the Timoshenko theory for built up columns and plates, considering columns with perforated cover plates (Timoshenko,1961) for the specific case of the member L9-L11 is shown in Appendix A.

The load-displacement curves obtained using the Riks procedure showed how the boundary conditions affect the maximum load as well as the perforations of the cover plates. The different cases analyzed where stiffer supports were used showed a higher critical load of about 16% than the critical load calculated using a rotation free support where the member doesn't have perforated cover plates or 26% where the cover plates are perforated.

In particular for the model that contains springs, temperature load and secondary moments, the critical load decreases and the load-displacement curve sudden drops showing a poor post buckling capacity when imperfections and temperature are introduced. The post buckling force – displacement plot shows a peak at about 2,000 kips (8´896 kN) which is comparable with the hand calculated buckling load in Appendix A. Once the maximum compression load is reached the load starts decreasing until there is a large drop at about 1,700 kips (7´561 kN) which results in the formation of a plastic hinge and a sudden loss of capacity for the member. The demand on the member according to the global model is about 1,800 kips (8´006 kN). Once the capacity of the deformed member is overcome by the applied load, the collapse of this non redundant structure is triggered. The post buckled deformed shapes obtained have also been compared to the recovered deformed members and it is shown in Figure 10-20 and Figure 10-24 the matching plastic hinges and deformations.

The thesis focused on technical aspects and did not attempt to assign responsibility among the involved parties. Nevertheless, the results of the analyses carried out in this work have been used by Thornton Tomasetti (TT) to enrich a nonlinear bridge model that was developed by the firm in LS-DYNA during the forensic investigation. The simulation performed by TT confirmed that the evidence did not support the US National Transportation Safety Board conclusion that a lateral instability at the under-designed U10 gusset was the fuse that resulted in the collapse. Instead, the model confirms that collapse initiated by the buckling of the bottom chord best matches the bridge collapse video and local failure behaviors. The results of the forensic investigation performed by TT were used in the litigation trial and resulted in a settlement in the legal case between the survivors and those who lost loved ones in the bridge collapse against the firm who was hired by the State of Minnesota to evaluate the bridge structural integrity.

The tragedy of the I-35 West Bridge collapse can serve as a cautionary tale for new taller, longer and lighter structures. As proven by history, at any time during the past, innovations and new technologies are developed and used in the design and construction bringing advantages but also carrying uncertainties related to the absence of solid experience or miss observations and care of the original intent of the design during the years. The effect of new technologies lasts beyond the design process. When all the steel is the same grade changes in

material strengths are not a critical focus of drawing revision and shop drawing review. However, as new stronger materials are introduced to the design their variety and potential impact on changes become important. In addition, the intent of the design innovations must be remembered in the inspection process as well. If a structure is lighter because it can move under a given loading condition, such as the temperature load effect, then the bearings and expansion joints must be maintained. In addition the structure needs to be thoroughly reviewed when retrofits take place.

APPENDICES

A. CAPACITY CALCULATION OF L9-L11

B. RIKS ANALYSIS

APPENDIX A – CAPACITY CALCULATION OF L9-L11

In the following paragraphs, the capacity of the member L9-L11, comprised of welded plates with perforations to form a built up box section, is calculated. The capacity is estimated using the AISC 360-05 Steel Guide as well as methodologies from the theory of plates (Timoshenko and Gere, 1961). Figure A1-1 shows the net and gross cross sections of L9-L11, the built up box member with perforations herein studied.

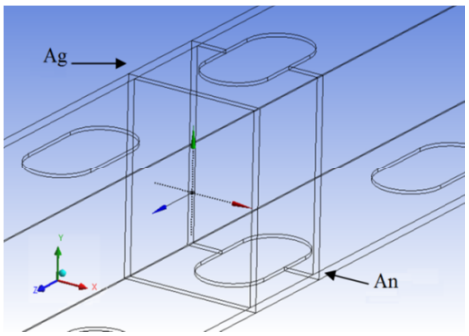

Figure A1-1 – Gross and Net Area of built up section with perforated cover plates

A1. COMPRESSIVE CAPACITY CALCULATION USING AISC 360-05

Using the dimensions shown in Figure A1-2 and according to Chapter B – Section B4 Table B4.1 in AISC 360-05, the built up section is classified as non compact for local buckling. See Table A1-1.

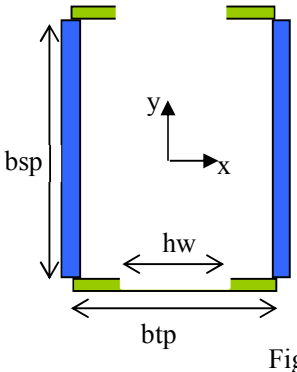

TOP PLATES				
btp	20.00	in	50,8	cm
thickness	0.50	in	1,2	cm
hw	10.00	in	25,4	cm

SIDE PLATES				
bsp	28.00	in	71,2	cm
thickness	0.94	in	2,4	cm

Figure A1-2 – Bottom chord L9-L11 cross section at perforation

Λ_r =	42.29	$\lambda_r = 1.49\sqrt{E/F_y}$
b/t =	40	top plates
b/t =	29.9	side plates
b/t <λr	**NON-COMPACT**	

Table A1-1– Section classification according to Table B4.1 AISC 360-05

Following the provisions of Chapter E – Section E.3 (AISC 360-05), the compressive strength for flexural buckling of a member without slender elements is calculated.

Section E.3 applies to compression members with *compact* and *non-compact section* as defined in Section B4, for uniformly compressed elements. The nominal compressive strength P_n, shall be determined based on the limit state of flexural buckling.

$$P_n = F_{cr} A_g \qquad (6) \qquad\qquad F_e = \frac{\pi^2 E}{(KL)^2} \qquad (7)$$

The flexural stress buckling F_{cr}, is determined as follows:

$$\frac{KL}{r} \leq 4.71\sqrt{\frac{E}{F_y}} \quad or \quad F_e \geq 0.44F_y \qquad F_{cr} = \left[0.658^{\frac{F_y}{F_e}}\right] F_y \qquad (8)$$

$$\frac{KL}{r} > 4.71\sqrt{\frac{E}{F_y}} \quad or \quad F_e < 0.44F_y \qquad F_{cr} = 0.877F_e \qquad (9)$$

Data:

K =	1	**E =**	29,000	ksi	**F_y =**	36	ksi	**L =**	38.4 ft
			200´000	MPa		250	MPa		1´167,5 m

Top-sides	**A_g =**	72.5	in^2	467,75	cm^2			
	r =	10.17	in	25,80	cm	(KL/r)	45.3	
	F_e =	139.29	ksi	960	MPa			
$F_e >= 0.44*F_y$	**F_{cr} =**	**32.31**	ksi	222	MPa			
	$P_n = F_{cr} A_g$ =	**2342**	kip	10´417	kN			
Net section	**A_{g_n} =**	62.5	in^2	403,23	cm^2	$(KL/r)_{eff}$	49.3	
	r_n =	9.35	in	23,74	cm			
	F_{e_n} =	117.8	ksi	812	MPa			
$F_e >= 0.44*F_y$	**F_{cr_n} =**	**31.68**	ksi	218	MPa			
	$P_n = F_{cr} A_n$ =	**1980**	kip	8´807	kN			
Sides only	**A_{g_sides} =**	52.5	in^2	338,71	cm^2	$(KL/r)_{side}$	57.0	
	r_sides=	8.08	in	20,5	cm			
	F_{e_sides} =	88.07	ksi	607	MPa			
$F_e >= 0.44*F_y$	**F_{cr_sides} =**	**30.34**	ksi	209	MPa			
	$P_n = F_{cr} A_{gsides}$ =	**1593**	kip	7´086	kN			

In particular it can be noted that using the critical buckling stress F_e for columns with perforated cover plates provided by the Eq. (5) shown again below the same capacity **P_n = 1980 kip** (8´807 kN) is obtained.

$$F_e = \frac{\pi^2 EI}{(L)^2} \frac{1}{1 + \frac{\pi^2 EI}{(L)^2}\left(\frac{9c^3}{64aEI_f}\right)} \qquad (5)$$

where

c =	20	in	71,12	cm	Length of perforation
a=	42	in	106,70	cm	Distance between perforations

Also, the compressive strength for torsional and flexural-torsional buckling of members without slender elements has been calculated for the L9-L11 member according to Chapter E – Section E.4 (AISC 360-05).

Section E.4 applies to singly symmetric and unsymmetric members, and certain doubly symmetric members, such as cruciform or built-up columns with compact and non compact sections, as defined in Section B4, for uniformly compressed elements.

The flexural stress buckling F_{cr} shall be determinate according to Equation (8) and (9), using the *torsional or flexural-torsional elastic buckling stress, F_e*, determined as follows:

a) For doubly symmetric members

$$F_e = \left[\frac{\pi^2 E C_w}{(K_z L)^2} + GJ\right] \frac{1}{I_x + I_y} \qquad (10)$$

The following quantities are calculated as shown in Figure A1-3 (Seaburg and Carter, 1997)

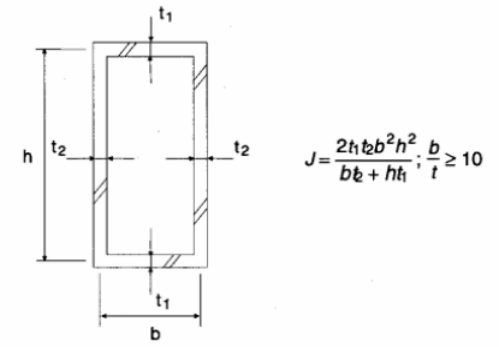

J =	9271	in^4	385,9	cm^4
I_x =	5953	in^4	247,8	cm^4
I_y =	7492	in^4	311,8	cm^4
G =	11,200	ksi	7´722	MPa
C_w =	0		0	
A_g =	72.5	in^2	467,7	cm^2

Figure A1-3 – Torsional constant from Seaburg and Carter, 1997

Therefore:

$F_e >= 0.44*F_y$	**F_e_torsion =**	7723.3	ksi	53´520	MPa	E4-4
	F_{cr}_torsion =	**35.9**	ksi	247	MPa	E3-2
	$P_n = F_{cr} A_g$ =	**2605**	kip	11´587	kN	

Chapter E – Section E6 (AISC 360-05) addresses the calculation of the *nominal compressive strength* P_n of built up members composed of two or more shapes or plates with at least one open side interconnected by perforated *cover plates* or *lacing* with *tie plates*. P_n shall be determined in accordance with Section E3, E4, or E7 (AISC 360-05) subjected to the modification given in Section E6.1 (a) (AISC 360-05).

(ii) For intermediate connectors that are welded or pre-tensioned bolted:

$$\left(\frac{KL}{r}\right)_m = \sqrt{\left(\frac{KL}{r}\right)_0^2 + 0.82\frac{\alpha^2}{(1+\alpha^2)}\left(\frac{a}{r_{ib}}\right)^2} \qquad (11)$$

$\left(\frac{KL}{r}\right)_0$ = Column slenderness of built up member acting as unit in the buckling direction being considered
a = Distance between connectors
r_i = Minimum radius of gyration of individual component
r_{ib} = radius of gyration of individual component relative to its centroidal axis parallel to member axis of buckling
h = Distance between centroids of individual components perpendicular to the member axis of buckling
α = Separation ratio = $h/2r_{ib}$

Therefore considering:

Only Sides plates

$\left(\frac{KL}{r}\right)_0$ =	45.33				$\left(\frac{KL}{r}\right)_m$ =	147.6		
a =	42	in	106,70	cm	**F_{e_m}=**	13.14	ksi	90,6 MPa
r_i =	0.27	in	0,68	cm		$F_e < 0.44*F_y$		
r_{ib} =	0.27	in	0,68	cm	**F_{cr_m}=**	**11.52**	ksi	79,4 MPa
h =	20.06	in	52,30	cm				
α =	37.07				**$P_n=F_{cr}A_{g\ side}$=**	**605**	kip	**2´691** kN
A_g_sides =	52.50	in ^{2}	338,71	cm ^{2}				

Sides plates + Cover Plate

$\left(\frac{KL}{r}\right)_0$ =	45.33				$\left(\frac{KL}{r}\right)_m$ =	55.03		
a =	42	in	106,70	cm	**F_{e_mt}=**	94.50	ksi	651,6 MPa
r_i =	1.21	in	3,07	cm		$F_e >= 0.44*F_y$		
r_{ib} =	1.21	in	3,07	cm	**F_{cr_mt}=**	**30.69**	ksi	211,6 MPa
h =	20.06	in	52,30	cm				
α =	8.29				**$P_n=F_{cr}A_{g\ eff}$=**	**1,918**	kip	**8´531** kN
A_g_eff =	62.50	in ^{2}	403,23	cm^2				

A2 BUCKLING CAPACITY CALCULATION USING PLATE THEORY

In order to calculate the *nominal compressive strength* P_n for local buckling of the built up section with perforated cover plates the elastic buckling stress F_e has been calculated using the theory of plates, and in particular using methodologies proposed in the buckling of thin plates (Timoshenko & Gere 1961). Figure A2-1 shows the perforated cover plate.

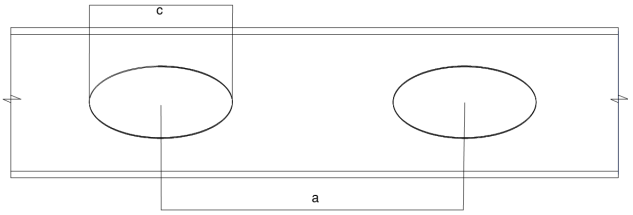

Figure A2-1– Perforated cover plate

The critical stress buckling F_{cr} has been determinated according to Equation (8) and (9) applying the adequate elastic buckling stress F_e calculated according to the different cases discussed in the following paragraphs.

In order to study the local buckling of a simply supported plate uniformly compressed in one direction, the critical value of the compressive stress F_e is calculated using Equations (12) where the coefficient k is calculated using Table 9-1 from Timoshenko and Gere, 1961. Figure A2-Figure A2-2 shows the geometry of the rectangular plate assumed for the calculation.

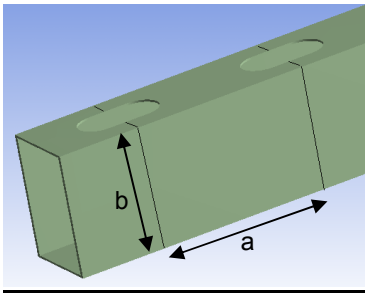

Figure A2-2 Rectangular plate assumed for the calculation

$$F_e = \frac{k_p \, \pi^2 E}{12(1-\nu^2)} \frac{h}{b^2} \qquad (12)$$

Data:

h =	0.94	in	2,38	cm	Plate Thickness
b =	28	in	71,12	cm	Plate Width
a	42	in	106,70	cm	Length of plate which is considered unsupported
a/b =	1.5				
v =	0.3				Poisson's ratio

K_p = 4.53 Value from Timoshenko and Gere, 1961 –Table 9-1

	Fe =	133	ksi	917	MPa	(9-7)
Fe >= 0.44*Q_s Fy	**Fcr =**	**32.15**	ksi	222	MPa	(E3-2)
	Pn = Fcr A_{side}=	**1688**	kip	7′508	kN	

The local buckling of one unsupported edge local plate buckling is calculated assuming the length of the plate as the size of the opening in the cover plate, see Figure A2-3.

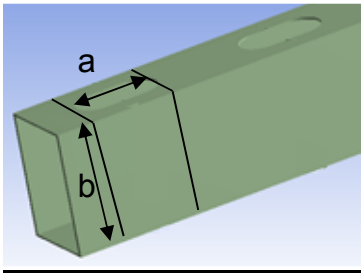

Figure A2-3 – Rectangular plate assumed for the calculation – Size of opening in cover plate

The elastic critical buckling flexural F_e is calculated using Equation (13) (Timoshenko and Gere, 1961).

$$F_e = \frac{k\,\pi^2 D}{b^2 h} \qquad (13)$$

In which k is a numerical factor depending on the magnitude of the ratio a/b and is equal to:

k_p u= 3.15 Value from Table 9-2 from Timoshenko and Gere, 1961

and D is the flexural rigidity of the plate calculated as follow

D = 2188 kip-in 247 kN-m $D = \frac{Eh^3}{12(1-\nu^2)}$

therefore

	Fe =	92.9	ksi	640	MPa	(9-7)
Fe >= 0.44*Q_s Fy	**Fcr =**	**30.61**	ksi	211	MPa	(E3-2)
	Pn = Fcr A_{side}=	**1607**	kip	7’148	kN	

Appendix B – RIKS METHOD

B1 STATIC POST BUCKLING USING THE MODIFIED RIKS METHOD

This research made use of the ABAQUS finite element analysis package for the stability analysis of a built up member. Two different methodologies exist for the buckling and post buckling problems (ABAQUS Theory Manual, 2007):

1) Eigenvalue buckling prediction

ABAQUS/Standard contains a capability for estimating elastic buckling by eigenvalue extraction. This estimation is typically useful for stiff structures, where the pre-buckling response is almost linear. The buckling load estimate is obtained as a multiplier of the pattern of perturbation loads, which are added to a set of base state loads. The base state of the structure may have resulted from any type of response history, including nonlinear effects. It represents the initial state to which the perturbation loads are added. The response to the perturbation loads must be linear up to the estimated buckling load values for the eigenvalue estimates to be reasonable.

2) Modified Riks algorithm

It is often necessary to obtain nonlinear static equilibrium solutions for unstable problems, where the load-displacement response can exhibit the type of behavior as shown in Figure B-1 that is, during periods of the response, the load and/or the displacement may decrease as the solution evolves. The modified Riks method is an algorithm that allows effective solution of such cases.

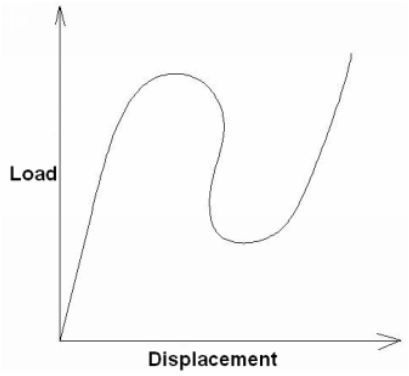

Figure B-1: Typical unstable static response

In this algorithm, it is assumed that the loading is proportional that is, that all load magnitudes vary with a single scalar parameter. In addition, the response is assumed to be reasonably smooth, meaning that sudden bifurcations do not occur. The essence of the

method is that the solution is viewed as the discovery of a single equilibrium path in a space defined by the nodal variables and the loading parameter. Development of the solution requires this path be traversed as far as required.

The modified Riks method in Abaqus finds static equilibrium at the end of each increment. However, unlike regular nonlinear static analyses, the load magnitude is also a solution variable. It can increase or decrease to satisfy static equilibrium, allowing the response to vary no monotonically.

Since both loads and displacements are unknowns, the concept of arc length is introduced. It is the distance along the equilibrium solution path in load displacement space. This measure is used to control the automatic time increment algorithm.

The results of interest are the current displacements which are available in the normal manner, and the current value s of the loads, which are given by referring to a load proportionality factor, identified by output variable LPF.

The concept of proportional loading is important in Riks method analysis, especially when using a multiple analysis steps. The current magnitude of the load in the structure is given by $P_{total} = P_0 + LPF\ (P_{ref} - P_0)$ where P_{ref} is the load pattern defined in the current RISK step. P_0 is the "dead load" (that is, any load or boundary condition applied in the previous step), and LPF is the load proportionality factor. Again, the LPF, may increase or decrease as the solution proceeds and is printed in the status file. It is worth noting the generality of the loading possibilities: that the "live" load, which is scaled up or down by the Riks algorithm, is added to any set of "dead" loads on the structure. The "live" load may be mechanical or thermal (or a combination of both).

The following Figures B-2 and B-3 show a close out of the model and the deformed shape using the two different methodologies.

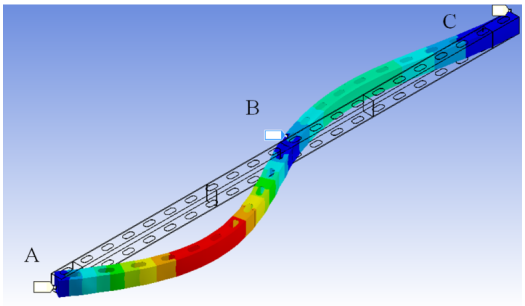

Figure B-2 – Abaqus Local Model –Elastic Buckling

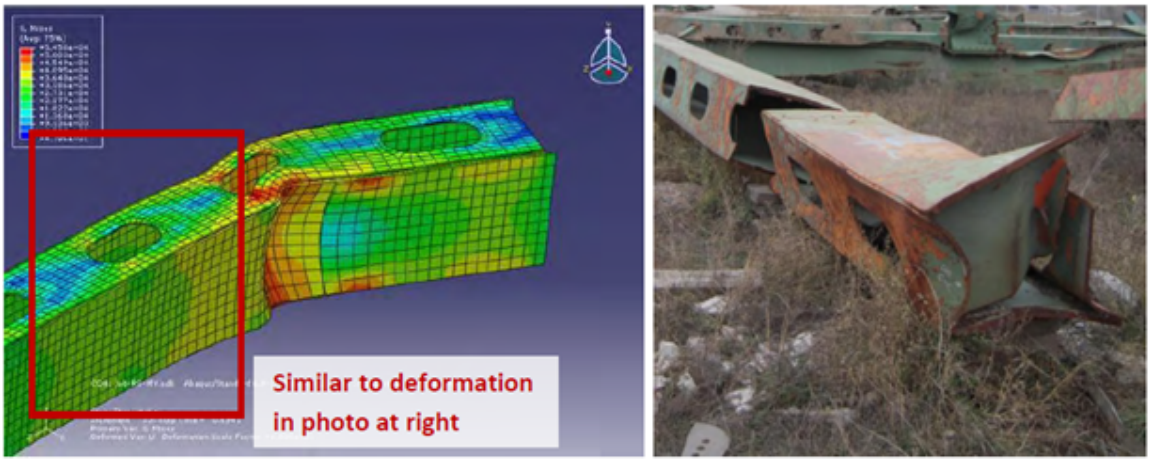

Figure B-3 –Abaqus Local Model – Post buckling behavior – RIKS method

INDICES AND BIBLIOGRAPHY

LIST OF FIGURES

LIST OF TABLES

LIST OF EQUATIONS

		Page	Notes:
(1)	$P[C] = P[C\|D]\ P[D\|E]\ P[E]$	49	
(2)	$\delta_2 = \frac{Q}{2}\left(\frac{3c}{4}\right)^3 \frac{1}{3EI_f} = \frac{9Qc^3}{128\,EI_f}$	61	Eq. (m) pg 141 (Timoshenko and Gere, 1961)
(3)	$\gamma = \frac{\delta_1 + \delta_2}{\frac{1}{2}a} = \frac{9Qc^3}{64aEI_f}$	61	Pg 142 (Timoshenko and Gere, 1961)
(4)	$\frac{1}{P_d} = \frac{9c^3}{64aEI_f}$	62	Eq. (n) pg 142 (Timoshenko and Gere, 1961)
(5)	$P_{cr} = \frac{\pi^2 EI}{l^2} \frac{1}{1 + \frac{\pi^2 EI}{l^2}\left(\frac{9c^3}{64aEI_f}\right)}$	62	Eq. (2-66) pg 142 (Timoshenko and Gere, 1961)
(6)	$P_n = F_{cr}A_g$	111	Eq. (E3-1) pg 33-Section E3 AISC 360-05
(7)	$\mathrm{F_e} = \frac{\pi^2 \mathrm{E}}{(\mathrm{KL})^2}$	111	Eq. (E3-4) pg 33-Section E3 AISC 360-05
(8)	$F_{cr} = \left[0.658^{\frac{F_y}{F_e}}\right] F_y$	111	Eq. (E3-2) pg 33-Section E3 AISC 360-05
(9)	$F_{cr} = 0.877F_e$	111	Eq. (E3-3) pg 33-Section E3 AISC 360-05
(10)	$F_e = \left[\frac{\pi^2 EC_w}{(K_z L)^2} + GJ\right] \frac{1}{I_x + I_y}$	112	Eq. (E3-4) pg 34-Section E3 AISC 360-05
(11)	$\left(\frac{KL}{r}\right)_m = \sqrt{\left(\frac{KL}{r}\right)_0^2 + 0.82\frac{\alpha^2}{(1+\alpha^2)}\left(\frac{a}{r_{ib}}\right)^2}$	113	Eq. (E6-2) pg 37-Section E3 AISC 360-05
(12)	$\mathrm{F_e} = \frac{\mathrm{k}\,\pi^2 \mathrm{E}}{12(1-\nu^2)} \frac{\mathrm{h}}{\mathrm{b}^2}$	114	Eq. (9-7) pg 355 (Timoshenko and Gere, 1961)
(13)	$\mathrm{F_e} = \frac{\mathrm{k}\,\pi^2 \mathrm{D}}{\mathrm{b}^2 \mathrm{h}}$	115	Eq. (j) pg 362 (Timoshenko and Gere, 1961)

BIBLIOGRAPHY

AASHTO-*LRFD Bridge Design Specifications*, (2007) by American Association of State Highway and Transportation Officials in Washington, D.C .4th Edition.

AASHTO-*LRFD Specifications* (1961), by American Association of State Highway and Transportation Officials in Washington, D.C.

ABAQUS, 2010. Abaqus Theory Manual. [Online] Available at: www.simulia.com

AISC 303-10, Code of Standard Practice for Structural Steel Buildings and Bridges by American Institute of Steel Construction.

AISC 360-05, Specification for structural steel buildings by American Institute of Steel Construction. ANSI/AISC 360-05.

Alashker, Y., Li, H. and El-Tawil, S. (2011), *Approximations in Progressive Collapse Modeling*, Journal of Structural Engineering, 137(9), 914-924.

Arangio S., Bontempi F. and Ciampoli M. (2011), *Structural integrity monitoring for dependability*, Structure and infrastructure Engineering, 7(1), 75-86.

Arup, (2011), *Review of international research on structural robustness and disproportionate collapse*, London: Department for Communities and Local Government.

Biezma, M. V., & Schanack, F. (2007). *Collapse of Steel Bridges*. Journal of Performance of Constructed Facilities. 21, pg. 398-405.

Biondini, F., Bontempi, F. and Malerba, P.G. (2004), *Fuzzy reliability analysis of concrete structures*, Computers and Structures, 82(13-14), 1033-1052.

Biondini, F. and Frangopol, D. (2009), *Lifetime reliability-based optimization of reinforced concrete cross-sections under corrosion*, Structural Safety, 31(6), 483-489.

Bontempi F. (2006), *Basis of design and expected performances for the Messina Strait Bridge*, Proceedings of the International Conference on Bridge Engineering – Challenges in the 21st Century, Hong Kong, 1-3 November 2006.

Bontempi, F., Giuliani, L. and Gkoumas, K. (2007), *Handling the exceptions: dependability of systems and structural robustness*, Invited Lecture, Proceedings of the 3rd International Conference on Structural Engineering, Mechanics and Computation

(SEMC), Cape Town, South Africa, September 10-12.

Bontempi, F. and Giuliani, L. (2008), *Nonlinear dynamic analysis for the structural robustness assessment of a complex structural system*, Proceedings of the 2008 Structures Congress, April 24-26, 2008, Vancouver, BC, Canada.

Bontempi F., Arangio S., (2010), *Dependability of Complex Bridge Structural Systems*. 5th Int. Conf. On Bridge Maintenance, Safety and Management (IABMAS 2010), Philadelphia, Pa. July 11-15 2010.

Brando, F., Iannitelli, A., Cao, L., Malsch, E., Panariello, G., Abruzzo, J., and Pinto, M. (2012), *Forensic Investigation Modeling (FIM) Approach: I-35 West Bridge Collapse Case Study*. Forensic Engineering 2012: pp. 48-57. Doi: 10.1061/9780784412640.006.

Canisius, T.D.G., Sorensen, J.D. and Baker, J.W. (2007), *Robustness of structural systems – A new focus for the Joint Committee on Structural Safety (JCSS),* Proceedings of the 10th Int. Conf. on Applications of Statistics and Probability in Civil Engineering (ICASP10), Taylor and Francis, London.

Carper, K. (2001), *Forensic engineering*. New York: Elsevier.

Cha, E. J. and Ellingwood, B. R. (2012), *Risk-averse decision-making for civil infrastructure exposed to low-probability, high-consequence events*, Reliability Engineering and System Safety 104, 27-35.

Chajes, A. (1974), *Principles of Structural Stability Theory*, Prentice-Hall Inc., Englewood Cliffs, New Jersey, USA.

Chen, W.F., and Lui, E.M. (1987), *Structural stability theory and implementation*, New York: Elsevier, USA.

Chen, W.F., and Lui, E.M. (1991), *Stability Design of Steel Frames,* CRC Press, Inc., Boca Raton, Florida.

Chen, W.F., Goto, Y. and Richard J.Y. (1996), *Stability Design of Semi-Rigid Frames*. John Wiley & sons, Inc., New York.

Choi, J-h. and Chang, D-k. (2009), *Prevention of progressive collapse for building structures to member disappearance by accidental actions*, Journal of Loss Prevention in the Process Industries, 22, 1016-1019.

Ciampoli, M., Petrini, F., Augusti, G. (2011), *Performance-Based Wind Engineering: Towards a general procedure*, Structural Safety 33: 367-378.

Clarin M., (2004), *High strength stees, local buckling and residual stresses*, Licentiate Thesis 2004:54, Lulea, University of Technology. <http://pure.ltu.se/portal/en/publications/high-strength-steel(44b79a40-b168-11db-bf9d-000ea68e967b).html>. <http://pure.ltu.se/portal/files/323740/LTU-LIC-0454-SE.pdf>

COST (2011), *TU0601 - Structural Robustness Design for Practising Engineers*, Canisius, T.D.G. (Editor).

Crosti, C., Duthinh, D. and Simiu, E. (2011), *Risk consistency and synergy in multihazard design*, Journal of Structural Engineering, 137(8), 844-849.

CSI "SAP2000 Analysis reference manual", Computers and structures Inc. Berkeley, California, USA, Sept. 2004.

DoD - Department of Defense (2009), Unified Facilities Criteria (UFC). *Report No. UFC 4-023-03: Design of buildings to resist progressive collapse.* Washington DC: National Institute of Building Sciences.

Ellingwood, B. (2002), *Load and resistance factor criteria for progressive collapse design*, Proceedings of Workshop on Prevention of Progressive Collapse, National Institute of Building Sciences, Washington, D.C.

Ellingwood, B.R. and Dusenberry, D.O. (2005), *Building design for abnormal loads and progressive collapse*, Computer-Aided Civil and Infrastructure Engineering, 20(3), 194-205.

Ellingwood, B.R., Smilowitz, R., Dusenberry, D.O., Duthinh, D. and Carino, N.J. (2007), *Report No. NISTIR 7396: Best practices for reducing the potential for progressive collapse in buildings*. Washington DC: National Institute of Standards and Technology (NIST). http://fire.nist.gov/bfrlpubs/build07/art008.html

Faber, M.H. and Stewart, M.G. (2003), *Risk assessment for civil engineering facilities: critical overview and discussion*, Reliability Engineering and System Safety, 80(2), 173-184.

FHWA (2011), *Framework for Improving Resilience of Bridge Design*, Publication No IF-11-016.

FHWA (2009), *"Load Rating Guidance and Example for Bolted and Riveted Gusset plates in truss bridges*".Publication No. FHWA-IF-09-014, February 2009.

Frangopol, M. D. & Curley, P., (1987), *Effects of damage and redundancy on structural reliability*. s.l., Journal of structural engineering, vol.113, No.7, July 1987.

Galal, K. and El-Sawy, T. (2010), *Effect of retrofit strategies on mitigating progressive collapse of steel frame structures*, Journal of Constructional Steel Research, 66(4), 520-531.

Galambos, T.V. (1968), *Structural Members and Frames*. Prentice-Hall, Inc.,Englewood Cliffs, New Jersey.

Garavaglia, E., Sgambi, L., Basso, N. (2012), *Selective maintenance strategies applied to a bridge deteriorating steel truss,* Bridge Maintenance, Safety, Management, Resilience and Sustainability - Proceedings of the 6th International Conference on Bridge Maintenance, Safety and Management, IABMAS 2012, Italy, Stresa, 8-12 July 2012.

Ghosn, M. and Moses, F. (1998), *NCHRP Report 406: Redundancy in Highway Bridge Superstructures*, TRB, National Research Council, Washington, D.C.

Giuliani, L. (2012), *Structural safety in case of extreme actions*, Special Issue on: "Performance and Robustness of Complex Structural Systems", Guest Editor Franco Bontempi, International Journal of Lifecycle Performance Engineering (IJLCPE), in press, ISSN (Online): 2043-8656; ISSN (Print): 2043-8648.

GSA - General Service Administration (2003), *Progressive collapse analysis and design guidelines for new federal office buildings and major modernization project*, Washington DC: GSA.

Hoffman, S. T. and Fahnestock, L. A. (2011), *Behavior of multi-story steel buildings under dynamic column loss scenarios*, Steel and Composite Structures, 11(2), 149-168.

HSE - Health and Safety Executive (2001), *Reducing risks, protecting people, HSE's decision-making process*, United King: Crown copyright.

International Standard ISO/FDIS 2394: *General principles on reliability for structures*, 1998.

ISDGA, Institute For Steel Development & Growth, online material accessed on September 2012. http://steel-insdag.org/TeachingMaterial/chapter43.pdf

Izzuddin, B. A., Vlassis, A. G., Elghazouli, A. Y. and Nethercot, D. A. (2008a), *Progressive collapse of multi-storey buildings due to sudden column loss - Part I: Simplified assessment framework*, Engineering Structures, 30(5), 1308-1318.

Izzuddin, B. A., Vlassis, A. G., Elghazouli, A. Y. and Nethercot, D. A. (2008b), *Progressive collapse of multi-storey buildings due to sudden column loss - Part II: Application*, Engineering Structures, 30(5), 1424-1438.

Jones, Arnold David (1976), *Trusses: a study by the Historic American Engineering Record*, Washington, D.C. : printed by the Montgomery C. Meigs original chapter of the Society for Industrial Archeology, National Museum of History and Technology, Smithsonian Institution. http://hdl.loc.gov/loc.pnp/pp.print

Kim, J. and Kim, T. (2009), *Assessment of progressive collapse-resisting capacity of steel moment frames,* Journal of Constructional Steel Research, 65(1), 169-179.

Kwasniewski, L. (2010), *Nonlinear dynamic simulations of progressive collapse for a multistory building*, Engineering Structures, 32(5), 1223-1235.

Malla, R.B., Agarwal, P. and Ahmad, R. (2011), *Dynamic analysis methodology for progressive failure of truss structures considering inelastic postbuckling cyclic member behavior*, Engineering Structures, 33(5), 1503-1513.

Malsch, E., Brando, F., Iannitelli, A., Abruzzo, J., Panariello, G., (2011), *The Causes of the I-35 West Bridge Collapse*, London, Proceedings 35th Annual symposium of IABSE.

Mella, P. (1997) *Dai sistemi al pensiero sistemico. Per capire i sistemi e pensare con i sistemi*. Franco Angeli, 1997.

Miyachi, K., Nakamura, S. and Manda, A. (2012), *Progressive collapse analysis of steel truss bridges and evaluation of ductility*, Journal of Constructional Steel Research, 78, 192-200.

MnDOT - Minnesota Department of Transportation, *Interstate 35W Bridge: Original Plans & Details*. http://www.dot.state.mn.us/I-35wbridge/history.html#steel, accessed online on December 2, 2009.

Nafday, A.M. (2011), *Consequence-based structural design approach for black swan events*, Structural Safety, 33(1), 108-114.

Nishino, F., Ueda, Y., Tall, L. (1966). *Experimental investigation of the buckling of plates with residual stresses*. Authorized reprint from the copyrighted "Test Method for

Compression Members" ASTM STP No 419, 1967, p.12.

Nishino, Fumio, and Lambert Tall. (1969). *Residual Stress And Local Buckling Strength Of Steel Columns*. Proceedings of the Japan Society of Civil Engineers. 1969, no. 172: 79-96.

National Transportation Safety Board (NTSB). (2007). *Loads on the bridge at the time of the accident.* Modeling Group Study Report No. 07-115.

National Transportation Safety Board (2008a), *Materials Laboratory Study Report 08-118, Calculation of differential temperature for I-35W bridge*, Nov 7 2008.

National Transportation Safety Board (2008b), *Collapse of I-35 W Highway Bridge, Minneapolis, Minnesota, August 1, 2007. Accident Report*, NTSB/HAR 08/03 PB 2008-916213, Washington D.C. 20594.

National Transportation Safety Board (2008c), *Structural and local failure study of gusset plate in Minneapolis bridge collapse.* Modeling group chairman final report 08-119, NTSBC070010, Nov 2008, Washington D.C. 20594.

Paik, J. K., & Thayamballi, A. K. (2003). *Ultimate limit state design of steel plated structures*. Chichster, England, J. Wiley.

Petrini, F., Ciampoli, M. (2012), *Performance-based wind design of tall buildings*, Structure & Infrastructure Engineering - Maintenance, Management, Life-Cycle Design & Performance, 8(10), 954-966.

Pilkey, W. D. (1994), *Formulas for stress, strain, and structural matrices*. New York.

Rezvani, F. H. and Asgarian, B. (2012), *Element loss analysis of concentrically braced frames considering structural performance criteria*, Steel and Composite Structures, 12(3), 231-248.

Riks, E. (1972), *The application of Newton's method to the problem of elastic stability*, Journal of Applied Mechanics, 39:1060-1065, 1972.

Saydam, D. and Frangopol, D. M. (2011), *Time-dependent performance indicators of damaged bridge superstructures,* Engineering Structures, 33(9), 2458-2471.

Seaburg, P. A., Carter, C. J., & American Institute of Steel Construction. (1997). *Torsional analysis of structural steel members*. Chicago, Ill: AISC.

Simulia 2009, ABAQUS Version 6.9-1 documentation collection, Dassault Systèmes

Sgambi, L., Gkoumas, K. and Bontempi, F. (2012), *Genetic Algorithms for the Dependability Assurance in the Design of a Long-Span Suspension Bridge*, Computer-Aided Civil and Infrastructure Engineering, **27**(9), 655-675.

Stang, Ambrose H., Greenspan, M. (1942), *Perforated cover plates for steel columns: compressive properties of plates having ovaloid perforations and a width-to-thickness ratio of 40*. Part of Journal of Research of the National Bureau of standards, Research paper RP1474, Volume 28, June 1942.

Stang, Ambrose H., Greenspan, M. (1948), *Perforated cover plates for steel columns: summary of compressive properties*. Part of Journal of Research of the National Bureau of standards, Research paper RP1880, Volume 40, May 1948.

Starossek, U. (2009), *Progressive collapse of structures*, London: Thomas Telford Publishing.

Starossek U. (2006), *Progressive collapse of bridges - aspects if analysis and design*, invited lecture, International symposium on sea-crossing long-span bridges, Mokpo, Korea, Feb. 15-17, 2006.

Starossek, U. and Haberland, M. (2010), *Disproportionate Collapse: Terminology and Procedures*, Journal of Performance of Constructed Facilities, 24(6), 519-528.

Starossek, U. and Haberland, M. (2012), *Robustness of structures*, Special Issue on: "Performance and Robustness of Complex Structural Systems", Guest Editor Franco Bontempi, International Journal of Lifecycle Performance Engineering (IJLCPE), in press, ISSN (Online): 2043-8656; ISSN (Print): 2043-8648.

Sverdrup & Parcel (1960), *Construction Plan for Bridge No.9340*, St. Louis, MO.

Tall L. (1966), *Welded built-up columns*, Fritz Engineering Laboratory Report No 249.29.

Timoshenko, S., Gere, J. M. (1961), *Theory of elastic stability*. New York, McGraw-Hill.

Ueda Y., Yao T., (1978), *Compressive strength of plate elements with welding residual stresses and deformation*, Welding Research Institute of Osaka University, <http://ir.library.osaka-u.ac.jp/meta-bin/mt-pdetail.cgi?smode=1&edm=0&tlang=1&cd=00033844>.

White. M.W., Thurlimenn B. (1956a), *Study of columns with perforated cover-plates*, Volume 244.1 di Fritz Laboratory report, Lehigh University, Institute of Research.

White. M.W., Thurlimenn B. (1956b), *Test of columns with perforated cover plates*, Volume 244.2 di Fritz Laboratory report, Lehigh University, Institute of Research.

White, Maxwell W., and Bruno Thurlimann. (1956c), *Study of columns with perforated cover plates*. Reprinted from AREA "American Ralway Engineering Association" bulletin no. 531, Sept.-Oct. 1956 pag 175 - 291. OCLC # 5633346, ISSN 0003-0694.

Wolff, M. and Starossek, U. (2010), *Cable-loss analyses and collapse behavior of cable-stayed bridges*, Bridge Maintenance, Safety, Management, Resilience and Sustainability - Proceedings of the 5th International Conference on Bridge Maintenance, Safety and Management, IABMAS 2010, Philadelphia, PA, 11-15 July 2012.

Yuan, W. and Tan, K. H. (2011), *Modeling of progressive collapse of a multi-storey structure using a spring-mass-damper system*, Structural Engineering and Mechanics, 37(1), 79-93.

Ziemian, R. D. (2010), *Guide to stability design criteria for metal structures*. Hoboken, N.J., John Wiley & Sons.